GridShield: Robust Control Algorithms to Prevent Power Outages

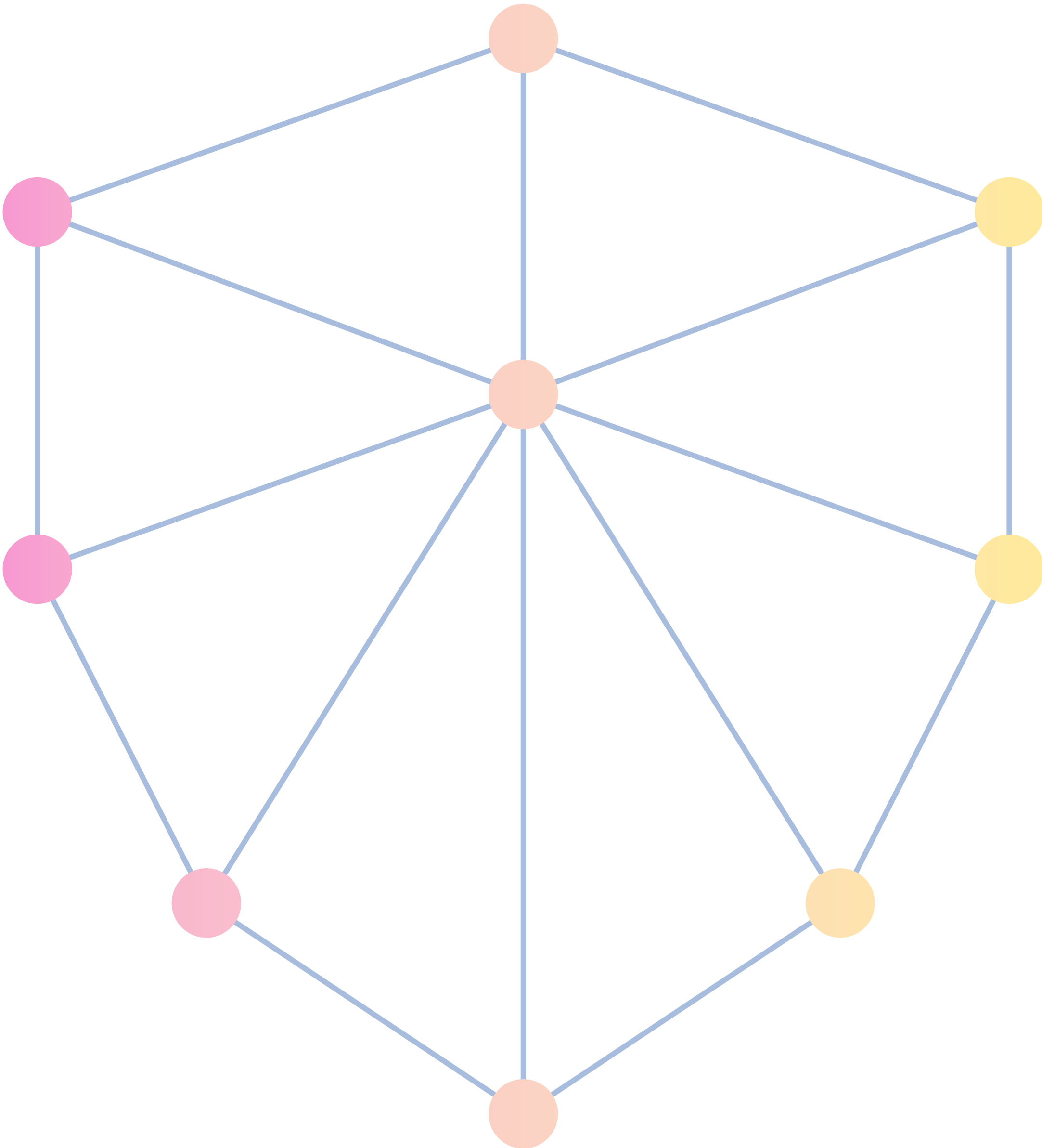

Ivo Varenhorst

June 29, 2022

University of Twente

UNIVERSITY
OF TWENTE.

Faculty of Electrical Engineering, Mathematics and Computer Science (EEMCS)

Master's Thesis, M-SET

GridShield: Robust Control Algorithms to Prevent Power Outages

Ivo Varenhorst

Chair Prof.dr. J.L. Hurink
EEMCS
University of Twente

Supervisor Dr.ir. G. Hoogsteen
EEMCS
University of Twente

Second supervisor Dr. M.N. Bañol Arias
EEMCS
University of Twente

External Dr. F.H.J.M. Coenen
BMS
University of Twente

Supervisor H. van Sambeek Msc
ElaadNL

June 29, 2022

Ivo Varenhorst
GridShield: Robust Control Algorithms to Prevent Power Outages
Master's Thesis, M-SET, June 29, 2022
Supervising Committee: Prof.dr. J.L. Hurink, Dr.ir. G. Hoogsteen, Dr. M.N. Bañol Arias, Dr. F.H.J.M. Coenen and H. van Sambeek Msc

University of Twente
Faculty of Electrical Engineering, Mathematics and Computer Science (EEMCS)
Drienerlolaan 5
7522 NB, Enschede, The Netherlands

Abstract

The growing number of electric vehicles (EVs) in the low-voltage distribution grid increase the grid load when charging and thereby the risk of overloading and damaging grid assets. Energy management systems (EMS) are an option to prevent grid congestion via smart charging. However, an EMS designed for controlling electric vehicle charging can fail, e.g. due to cyber-attacks or failure of communication systems. Therefore, a robust fallback control mechanism is required to prevent congestion and overloading problems in the grid.

This thesis presents implementations for GridShield, a novel concept designed to act as such a fallback control mechanism. In the event of an EMS failure, it must minimize excessive power draw at the transformer while still maximizing comfort under the imposed GridShield constraints. This means that the energy not supplied to the EVs due to the intervention of GridShield should be minimized. For robustness, GridShield uses a one way standalone communication network. In this thesis, the aim is to develop a control algorithm for GridShield that has minimal excessive power draw, while providing maximum comfort. To develop such an algorithm, congestion management and control strategies from multiple fields are considered. The proposed algorithm must be robust enough to deal with unexpected events such as variations in the number of vehicles simultaneously charging. Discomfort caused to users must meanwhile be minimized in the fairest possible way.

The GridShield system is tested in various simulation scenarios. The scenarios include a residential neighborhood, but also a public parking lot with EV chargers. Recommendations about what control strategies work best for a GridShield system are made based on the simulation results. The validity of the simulation results is verified through a real-world test of a GridShield system at the SlimPark site at the University of Twente. The results show that GridShield can be used to effectively decrease grid power limit violations caused by EV charging by 85% to 94% in the presented scenarios, compared to a situation where GridShield is not active, thereby increasing the reliability and longevity of grid assets.

Dankwoord

Twee jaar geleden begon ik aan de Master Sustainable Energy Technology nadat ik een half jaartje Embedded Systems had gedaan, zonder enig idee waar ik nou echt naartoe wilde. Toen Johann en Bart me een half jaar geleden attendeerden op het bestaan van de Energy Group, vond ik eindelijk een onderzoeksrichting waar ik echt enthousiast van werd. Voor ik het wist was ik bijna dagelijks bij de groep te vinden, en zo is deze thesis ontstaan. Via deze weg wil ik iedereen bedanken die me heeft geholpen en gesteund tijdens dit onderzoek.

Thank you to Gerwin and Nataly, my daily supervisors at the UT, for our weekly interesting meetings and discussions, which were very important to the research. Gerwin, bedankt ook voor je begeleiding van Felix en mij tijdens DEMS, jouw geloof in onze paper deed mij ook in mezelf geloven. Als iemand zich afvraagt of je ons een warm welkom hebt gegeven, zegt het denk ik genoeg dat we beiden met veel plezier onze Master thesis bij jou schrijven. Ik kijk er naar uit nog meer met je te werken!

Danke Felix, dass du dich mit mir auf diese GridShield Reise begeben hast. Your relentless hunger to publish our DEMS paper pushed me to go the extra mile, which was well worth the effort! Johann, Bart, and all Energiehok-inhabitants, thank you for the coffee breaks and the great atmosphere every day.

Bedankt aan Stan en Bart, die een grote rol hebben gespeeld in de SlimPark metingen die uiteindelijk in deze thesis terecht zijn gekomen. Zonder jullie was dat niet gelukt. En naast Stan natuurlijk bedankt aan de rest van het GridShield team bij Elaad. Hanna, Stefan, Marisca en Jesse, bedankt voor alle discussies en ideeën.

Bedankt aan mijn studievrienden, jullie zijn met te veel voor deze pagina, maar ik weet zeker dat dat biertje en die GiTo van laatst nog lang niet onze laatsten zijn ;)

Bovenal wil ik mijn vader bedanken (bij de Nobelprijs sta je als eerste pap ;)), en jou natuurlijk mama voor al het eten dat ik iedere keer weer op mocht eten bij jou als ik bij Elaad ging werken. Willem, bedankt voor de speciaalbiertjes die we dan dronken, en voor de goede hoeveelheid geouwehoer die we daarbij over tafel slingerden.

Paps en mams, Tobias en Mira, ook al konden we het inhoudelijk niet in detail over de thesis hebben, toch zijn jullie onvervangbaar en mijn allerbelangrijkste support. Zonder jullie was deze thesis niks geworden, dankjulliewel!

Contents

Introduction

1

Chapter Objective: In this chapter, the scope of this thesis and the research questions are introduced.

Chapter Contents

1.1 The Energy Transition

Global energy demand is ever increasing. While traditionally we fulfilled our energy needs by consuming fossil fuels, there is an increasing demand for renewable, locally generated alternatives to fossil fuels. This demand originates not only from climate change conferences such as the COP26 conference in Glasgow in 2021, which aims to limit global warming to $1.5°C$ compared to pre-industrial levels [1]. The Ukraine war and the resulting energy crisis with Russian gas suppliers prove the value of energy independency. While in 2021, 40% of European gas was supplied by Russia [2], there is now a strong desire to be energy independent.

The EU plans to abandon the use of Russian fossil fuels with a €300 billion plan well before 2030 [3]. One of the main pillars of this plan is to significantly boost the local production of green energy such as solar and wind power. However, green energy sources introduce intermittency on the supply side of an energy system. Solar energy is only available when the sun shines, and wind energy is only available when the wind blows. To deal with this intermittency, energy systems must be able to deal with the peaks that are introduced by renewable energy sources (RES). When looking at the Netherlands, we see that the electricity grid is often at its maximum capacity already with the current amount of RES installed, limiting the possibility of adding more RES to the national energy system.

On the demand side of the energy system, the growing economy, digitalization, and other factors such as the switch from fossil powered internal combustion engine vehicles (ICE vehicles) to electric vehicles (EVs) also place a strong burden on the grid. Companies that require a large grid connection are often refused by the distribution system operators (DSOs) because the grid is already at its maximum capacity [4]. Reinforcing the grid is costly, involves a slow process, and requires many technicians which are not readily available.

In residential areas, the transition from fossil fuel powered appliances to electric appliances is increasing the grid load of households significantly. Such appliances include EVs, but also heat pumps (HPs), induction cooking stoves and more. These appliances have a high power demand compared to the power demand of a traditional household. This introduces challenges to keep the grid operational. For instance, the grid voltage must be kept within bounds, and the power constraints of the grid must be respected to prevent grid overloading and damage.

1.2 Electrical Appliances

Emerging electrical appliances such as heat pumps, home batteries, and EVs can use significant power compared to an average household, but they also provide flexiblity in their own unique ways. In this work, we focus on one of these appliances: EVs.

Rising oil prices, government tax schemes where consumers can get a €3350 tax bonus when buying a new EV [5], companies pay less taxes for a company EV than for an ICE vehicle, EV owners pay no road tax nor BPM [6], and a general desire to be green, all accelerate the transition from ICE vehicles to EVs. Instead of refilling at the petrol station like ICE vehicles, EVs are charged at home or at a local charging point. This new paradigm is convenient for the user, but EVs can draw large amounts of power, up to 7.2 kW per phase for at home chargers. This puts additional stress on the already-stressed grid. This effect is amplified further because EVs often arrive at home in the evening when demand is already high, and then start charging at high power. On top of that, most EVs in a neighborhood will arrive home roughly simultaneously. All these effects make the peak load that occurs from EV charging increase.

While the peak load of EV charging in the evening, when electricity demand is already high, can cause violations of grid restrictions, most EVs do not actually need to charge at high power when arriving at home. By decreasing charging power when the grid load is too high, impact on the grid from charging EVs can be decreased significantly.

Dutch cars drove less than 36 kilometers per day on average in 2019 before the COVID-19 crisis [7]. This means that EV batteries do not generally need a full charge every night; they usually only require a few kWhs per night instead. This means EV charging can be postponed and done later in the night, and/or that charging can be done at a reduced rate. Another factor to consider for the grid load of EVs is V2G - By reversing the power flow and providing power from the vehicle to the household or the grid, EVs can locally provide additional power when necessary. Thus, smart coordination of EVs can help stabilize grid operation. This presents an opportunity to increase the penetration of EVs without reinforcing the grid. To use this flexibility provided by EVs to prevent grid overloading, smart coordination of the grid is required. Thus, we look into smart grids, which are introduced in Section 1.3.

1.3 Smart Grids

Smart grids can be a possible solution to the problems that arise in local grids. The International Energy Agency (IEA) defines a smart grid as follows [8, p. 6]:

> "*A smart grid is an electricity network that uses digital and other advanced technologies to monitor and manage the transport of electricity from all generation sources to meet the varying electricity demands of end-users. Smart grids co-ordinate the needs and capabilities of all generators, grid operators, end-users and electricity market stakeholders to operate all parts of the system as efficiently as possible, minimising costs and environmental impacts while maximising system reliability, resilience and stability.*"

While the introduction of a smart grid introduces additional dependence on an operational ICT system to safeguard the supply of electricity, a smart grid also has many advantages. It can provide better utilization of grid assets, since production and demand peaks can be spread more evenly over time. Current power profiles of local grids in residential areas show clear peaks in the evening as shown in Fig. 1.1. This effect will be amplified when more electric appliances such as EVs and heat pumps are put in place. Meanwhile, local power generation, e.g. from solar panels, introduces production peaks in the afternoon, where demand is low. However, with flexible controllable devices that can adapt their power profile to grid requirements, a smart grid can mitigate these peaks. By utilizing the flexibility of devices such as batteries or EVs to charge in the afternoon (thereby decreasing the solar power generation peak in the grid), while supplying power through V2G in the evening (thereby decreasing the demand power peak in the grid), generation and consumption become more coordinated, significantly decreasing peak grid loads. To coordinate the available flexibility in a smart grid, a system that manages energy production and consumption is required. Section 1.4 looks into such systems that can manage energy flexibility for better utilization of the grid.

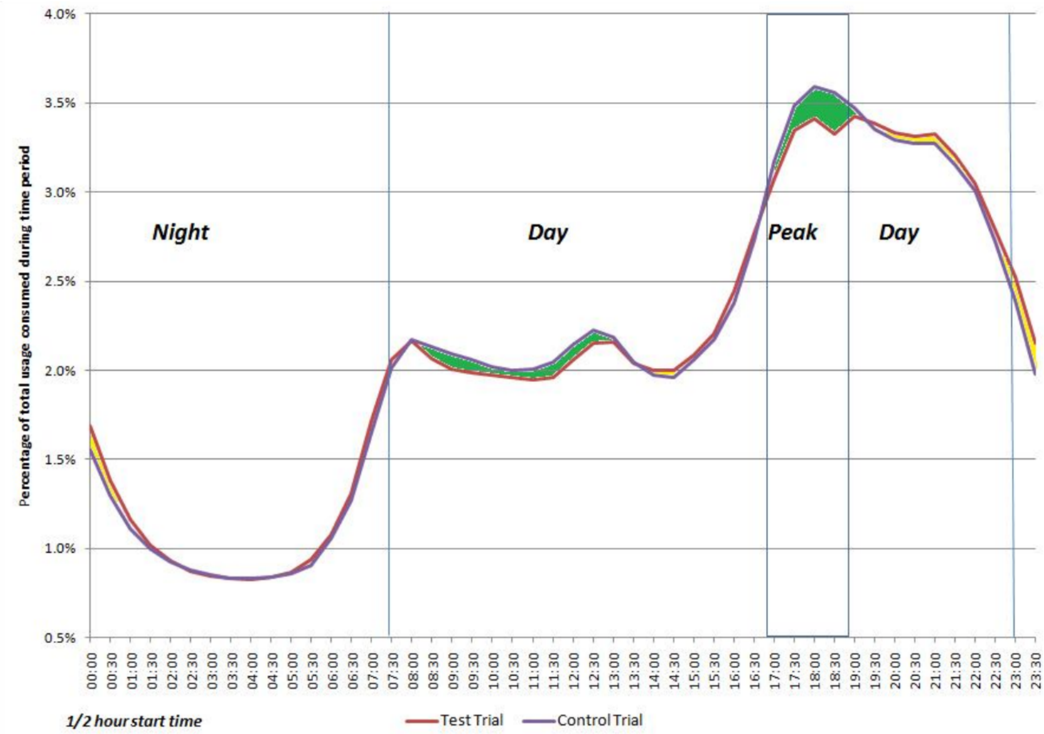

Fig. 1.1: Changes in load distribution profile across an average day (Monday to Friday) for test and control groups during measurements from 1st January to 31st December 2010 in a residential area in Ireland [9].

1.4 Energy Management

An energy management system (EMS) is a system that can steer flexibility of the devices it controls for optimal usage of the local grid. The target of an EMS is e.g. to keep the power flowing through the grid within certain pre-defined limits. It must prevent the combined power of the loads from exceeding power limits, but it must also deliver as much power as possible within the bounds of the grid limits. In other words, such an EMS must:

- Minimize excessive power draw at a transformer level.
- Minimize energy delivery curtailed.

However, an EMS can fail. This could e.g. be due to communication failures between devices, hardware failures, software bugs, or cyber attacks. When an EMS fails, this can cause multiple problems. When the EMS should tell devices to limit their power consumption, but fails to do so due to one of the aforementioned reasons, the grid may be overloaded. On the other hand, when devices are erroneously forced not to use any power by the EMS, this will cause user discomfort in the form of e.g. empty car batteries or cold houses. Worse, in the event of high production, the grid may be overloaded when there is no consumption to balance out the production. When such EMS issues are not resolved, sustained grid overloading can cause high wear, and in the event of significant overloading, physical damage to the grid may be caused. To prevent these problems from occurring in case of a failure, a backup system for an EMS is required. This is the main focus of this work: *EMS backup systems*.

1.5 Research Questions

To cope with possible failures of an EMS, an emergency fallback control system is required. In this work, we focus on EV charging. Hence, our main research question is:

How to robustly and adequately implement emergency fallback control of EV charging to avoid grid congestion?

The following sub-questions are formulated to deal with this main question:

- *What are the main objectives of such an EV charging control emergency fallback system and how can its performance be measured?*
- *How can general control concepts aid in avoiding grid congestion?*
- *How could an EV charging emergency fallback system be practically implemented?*
- *How will EV charging emergency fallback systems impact user comfort and social behavior?*

1.6 Thesis Outline

Chapter 2 deals with literature related to Energy Management Systems that holds relevance for EMS backup solutions in residential areas. Chapter 3 describes how the GridShield system discussed throughout this thesis is modeled. Chapter 4 details the implementation of the algorithms used to control the system of Chapter 3. Chapter 5 presents the results obtained from the implementation of the algorithms in simulations and during real-world tests. Chapter 6 discusses the social implications and effects of an EMS emergency backup system. Finally, the research questions from Section 1.5 are answered in Chapter 7 and suggestions for future work are presented.

Literature Review

2

Chapter Objective: This chapter serves to review literature relevant to the presented research.

Chapter Contents

2.1 Energy Management Systems

The emergence of new electrical appliances such as EVs and heat pumps, that significantly increase peak power demands compared to current household devices, has introduced significant additional stress on local grid assets. This additional stress can cause wear and damage to local grid assets and potentially even blackouts. However, since these new appliances also offer high flexibility in their consumption profile, the stress they cause on the local grid can be minimized through systems that steer this flexibility. Such an energy management system (EMS) can steer the demand of these appliances through demand side management (DSM) to e.g. maximize self-consumption of locally produced solar power, or steer them to reduce their power consumption when the household load is high because the electric stove is on. The International Electrotechnical Commission (IEC) defines an EMS in the IEC 61970 standard [10] as:

> *"a computer system comprising a software platform providing basic support services and a set of applications providing the functionality needed for the effective operation of electrical generation and transmission facilities so as to assure adequate security of energy supply at minimum cost."*

To prevent wear and damaging of local grid assets caused by overloading, an EMS must limit local energy consumption when required. Overloading of the local grid can occur at multiple levels. Household grid connections are protected through a fuse, which imposes a limit to the local consumption of a household. Thus, at a household level, the power consumption must be prevented from exceeding this fuse limit through DSM, for example by temporarily reducing the power of an EV charging session when the stove is on and the washing machine is operating. At the MV/LV transformer level, the total energy demand of a neighborhood must not exceed the fuse and capacity limits of the transformer. An EMS must prevent the combined consumption profile of all local households from exceeding this transformer limit, e.g. by reducing EV charging power when all EVs return from work and start charging. Numerous approaches have been researched to steer household appliances to respect local grid limits [11]. An EMS must respect the needs of consumers and allow high power consumption when the grid can facilitate this, but should also intervene and allow the grid operator to decrease consumption when required to protect grid assets.

Siano surveyed various implementations of DSM [12]. Many of these use price signals as steering signals to decrease peak loads at the MV/LV transformer level, such as time-of-use pricing (TOUP) and day ahead pricing (DAP). TOUP uses historical data to increase prices at times where consumption was high historically (typically in the evening), while DAP uses market principles to balance supply and demand for the next day. For both strategies, the aim is to shift peak loads to hours where typical consumption is less high, which should result in a lower peak demand. However, McKenna et al. showed that this does not necessarily decrease the peak load, it only shifts the peak load in time [13]. Worse, the peak load can actually increase, since decreased prices lead to higher synchronization of loads amongst households. These effects are visible in Fig. 2.1 and Fig. 2.2. In the figures, we see that e.g. cooling power increases before and after a time period where prices are high, while the power use for cooling during these high price periods is very low. The result of this shift of peak power consumption in time produces peaks that are higher than the peak without DSM, an effect that is distinctly noticeable after the increased price period in Fig. 2.1. This shows that DSM using TOUP or DAP can have an effect directly opposite to what DSM is trying to achieve.

To address this load synchronization problem, other steering heuristics have been proposed. For example, Gerards et al. proposed the profile steering heuristic, which uses a desired power profile as a steering signal instead of pricing schemes [14]. The aim of profile steering is to minimize the distance between a desired profile $\vec{p} = [p_1, ..., p_N]^T$ (usually a profile without peaks, i.e. a flat profile), and the profile

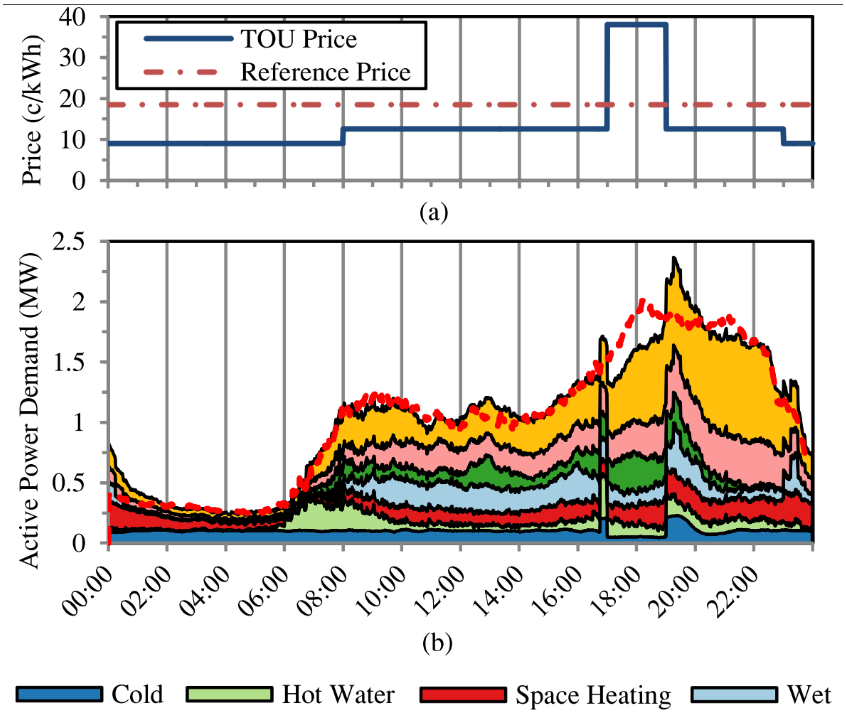

Fig. 2.1: Time-of-use pricing (TOUP) pricing scheme (a) and resulting power consumption (b) [13].

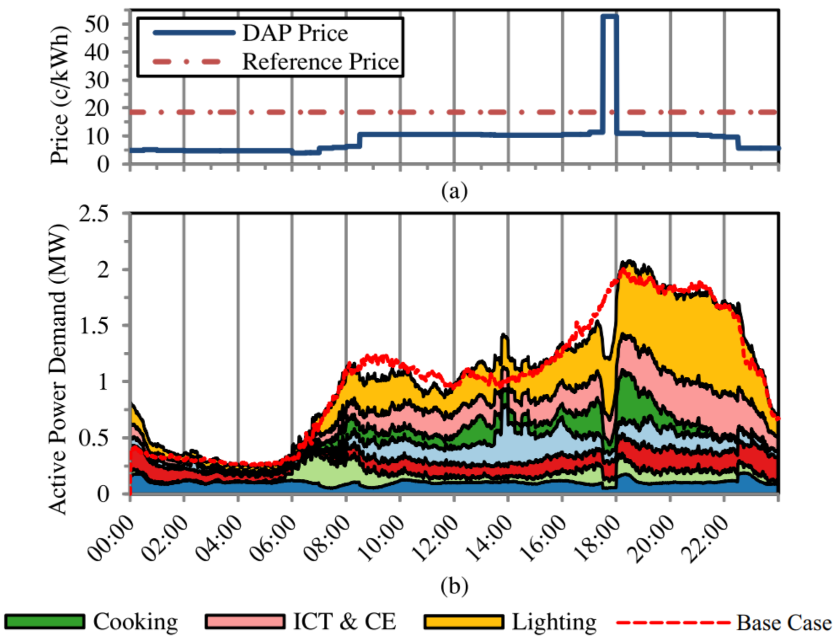

Fig. 2.2: Day ahead pricing (DAP) pricing scheme (a) and resulting power consumption (b) [13].

resulting from the algorithm $\vec{x} = [x_1, ..., x_N]^T$. In their paper, the euclidean distance $||\vec{x} - \vec{p}||_2$ is used. Profile steering can mitigate the peak load shifting effect present in TOUP and DAP schemes and thus prevent excessive grid load, by minimizing this euclidean distance. However, research into methods to incentivize users to make their appliances adopt the power profiles generated by the profile steering heuristic is still ongoing. The value of flexibility users are willing to provide must first be quantified.

As an indication of grid load, The German Association of Energy and Water Industries (BDEW) introduced the traffic light concept, which indicates the current stress on the grid [15]. A graphical representation is presented in Fig. 2.3. When the grid is safely within limits, this is regarded as a green light situation, and no intervention from the DSO is required. In green light conditions, free market operation is in full effect. Free market operation can introduce power problems however, even when DSM heuristics are applied as e.g. shown for the TOUP and DAP approaches in Fig. 2.1 and Fig. 2.2. These problems may introduce an amber situation, during which the EMS must allow the DSO to limit production and consumption where possible in a fair way as a means to prevent the grid from going to a red light situation where it is exceeding its limits. Where possible, the goal is to still allow market mechanisms to take effect. This becomes impossible in a red light situation, where the EMS must allow direct control by the DSO over all flexible production and consumption to prevent damage from occurring. The DSO is authorized to overrule any market mechanisms in this event. If a red light situation occurs, this usually means the EMS, instructed by the DSO, will intervene as hard as possible to prevent damage. However, an EMS can fail. This can be due to hardware failures, software bugs, cyber-attacks, or other unforeseen complications. In such an event, a red light situation cannot be resolved by DSO through direct control of the EMS, and worse, it may not respond to the situation as intended.

When the EMS fails while there is a red light situation, the need for an EMS backup solution is introduced. A simple backup solution would be to turn off all flexible loads and generators entirely. This will generally allow the grid to operate within limits again, but will also cause significant user discomfort; car batteries will not be charged and houses will become cold because heat pumps are turned off. A better backup solution can curtail the flexible loads and generators just enough to prevent grid overloading, while still delivering as much energy as possible. Shortly put, a good backup solution must:

- Minimize excessive power draw at a transformer level.
- Minimize energy curtailed by the backup system.

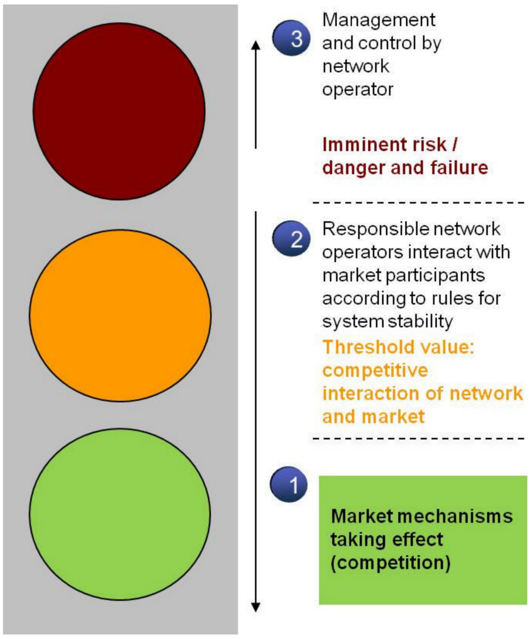

Fig. 2.3: Visualisation of the traffic light concept adapted from [15].

- Maximize user comfort under these constraints.

Backup solutions for EMS failures are the focus of this work. This chapter surveys literature that holds relevance for control strategies of such backup systems. We first introduce how electrical power overloads can occur and what actions can be taken to increase the power that can be delivered through the grid without needing to reinforce it. Then, we look into strategies to control power levels to stay within bounds. For this, we look at droop control, a strategy from the field of electrical grids, but we also look at other fields such as ICT and control engineering to draw inspiration from algorithms developed there.

2.2 Reactive Power Control and Phase Balancing

Grid damage from overloading occurs when the apparent power at a transformer, i.e. the combination of active and reactive power, exceeds transformer limits. From a generator and consumer standpoint, we are only interested in the delivery of active power, since active power is what is measured at the meter for payments, and active power is what can be turned into useful work from the power socket. Reactive power is generally an undersireable side effect. However, significant amounts of reactive power can flow through the grid, especially in three-phase grids such as we often have in Europe where the power between phases can be very unbalanced. This

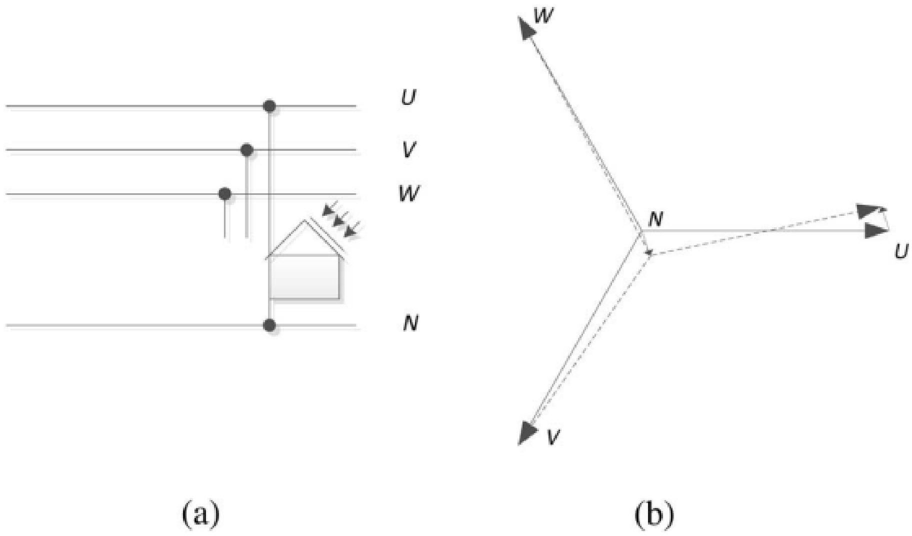

Fig. 2.4: Neutral-point shifting due to the absorption of reactive power in phase U: (a) PV inverter connected to phase U and (b) phase voltages before and after absorption of reactive power in phase U [17].

reactive power can undesirably load the grid and prevent more active power from being put into it. Thus, we look into reactive power control and phase balancing, as they can increase active power delivery.

In our three-phase grid, local generators such as PV inverters and consumers such as heat pumps are often connected to the grid on one phase only. These loads are rarely distributed evenly over the phases. Degroote et al. [16] showed that in an unbalanced three-phase four-wire grid, a neutral-point shifting effect occurs when single phase loads or inverters are connected that consume or inject significant amounts of active power. The uneven distribution of these single phase loads over the three phases causes a return current to flow through the neutral conductor, which introduces reactive power flow. The reactive power flow undesirably causes voltage swings and an increase of the apparent power in the grid, resulting in a loss of active power capacity. By controlling the reactive power in the other phases, the current through the neutral conductor can be decreased. This decrease of reactive power allows for an increase of active power without an increase in apparent power. The phase unbalance problem is depicted in Fig. 2.4. When a PV inverter absorps reactive power in phase U, the phase voltage of phase W increases while the voltage of phase V decreases [17]. Such unbalance effects make a grid significantly more vulnerable to overvoltage effects [18], and also result in higher currents, which cause overloading.

In [17], Weckx et al. found that by controlling the active and reactive power flow of PV inverters, less active power had to be curtailed and reactive power use was near-optimal compared to their base case of no control. Other examples of the use of reactive power control and phase balancing to increase active power delivery have been investigated. Paudyal et al. [19] show that when EVs charge in the fourth quadrant, i.e. injecting reactive power while charging, the time required to fully charge them can be significantly reduced. In their example, they are considering EVs charging with dynamic energy prices. In such a situation, it is beneficial to charge when prices are lowest, but since the hours of low prices are the same for all connected EVs, the charging power at low energy prices that is allowed by the EMS is limited. In their example, the reactive power injection allows the EVs to charge at higher active power at times of cheap electricity, reducing the price payed by customers to fully charge their vehicle. Simultaneously, the time it takes to fully charge the EVs is also decreased since more active power can be delivered to them in the same time frame.

Reactive power control and phase balancing can lead to an increase in capacity for active power. Going back to our objectives of minimizing excessive power draw at a transformer level while minimizing energy delivery curtailed, we see that reactive power control and phase balancing can lead to an increase of energy delivery without adding excessive power draw. Thus, when possible, these strategies should be considered for use in an EMS backup system.

2.3 Power Control Strategies

An EMS backup system must control the power use of a set of devices. In this section, we investigate what power control strategies have been proposed in literature, that could also be applied to EMS backup systems. We start with looking at power control strategies for inverters in Subsection 2.3.1, which are designed to increase grid stability by mimicking the behavior of the inertia in traditional generators.

We also look at other fields to find inspiration for control strategies that may apply to EMS backup systems. In Subsection 2.3.2 we consider protocols that are widely used in the Internet to deal with congestion, and in Subsection 2.3.3 we look into the field of control engineering.

2.3.1 Droop Control

To maintain the frequency and stability of the grid, mankind used to rely on fossil-powered AC power generation plants. These plants have an inherent inertia that stabilizes the grid in the event of sudden power surges or drops. However, modern and especially renewable energy sources (RES) usually generate DC power, which is converted to AC by inverters before being supplied to the grid. These inverters do not have the inertia characteristic of conventional power plants. Therefore, coordination of these RES is essential to mimic the stabilizing behavior of conventional power plants in renewable energy generators, which is required to meet the increasing demand for electricity [20].

The droop characteristics of conventional power plants can be mimicked using locally measured indicators of the current stability status of the grid, such as voltage or frequency. As an example, when the voltage drops below a pre-defined limit in a flexible RES power plant, the output power is increased, to rectify the voltage level. When the voltage increases, the reverse happens and the output power is decreased. Similar algorithms apply to other grid status indicators. Voltage and frequency droop control are both considered well-established methods [21], [22].

The aim of an EMS backup solution is to decrease demand when the power in a grid exceeds transformer limits. However, controlling demand has similarities to controlling generation. Droop control algorithms can thus be modified to be used as an EMS backup solution that controls demand side consumption instead of generator side production. Marinelli et al. showed that droop control algorithms can be used to steer EV charging based on grid status measurements at a centralized location [23]. They validated their results in field tests with three Nissan Leafs, where they implemented droop control using power, voltage and current measurements [24], [25].

During the practical tests, the authors encountered some practical considerations which should be kept in mind when designing an EMS backup system. The authors found that the EVs had varying reaction times; within a range of 1 to 5 seconds depending on their production year. The newer vehicles in their test were quicker to respond as visible in the bottom plot in Fig. 2.5, while the top plot in Fig. 2.5 shows that the older EV used in the test has a slower response time of up to 5 seconds [25]. Additionally, while the control signals in Fig. 2.5 should be an upper limit to the allowed charging current, it is of note that the EV in the upper plot in the figure charges at a rate 1 A higher than the control signal allows. The authors suspect this was caused by a charger firmware update.

Another interesting result from the field tests was that the EVs only have a limited set of charging powers they can use. In this example, the charger current could be modulated between 6 and $16\ \mathrm{A}$ with steps of $1\ \mathrm{A}$. Hence, a discrete version of droop control instead of a continuous version was implemented.

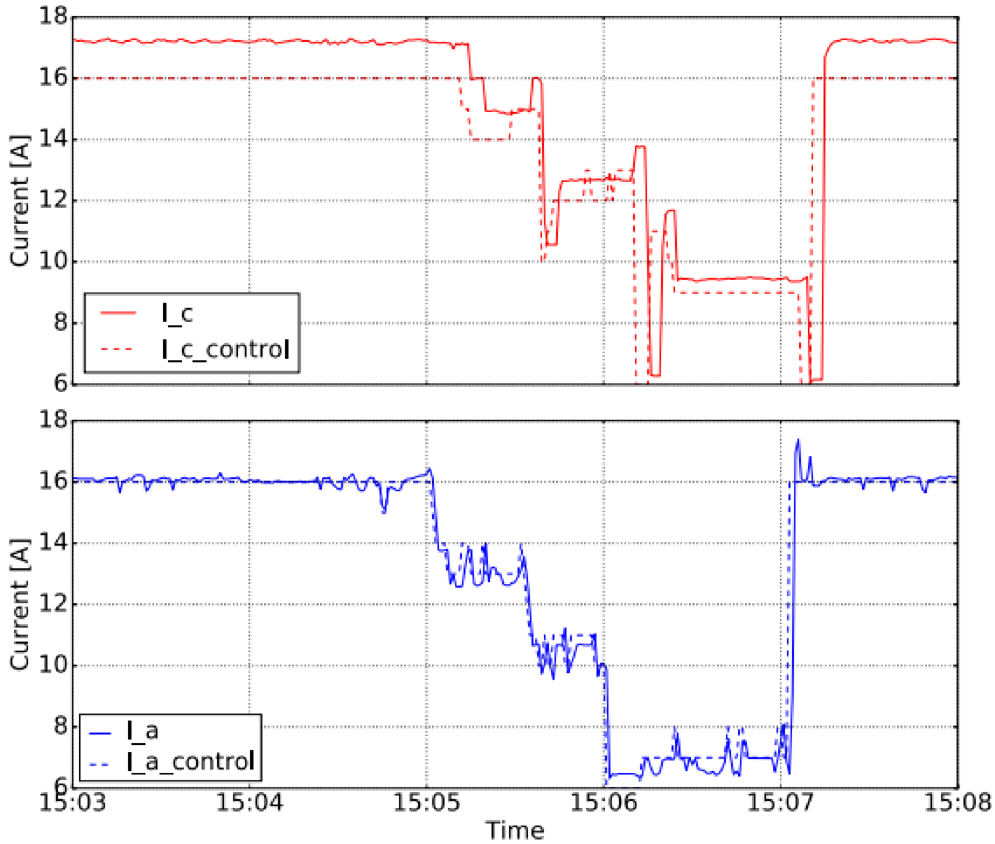

Fig. 2.5: Charging current control signal and measured resulting current for EV smart charging–test in [25].

The field tests from [23]–[25] show that droop control can be used to keep the consumption of EVs within grid limits, where without the control the maximum grid limits would have been exceeded. This makes it a viable solution for EMS backup solutions which should be considered during development of a control algorithm.

2.3.2 Internet Transmission Control Protocol (TCP)

This subsection introduces congestion management concepts that are used in the transmission control protocol (TCP), a well known and exhaustively researched field describing Internet protocols. The aim of TCP implementations is to achieve fair usage of limited bandwidth among multiple distributed agents by minimizing network congestion while maximizing network throughput [26]. Considering that congestion in the Internet can be considered analogous to grid violations in the power grid and network throughput can be considered analogous to energy delivered in a power grid context, a study of how congestion problems are solved in the Internet can provide valuable solutions for energy management backup systems. In this subsection, we first discuss early TCP implementations, after which we investigate recent advancements which improve TCP performance further. We aim to find how these implementations can apply to the power grid.

To determine what transmission rate a sender can use on a network, TCP implementations use a congestion window $cwnd$. This congestion window determines what the maximum sending rate for the transmitter is. Ideally, TCP implementations aim to keep the value of $cwnd$ as large as possible to maximize usage of the available bandwidth, but without transmitting too much since that would cause congestion.

Additive Increase, Multiplicative Decrease (AIMD)

The original implementation of TCP used an additive increase, multiplicative decrease (AIMD) algorithm. The potential of the use in power grids of AIMD has been studied in recent years for various situations, including frequency control for grid stabilization [27], control strategies for PV microgenerators [28], and EV charging policies [29].

The AIMD algorithm is divided into two phases: an additive increase and a multiplicative decrease phase. When a collision is detected, where a packet is not acknowledged which indicates network congestion, the AIMD algorithm enters the decrease phase. During the decrease phase, the algorithm decreases $cwnd$ exponentially by multiplying it by a factor $\beta < 1$, until operation continues within the network limits again. Then, a new increase phase commences. A plot of $cwnd$ displays a sawtooth like behavior over time, going down rapidly while going up slowly in loops. During stable network conditions, AIMD implementations thus hover around the optimal sending rate, while the rapid decrease phase also makes AIMD robust to changes in network conditions. Chiu et al. [30] showed intuitively how multiple distributed agents running AIMD algorithms will ultimately converge to a fair distribution of the available bandwidth in Fig. 2.6. In this figure, we see that when User 2 initially was assigned significantly more bandwidth than User 1, AIMD will naturally transition to a state where the bandwidth is distributed equally between the two users. This is because the rate of User 2 goes down faster than that of User 1. AIMD converges to a point which is both fair and maximizes the use of available bandwidth. The use of AIMD in TCP was first widely adapted in *TCP New Reno*, which was first officially introduced in RFC2001 in 1997 [31]. Modern TCP implementations are still based on this algorithm. The widespread use of AIMD in TCP congestion protocols makes it one of the best examples of a distributed control system [32].

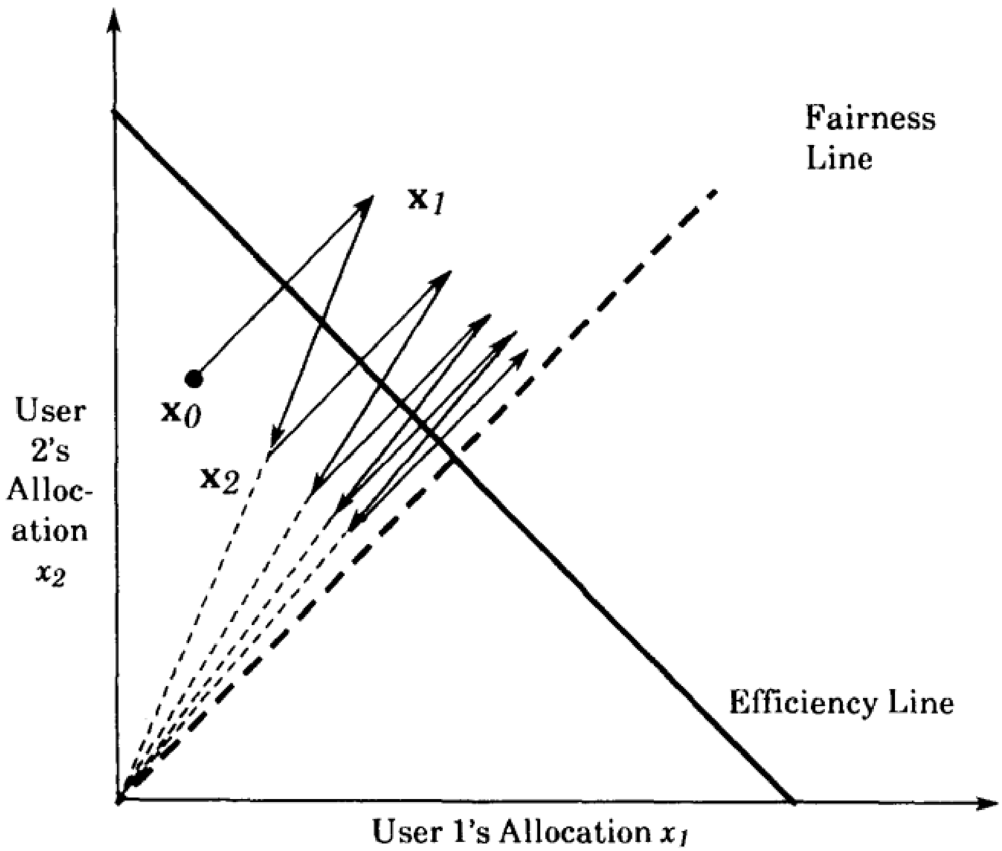

Fig. 2.6: visualisation by Chiu et al. of how an AIMD implementation converges to the optimal point [30].

TCP Advancements

To improve upon the performance of early TCP implementations like TCP New Reno, many new implementations have been suggested over the years to increase performance, including TCP Vegas, TCP Cubic, C-TCP, TCP BRR, and TCP Elastic [33]. While all of these differ from New Reno in some ways, all are still based on an AIMD algorithm. For the sake of brevity, we will not discuss and compare all existing TCP implementations, but we will focus on two implementations in detail instead: TCP Vegas and TCP Elastic.

TCP Vegas tries to improve on TCP New Reno by making estimations on how "congested" the network is, using round trip time (RTT) measurements. This allows it to predict congestion and thus prevent congestion from occurring in the first place, instead of reacting to it like TCP New Reno does. Such a heuristic allows TCP Vegas to achieve 40% to 70% better throughput with one-fifth to one-half of the losses compared to TCP Reno [34].

TCP Vegas has an increase phase that initially is similar to AIMD. However, it aims to stop congestion before it occurs by making an estimate of the congestion in the network based on a base RTT, RTT_{base}. The value of RTT_{base} is set to the minimum of all measured RTTs, which commonly is the first segment sent by the connection [35]. Assuming no congestion will occur, the expected throughput is determined through (2.1).

$$Throughput_{\text{Expected}} = \frac{cwnd}{RTT_{base}} \tag{2.1}$$

However, when the network begins to fill, the expected throughput may be higher than the actual throughput of the data that is transmitted. The actual throughput is determined using (2.2).

$$Throughput_{\text{Actual}} = \frac{cwnd}{RTT} \tag{2.2}$$

The congestion window is adjusted based on the difference between the expected and actual throughput. Because the RTT will go up before congestion occurs due to buffers in the network, adjusting the window based on the RTT allows TCP Vegas to stop increasing $cwnd$ before congestion occurs. To determine when the algorithm should stop increasing $cwnd$, two thresholds a and b are defined, where $a < b$. When the difference between the expected and actual throughput is smaller than a, no congestion occurs and TCP Vegas increases $cwnd$ linearly during the next RTT. A sign of noticeable congestion in the network is observed when the difference is larger than b, to which TCP Vegas reacts by decreasing $cwnd$ during the next RTT. To prevent oscillations, a deadband is implemented when the difference is larger than a but smaller than b, where $cwnd$ is left unchanged. Traditionally, TCP Vegas implementations use $a = 1$, $b = 3$, which means that each Vegas flow tries to keep at least one packet, but no more than three packets queued in the network [36]. However, it has been shown that increasing the value of these parameters can improve the performance of TCP Vegas in certain situations [36], [37].

Where standard AIMD implementations go back and forth around the optimal transmission rate, an ideal implementation of TCP Vegas stays just below the optimal transmission rate continuously, allowing it to operate closer to the limit for longer periods of time. However, TCP Vegas has not widely been implemented in the Internet because it is too cautious when co-existing with other TCP implementations such as TCP New Reno, which more aggressively claim bandwidth. A TCP Vegas implementation co-existing with a TCP New Reno implementation will reduce its sending rate before the TCP New Reno implementation does, causing it to unfairly give up too much bandwidth [38]. In such situations, increasing the values of a and b above the standard values of $a = 1$ and $b = 3$ can improve the performance of TCP Vegas, but it will not perform as well as when TCP Vegas is operating standalone [36]. A TCP Vegas based implementation of an energy management backup system that is standalone and thus will not have to co-exist with other congestion protocols, could outperform an implementation based on standard AIMD.

While TCP Vegas was not widely implemented in the Internet, its strategy of predicting congestion and acting before it occurs remained a topic of interest in TCP research. In 2019, Alrshah et al. [33] introduced TCP Elastic, which also uses RTT measurements to predict how congested the network is, and thus how quickly it can increase its throughput. TCP Elastic outperforms the current standard implementations of TCP on Windows and Linux. It also outperforms newer TCP algorithms such as TCP BRR introduced by Google in 2016 [39], achieving 14% to 81% higher throughput than these other implementations.

TCP Elastic uses a utilization rate $UR = \frac{RTT_{current}}{RTT_{max}}$ to keep track of how congested the network is, where $RTT_{current}$ is the current RTT and RTT_{max} is the maximum RTT measured since the connection was established. TCP Elastic estimates the maximum possible congestion window $cwnd_{est}$, i.e. the maximum transmission rate before congestion occurs, based on this UR through (2.3).

$$cwnd_{est} = \frac{cwnd_{current}}{UR} \tag{2.3}$$

TCP Elastic uses this estimate of the maximum congestion window to introduce a novel window-correlated weighting function WWF through (2.4).

$$WWF = \sqrt{cwnd_{est}} \tag{2.4}$$

The $cwnd$ of TCP Elastic is finally updated using this WWF through (2.5).

$$cwnd_{new} = cwnd_{current} + \frac{WWF}{cwnd_{current}} \tag{2.5}$$

Using this WWF allows TCP Elastic to go through the first stage of the increase phase significantly faster than other AIMD algorithms, but without noticeable overshoot at the final stages of the increase phase. This is what allows it to perform better than other algorithms. The improvements made by the WWF of TCP Elastic for Internet applications could be translated to improvements for a TCP based energy management backup system.

2.3.3 PID Control

The goal of the energy management backup system we require is in essence to control a system to stay within certain bounds, i.e. to prevent a set of electrical loads from exceeding the power limits of a transformer. To control a system to stay within bounds, a general purpose control strategy such as a PID based controller [40] can be applied. Introduced over 90 years ago, PID controllers still have a dominant role in engineering control systems, with over 95% of process control loops being still being designed based on PID controllers [41]. PID control has been introduced into power grid solutions for PV inverters [42] and grid load variance reduction through EV charging [43]. Thus, it can also be considered for application to our problem.

In general, a PID controller steers a signal to a given setpoint $r(t_\mathrm{k})$, which in our case could be the maximum allowable power at a transformer. The general formula for a discrete time PID based controller as mentioned in [44] is given in (2.6). In this equation, K_p, K_i and K_d are parameters whose values can be tuned to change the proportional, integral, and derivative terms of the controller. The $e(t_\mathrm{k})$ term in (2.6) is a measure of the observed error between the measured plant output $y(t_\mathrm{k})$ and the reference point $r(t_\mathrm{k})$, i.e. $e(t_\mathrm{k}) = r(t_\mathrm{k}) - y(t_\mathrm{k})$. The controller output $u(t_\mathrm{k})$ is used as input for the plant to steer its output to the desired setpoint $r(t_\mathrm{k})$.

$$u(t_\mathrm{k}) = K_\mathrm{p} e(t_\mathrm{k}) + K_\mathrm{i} \sum_{\mathrm{j}=1}^{\mathrm{k}} e(t_\mathrm{j}) \Delta t + K_\mathrm{d} \frac{e(t_\mathrm{k}) - e(t_{\mathrm{k}-1})}{\Delta t} \tag{2.6}$$

Despite having been introduced over 90 years ago, no heuristic has been found to optimally tune a PID controller. It is said that PID controllers are still poorly understood and tuned in a many applications [45]. Still, the widespread application of PID control shows that it can provide a reliable control mechanism. The International

Federation of Automatic Control (IFAC) committee even states "*we still have nothing compared to PID*" [46]. A PID controller implementation can thus be of interest for our energy management backup system.

2.3.4 Summary

To implement an EV charging control emergency fallback mechanism, a congestion control algorithm is required. Such an algorithm could be developed on the principles of droop control, presented in Section 2.3.1. The AIMD algorithm presented in Section 2.3.2 and the improvements made over it for implementation in the Internet congestion protocol suite TCP also provide an idea upon which an EV charging control emergency fallback mechanism could be based. Another option from literature is to base the mechanism on principles of PID control, presented in Section 2.3.3. The implementation of algorithms based on the findings in this chapter is presented in Chapter 4.

3 Model

Chapter Objective: This chapter describes how the GridShield system discussed throughout this thesis is modeled.

Chapter Contents

3.1 Introduction

Grids in the Netherlands are designed based on a rule of thumb that a peak capacity $P^{\text{max}}_{\text{household}}$ of 2.6 kW per household should be accounted for [47, Chapter 13]. Since simultaneity between household peaks is traditionally low, a simultaneity factor f of 0.46 is used for a neighborhood of 100 households. As a consequence, a grid for a 100 household neighborhood is designed for a peak demand of $100\ P^{\text{max}}_{\text{household}}\ f \approx 120$ kWh, even when individual peaks of a household can well exceed 2.6 kW. However, there is an emergence of high power electrical appliances on the demand side of the grid, which require large amounts of power and have a high simultaneity due to their prolonged periods of high power demand. As a result, the conventional wisdom that 2.6 kWh of capacity per household is enough and that only a low simultaneity factor must be accounted for, no longer applies. Energy Management Systems are being introduced to deal with this, but their rollout is slow and they can fail. Hence, we need a backup solution that can limit demand when everything else fails to do so, to prevent grid overloading and damage. To counteract a failing EMS, such a solution should be completely separated from the EMS. While an EMS can use *the Internet* for communication, a backup solution requires a *standalone separate communication network*. This chapter describes how our model of such a solution, called *GridShield*, can be set up.

3.2 Setup

To understand the implementation of the various GridShield control algorithms in this report, we must first understand the setup and topology of a GridShield system. Such a system can work with any type of controllable appliance, but in this work we focus on EVs. Multiple variations on this setup exist, with different numbers of EVs in different toplogies, but the main characteristics of the model always remain the same. We have a central point of connection, e.g. a transformer, which has a GridShield sender module that sends out a message when it measures congestion at the transformer. This message is received by GridShield receiver modules at flexible devices, e.g. electric vehicle supply equipment (EVSE), that use the received message to limit the power consumption they allow if that is required to protect the grid from grid limit violations. In this work, we focus on EVSEs, but note that GridShield could be adapted to also work with other device types, e.g. heat pumps.

The GridShield system is schematically layed out in Fig. 3.1, where the transformer with its GridShield sender module on the left and the EV chargers with their GridShield receiver modules on the right. In Section 3.3, we describe how the transformer GridShield module behaves and what signals it can send, and in Section 3.4 we describe the behavior of the GridShield receiver modules at the EV charging stations upon receiving a message from the GridShield sender module at the transformer. Together, these two modules form the foundation upon which the GridShield system is built. In Section 3.5, we describe how these modules communicate with each other. To deal with larger networks of more than one connection point, we also describe how a multi-layer version of this GridShield system is set up in Section 3.5.

We use the following terminology in this thesis. A congestion event is detected, when the power $P_{\text{trafo}}(t)$ of any of the three phases at the transformer exceeds its power limit: $P_{\text{trafo}}(t) > P_{\text{trafo}}^{\max}$. Furthermore, for every time interval t, a charging station chooses the minimum value of the desired charging power determined by the EMS $P_{\text{EV}}^{\text{desired}}(t)$, the maximum allowed charging power $P_{\text{EV}}^{\max}$, and the charging power determined by GridShield (GS) $P_{\text{EV}}^{\text{GS}}(t)$: $P_{\text{EV}}(t) = \min\left(P_{\text{EV}}^{\text{desired}}(t), P_{\text{EV}}^{\max}, P_{\text{EV}}^{\text{GS}}(t)\right)$.

In this chapter, we focus on *power* based GridShield systems, which measure power and steer charging power. In these models, the EVSEs are modeled as a constant

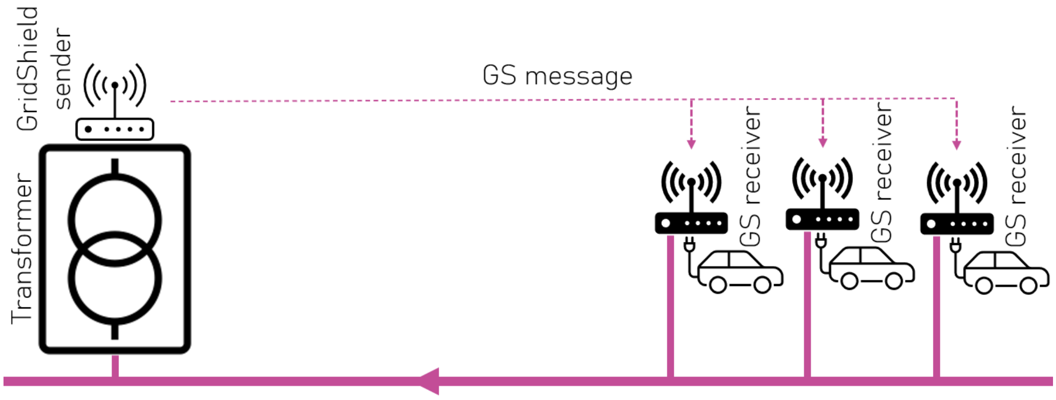

Fig. 3.1: Schematic overview of basic GridShield (GS) implementation.

power load. For a *current* based implementation we only have to exchange the power P with the current I in the formulations. When we use current based control, the EVSEs become constant *current* loads, and thus the resulting power from current based control varies with fluctuations in local voltage, which non-linearly depends on factors such as local generation and consumption. However, the basic principle of operation of the described systems remains the same.

The inverters used in EV charging consume or produce reactive power as detailed in Chapter 2. Control over this reactive power could be used to decrease the charging grid load, but due to technical gaps reactive power control is not supported by EVs and thus we do not consider it further in this work.

3.3 GridShield Sender

All power flows in a local grid go through a central connection point, e.g. a transformer, that exchanges energy with the main grid. This makes the central connection point susceptible to overloading: when many loads that are connected to it simultaneously draw a significant amount of power, the individual connections may not necessarily get overloaded, but the central connection point may be. An EMS must prevent such a scenario from occurring. A transformer is usually connected to its loads through three phases. Each phase of the transformer has a power limit. When the transformer power exceeds this limit on one of the phases, grid overloading and damage may occur. An EMS should prevent the power on every phase from exceeding this limit.

In a GridShield system, the transformer has a GridShield sender module which can transmit a signal to the GridShield receiver modules further described in Section 3.4.

This GridShield sender module measures the power of each phase of the transformer. When an overload on one of the phases is measured, the GridShield sender module transmits a signal. The contents of this signal depend on the chosen GridShield algorithm. These algorithms are discussed in Chapter 4. The GridShield sender module gets no direct response from the GridShield receiver modules. The only available feedback after transmitting a message, is the power of every phase that should have changed due to the GridShield signal. Note that while the GridShield message should change the power measured on the phases, the power also depends on other factors such as a change in baseload.

3.4 GridShield Receiver

In this work, we use GridShield to limit the charging power of EVs when that is required to prevent grid overloading. EVSE devices supplying power to EVs can have a high grid load, up to the load of 10 households [48]. The power demand profile of EVs is variable, and depends on multiple factors such as:

- the properties of a specific EV model, which e.g. dictate how many phases it supports, and the maximum power $\hat{P}_{\mathrm{EV}}^{\max}$ this EV can draw per phase.
- User behavior, which dictates when an EV starts and stops charging.
- User behavior also determines how much energy an EV will require during a charging session (when an EV covers more distance, its state of charge (SoC) will be reduced further, increasing its energy demand)
- EV settings can be changed to for instance limit the maximum charging power of the EV below its manufacturer limit, as a means of prolonging battery life.

The final charging power of an EV $P_{\mathrm{EV}}(t)$ depends on these factors. However, properties of the EVSE unit that an EV is connected to must also be taken into account. An EVSE has a maximum charging power per phase $\hat{P}_{\mathrm{EVSE}}^{\max}$, which could be less than the maximum charging power of the EV that is connected to it. The maximum charging power $P_{\mathrm{EV}}^{\max}$ an EV can charge with at an EVSE within the limits of the available hardware is thus defined by (3.1).

$$P_{\mathrm{EV}}^{\max} = \min\left(\hat{P}_{\mathrm{EV}}^{\max}, \hat{P}_{\mathrm{EVSE}}^{\max}\right) \tag{3.1}$$

Besides the hardware limit of the maximum possible charging power in (3.1), an EMS may send a control signal to an EVSE unit to limit its maximum *allowed* charging power $P^{\max}_{\mathrm{EVSE}}(t) \leq \hat{P}^{\max}_{\mathrm{EVSE}}$, such that the EV charges at the power level desired by the EMS, i.e. $P^{\max}_{\mathrm{EVSE}}(t) = P^{\mathrm{desired}}_{\mathrm{EV}}(t)$. When $P^{\mathrm{desired}}_{\mathrm{EV}}(t) \leq P^{\max}_{\mathrm{EV}}$, the charging power of the EV is limited to $P^{\mathrm{desired}}_{\mathrm{EV}}(t)$.

In our GridShield system, a GridShield receiver module is connected to the EVSE to receive and apply commands sent by the GridShield sender module. The GridShield receiver module can control the allowed power through the maximum power allowed by GridShield $P^{\mathrm{GS}}_{\mathrm{EV}}(t) \leq \hat{P}^{\max}_{\mathrm{EVSE}}$, which is a separate limit from $P^{\mathrm{desired}}_{\mathrm{EV}}(t)$. The final charging power of an EV $P_{\mathrm{EV}}(t)$ is always decided through (3.2), which chooses the lowest of the described limits.

$$P_{\mathrm{EV}}(t) = \min\left(\hat{P}^{\mathrm{desired}}_{\mathrm{EV}}(t), P^{\max}_{\mathrm{EV}}, P^{\mathrm{GS}}_{\mathrm{EV}}(t)\right) \tag{3.2}$$

Note that due to technical gaps, most EVSE units (and hence their GridShield Receiver modules) have no information on the charging power of the EV that is connected, and thus cannot directly decrease it. They only know the maximum charging power $\hat{P}^{\max}_{\mathrm{EVSE}}$ they can allow. Hence, upon receiving a GridShield signal, the maximum *allowed* charging power in the EVSE is changed by the GridShield receiver module. Since $P_{\mathrm{EV}}(t) \leq P^{\mathrm{GS}}_{\mathrm{EV}}(t)$, this method will always decrease $P_{\mathrm{EV}}(t)$ eventually, but it will not necessarily decrease $P_{\mathrm{EV}}(t)$ directly. As a result, it may take multiple GridShield control iterations before an effect in $P_{\mathrm{EV}}(t)$ is measured, due to the possibility that $P^{\mathrm{desired}}_{\mathrm{EV}} < P^{\max}_{\mathrm{EV}}$, or $\hat{P}^{\max}_{\mathrm{EV}} < \hat{P}^{\max}_{\mathrm{EVSE}}$.

In short, in our model, the power that an EV charges with at an EVSE unit depends on:

- The properties of the EV and the EVSE unit $P^{\max}_{\mathrm{EV}}$.
- The EMS control signals sent to the EVSE unit $P^{\mathrm{desired}}_{\mathrm{EV}}(t)$.
- The charging power limit imposed by GridShield $P^{\mathrm{GS}}_{\mathrm{EV}}(t)$.

All of these elements can dictate the maximum charging power. The element that dictates the lowest charging power is always the charging power that is finally chosen.

3.5 Communication Network Architecture

Since the safe and reliable operation of the grid depends on GridShield, the communication between the GridShield sender and receiver modules is mission-critical and must therefore be very robust. To this end, GridShield uses a stand-alone network for communication between the sender and receiver modules. Before discussing what algorithms could be used to implement GridShield, we first discuss the architecture of this network. The GridShield sender module sends messages to the GridShield receiver modules, which use the information in the message to change the charging power of the EVs. We consider two possible approaches to the setup of this network:

- Centralized: The GridShield *sender* runs a power control algorithm and sends the result to the GridShield receivers. They adjust the EV charger maximum power accordingly.
- Decentralized: The GridShield *receivers* run the power control algorithm; the sender only informs the chargers that congestion occurs or does not occur.

Both architectures use the topology of Fig. 3.1. The difference between the two approaches lies in the content of the message that the GridShield sender transmits. A fully centralized approach may require more messages and thus requires a higher bandwidth. On the other hand, it introduces less computational overhead since most of the computations happen at the transformer side of the system. Finally, it makes updating the system easier; changes to the implementation only need to be implemented on the transformer side, not on the receiver side. A fully centralized approach may also allow for more fine-grained control, since the actual state of the grid is known to the GridShield module running the control algorithm. In a fully decentralized system, the only available information is whether or not there is congestion. In future standards, the technical gaps described in Section 3.4 may be overcome and more specific information about the EV may become available to an EVSE unit and thus to the GridShield sender module. As the available information increases, a (partially) decentralized approach becomes more interesting. The centralized and decentralized approach are further explained in Subsection 3.5.1 and Subsection 3.5.2 respectively. Finally, we discuss how a multi-layer GridShield architecture could be set up for when a major central connection point has multiple minor connection points connected to it, all with their own GridShield sender modules.

3.5.1 Centralized Approach

The centralized GridShield architecture is schematically presented in Fig. 3.2a. In the event of a congestion problem, a message is sent from the GridShield sender module at the transformer to the GridShield receiver modules at the EVSEs. In the centralized approach, this message ϕ is always a factor by which the EV chargers must reduce their power, i.e. $0 \leq \phi \leq 1$. When $\phi = 1$, no congestion occurs and GridShield does not intervene. When $\phi = 0$, all EVs have to completely stop charging. Any factor in between is a factor by which the maximum charging power of the EVSE units must be reduced. In summary, upon receiving the message, the maximum allowed charging power of the EVSEs is determined by (3.3).

$$P_{\mathrm{EV}}^{\mathrm{GS}} = \phi(t) \cdot P_{\mathrm{EV}}^{\max} \tag{3.3}$$

Thus, the only logic that happens at the receiver side is multiplying the maximum charging power by this factor ϕ.

3.5.2 Decentralized Approach

The decentralized GridShield architecture is schematically presented in Fig. 3.2b. Compared to the centralized architecture of Fig. 3.2a, the processing happens locally at the chargers, while the message ϕ is simpler. We only send a message from the GridShield sender to the GridShield receivers indicating that congestion occurs. In our example of EV charging in Fig. 3.2b, the GridShield message could have three possible states:

- -1, indicating too much power is being injected in the grid and consumption must be increased/V2G delivery reduced.
- 0, indicating the grid is operating within limits.
- 1, indicating too much power is being drawn from the grid and consumption must be decreased/V2G delivery increased.

The GridShield receivers adjust the power of the EV chargers based on what algorithm they apply locally. An advantage of this approach is that more local data can be used in the decision making at the receivers, especially in the future when new charging protocols emerge.

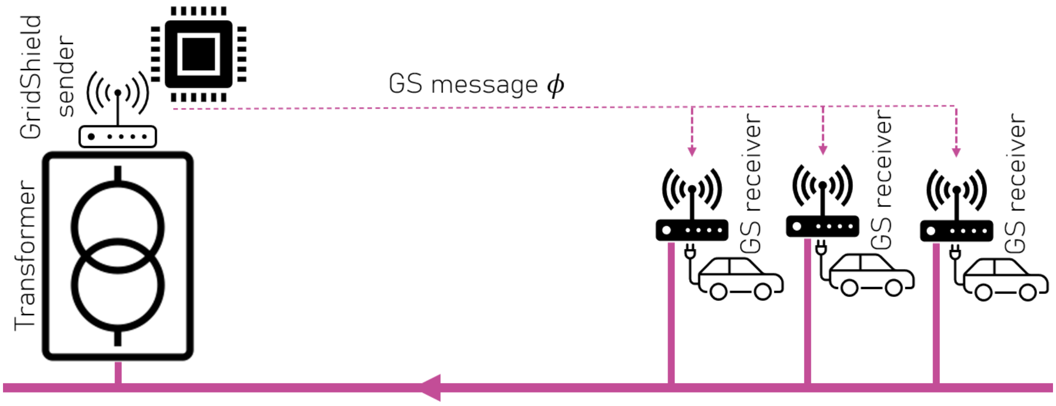

(a) Centralized GridShield Architecture.

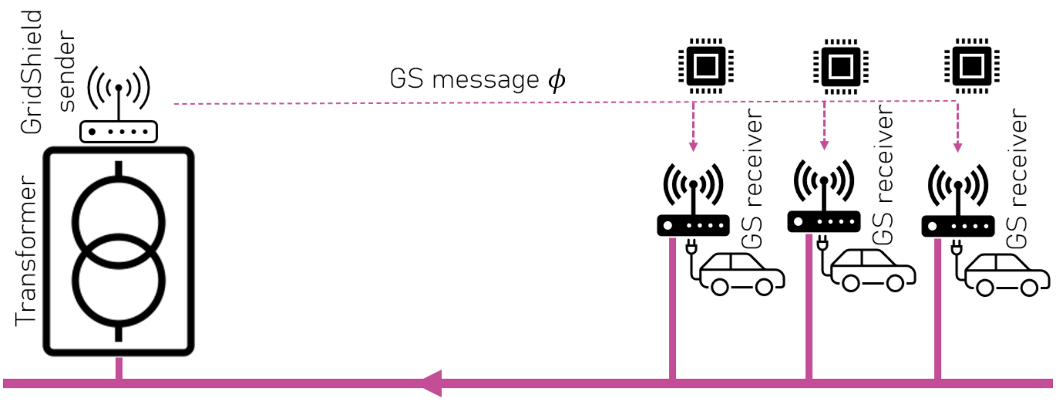

(b) Decentralized GridShield Architecture.

Fig. 3.2: Two possible GridShield architectures.

3.5.3 Multi-layer GridShield

In a single layer GridShield module, the GridShield sender module only transmits data and the GridShield receiver module only receives it. When we have a major central connection point with multiple minor connection points connected to it however, it may be desirable to have a multi-layer GridShield setup. That way, when only one of the minor connection points is overloaded, the power reduction by GridShield can be limited to that minor section of the grid. On the other hand, when all minor connection points individually are within bounds, but the major central connection point is over the limit, the power at all connection points should be reduced equally.

To create a multi-layer GridShield system, no changes need to be made to the message ϕ. Since ϕ is already a factor applied to the charging power, it can be multiplied with a factor from a higher level GridShield module in (3.4). In this equation, ϕ^*_{child} is the locally generated message of a lower level child GridShield sender, ϕ_{parent} is the message of a higher level parent GridShield sender module, and ϕ_{child} is the final message of the child.

$$\phi_{\text{child}} = \phi^*_{\text{child}}\phi_{\text{parent}} \tag{3.4}$$

3.5.4 EV Discrete Charging Powers

EVs are often only able to charge at a few given charging powers. For example, Martinenas et al. [25] found that each test vehicle of their set of three Nissan Leafs only supported charging rates from 6 A to 16 A with steps of 1 A. This has significant implications for control algorithms; it becomes impossible to send a factor that is always exactly applied to the maximum charging power. Instead, the charging power of the EV will be rounded to the nearest actual available charging power in the set of discrete charging powers. Since this has implications for the effect of the control signal, it must be integrated into the model.

Due to the limited set of available charging powers, the granularity of the EV power control is limited. This problem can be partially overcome by choosing the power level based on the desired (unobtainable) power. When the desired power $P_{desired}$ is not at at one of the available discrete power levels but in between the available levels P_{lower} and P_{higher}, i.e. $P_{lower} < P_{desired} < P_{higher}$, we may use a randomization algorithm to achieve that the average charging power of all EVs approximates the desired power $P_{desired}$ better with an increasing number of

EVs. When $P_{lower} << P_{desired} < P_{higher}$, we have to use a high probability of selecting P_{higher}, whereas when $P_{lower} < P_{desired} << P_{higher}$, we have to use a high probability of selecting P_{lower}. To do this, we apply the following power selection algorithm. We first determine the difference between the available powers levels ΔP in (3.5).

$$\Delta P = P_{higher} - P_{lower} \tag{3.5}$$

Based on this difference, we decide whether to choose P_{higher} or P_{lower}. Let A be the the event that we choose P_{higher}. Then the probability $\mathrm{P}(A)$ is given by (3.6).

$$\mathrm{P}(A) = \frac{P_{higher} - P_{desired}}{\Delta P} \tag{3.6}$$

Now, each EV decides whether to choose P_{higher} based on this probability of A, and in case an EV decides not to choose P_{higher} it chooses P_{lower} as its new charging power.

In this chapter, we presented a structure on which GridShield systems can be implemented. In the next chapter, we present algorithms that can use this GridShield structure to steer EV charging to comply with grid limits.

GridShield Power Control Algorithms

4

Chapter Objective: This chapter describes how the control algorithms that are considered for GridShield are implemented.

Chapter Contents

4.1 Introduction

In Chapter 2, we introduced various algorithms from different fields that may apply to an EMS backup system such as GridShield. In Chapter 3, we introduced how the communication structure of GridShield could be implemented. In this chapter, we discuss how algorithms can be implemented for GridShield using the communication structure of Chapter 3. We assume a GridShield system that has the same topology as the system described in Chapter 3.

We only consider centralized GridShield topologies here, where the algorithms are performed at the GridShield sender module and the GridShield receiver modules only apply a multiplication factor to their maximum charging power that they receive from the GridShield sender module. Changing to a decentralized topology makes the implementations slightly different, but would not change the overall principle of the algorithms described in this chapter.

In all of the centralized GridShield implementations presented in this chapter, the GridShield sender module decreases its maximum charging power multiplier $\phi(t)$ when it detects a congestion problem. This multiplier $\phi(t)$ is then sent to all charging stations, which apply the received message to their maximum charging power allowed by GridShield, i.e. $P_{\text{EV}}^{\text{GS}}(t) = \phi(t)P_{\text{EV}}^{\max}$. We only describe power based control in this chapter, but note that the same methods are interchangeable with current based control as was explained in Chapter 3.

4.2 AIAD

The additive increase, addtive decrease (AIAD) algorithm is the algorithm used in the original GridShield implementation by Kerkhoven [49]. A block diagram of the algorithm is provided in Fig. 4.1. The algorithm is structured into two phases: an increase and a decrease phase. The GridShield charging power of every EV is initialized to the maximum allowed charging power: $P_{\text{EV}}^{\text{GS}}(t) = P_{\text{EV}}^{\max}$. The message $\phi(t)$ is intialized to $\phi(0) = 100\%$.

Upon detection of a congestion event at the transformer, we enter the *additive decrease phase*. In this phase, a controller uses a fixed step size s to decrease the value of the signal $\phi(t)$ in every control interval while the congestion problem lasts: $\phi(t) = \phi(t-1) - s$. This step-wise decrease is repeated until the congestion problem is solved. Once $P_{\text{trafo}}(t)$ does not exceed the power limit anymore, the *additive increase phase* starts where we apply $\phi(t) = \phi(t-1) + s$.

Oscillations between the increase and decrease phase may occur around $P_{\text{trafo}}^{\max}$ if we immediately start the increase phase when we are below the limit. These oscillations are undesirable as they can e.g. cause voltage swings. Hence, we introduce a deadband to prevent them. The power $P_{\text{trafo}}(t)$ is reduced until it is below the transformer power limit, but the increase phase is only entered when the power is below a certain restoration limit ($P_{\text{trafo}}(t) < P_{\text{trafo}}^{\text{rest}}$). Effectively, the algorithm does not change $\phi(t)$ when $P_{\text{trafo}}^{\text{rest}} \leq P_{\text{trafo}}(t) \leq P_{\text{trafo}}^{\max}$. Only when $P_{\text{trafo}}(t) < P_{\text{trafo}}^{\text{rest}}$ the additive increase phase starts, where $\phi(t)$ is gradually increased by the step size s, until $\phi(t) = 100\%$ or $P_{\text{trafo}}(t) \geq P_{\text{trafo}}^{\text{rest}}$.

The performance of the AIAD GridShield algorithm can be tuned using the following parameters:

- The increase/decrease step size s.
- The restoration limit $P_{\text{trafo}}^{\text{rest}}$.

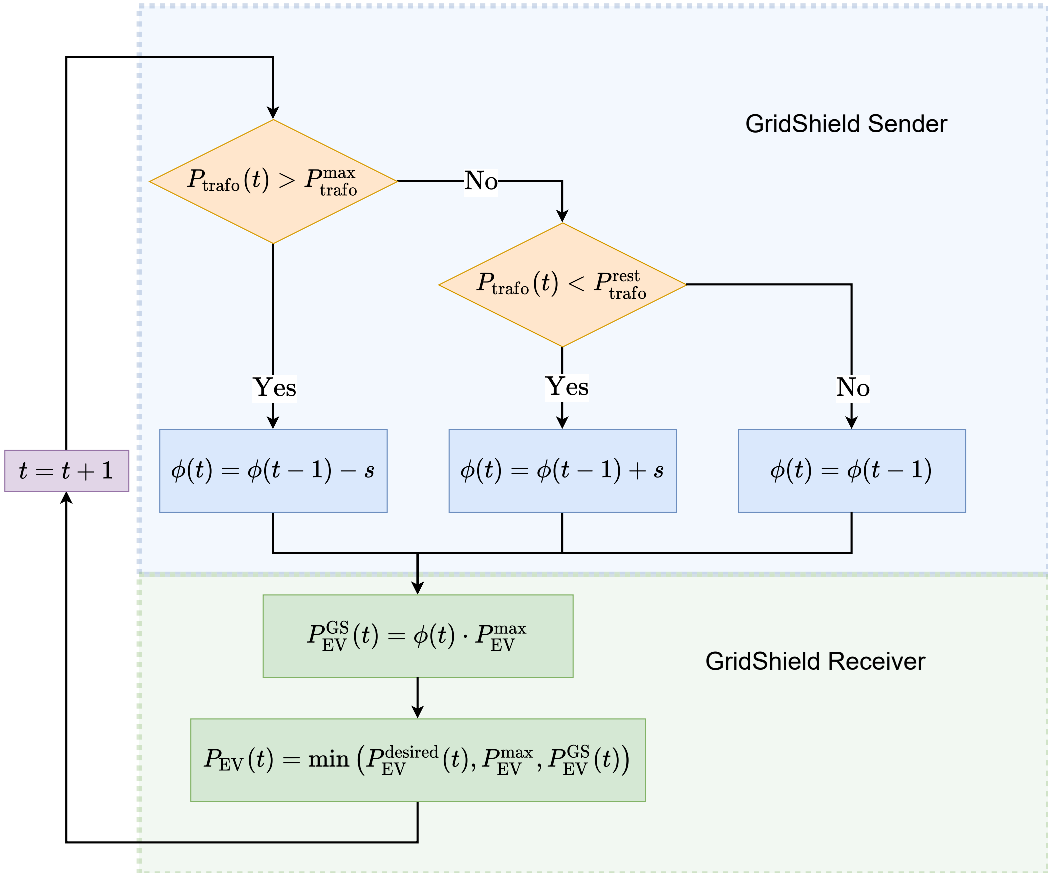

Fig. 4.1: Block diagram of AIAD GridShield algorithm. Blue: sender side implementation. Green: receiver side implementation.

4.3 AIMD

The AIMD algorithm principle was first introduced in the Internet TCP as described in Chapter 2 [26]. Similar to the AIAD approach, the AIMD algorithm consists of two phases. AIMD uses a different decrease phase however, to achieve better performance. A block diagram of the algorithm is provided in Fig. 4.2.

When the GridShield sender module detects a congestion problem, it will decrease its maximum charging power multiplier $\phi(t)$ by a factor β, i.e. $\phi(t) = \beta\phi(t-1)$. This results in an exponential reduction of the charging power. The multiplier $\phi(t)$ is then sent to all charging stations, which reduce their $P_{\text{EV}}^{\text{GS}}(t)$ by the received factor $\phi(t)$. This charging power decrease $P_{\text{EV}}^{\text{GS}}(t) = \phi(t)\ P_{\text{EV}}^{\text{max}}$ is repeated every control iteration until the transformer power limit is not exceeded anymore.

When the congestion problem is resolved, the charging stations enter the additive increase phase, where $\phi(t)$ is increased linearly by an additive constant $\alpha > 0$: $\phi(t) = \phi(t-1) + \alpha$. Similar to the AIAD algorithm, oscillations may occur around $P_{\text{trafo}}^{\text{max}}$, albeit slower since there is a speed difference between the increase and decrease phase. To counteract the oscillations, we deviate from the AIMD implementation of Chapter 2 and incorporate a deadband similar to the deadband in AIAD, where the algorithm does not change $P_{\text{EV}}^{\text{GS}}(t)$ when $P_{\text{trafo}}^{\text{rest}} \leq P_{\text{trafo}}(t) \leq P_{\text{trafo}}^{\text{max}}$. We define a scalable deadband by introducing a parameter γ, where $P_{\text{trafo}}^{\text{rest}} = \gamma P_{\text{trafo}}^{\text{max}}$. Only when $P_{\text{trafo}}(t) < P_{\text{trafo}}^{\text{rest}}$, the additive increase phase is entered. The system resumes normal operation, when $P_{\text{EV}}^{\text{GS}}(t)$ reaches the value of $P_{\text{EV}}^{\text{desired}}(t)$ without causing a new congestion event.

The performance of the AIMD GridShield algorithm can be tuned using the following parameters:

- The increase step size α.
- The decrease factor β.
- The restoration limit factor γ.

4.4 Elastic

The Elastic algorithm for GridShield is based on TCP Elastic which has been further described in Chapter 2 [33]. A block diagram of the algorithm is provided in Fig. 4.3. As can be observed in Fig. 4.3, the decrease phase is the same as the decrease

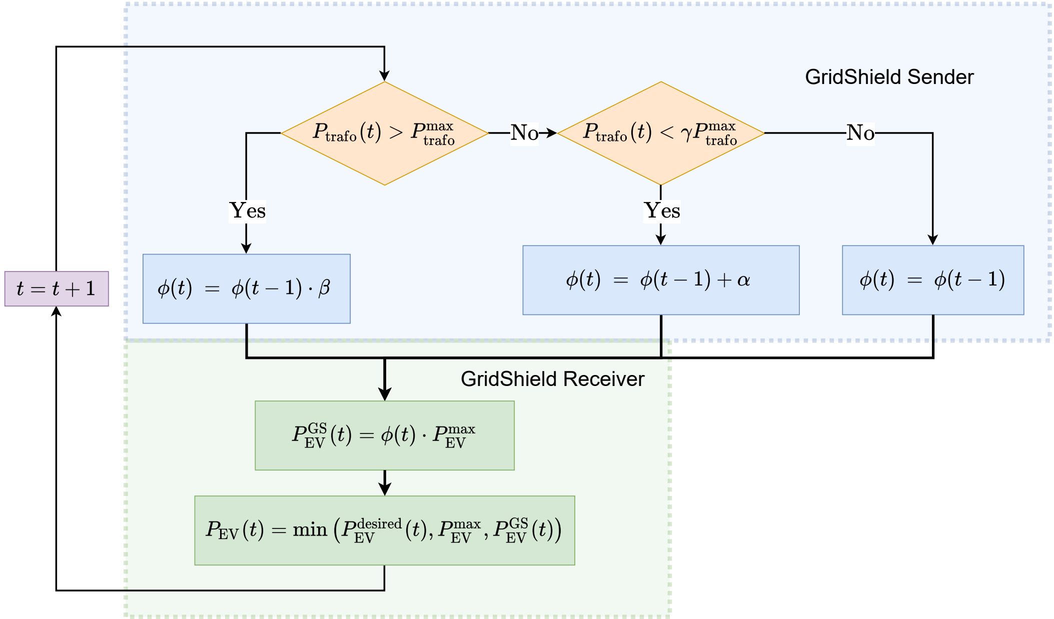

Fig. 4.2: Block diagram of AIMD GridShield algorithm. Blue: sender side implementation. Green: receiver side implementation.

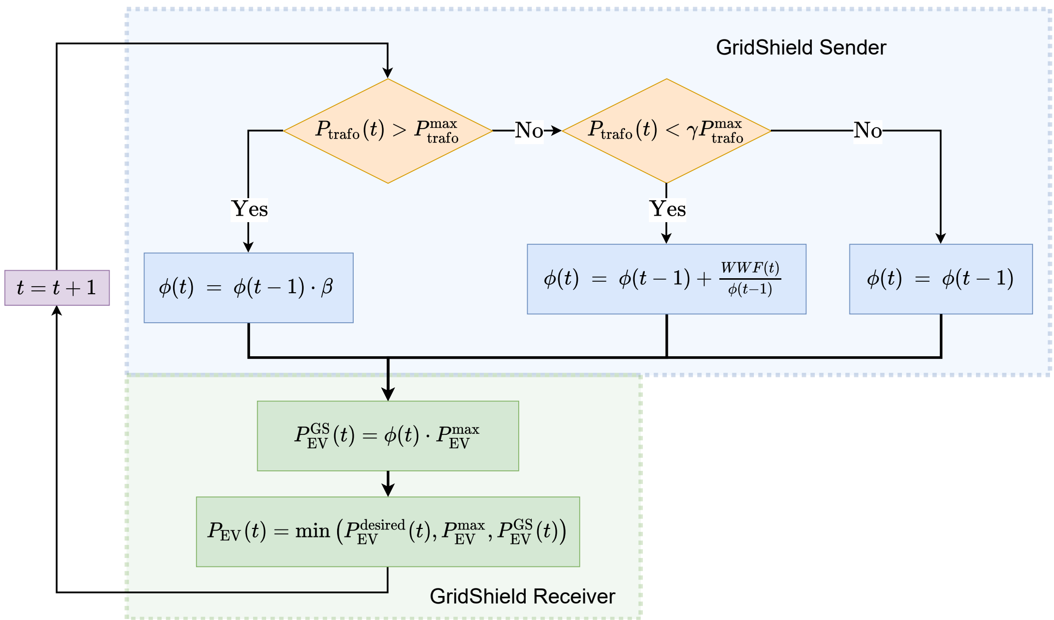

Fig. 4.3: Block diagram of Elastic GridShield algorithm. Blue: sender side implementation. Green: receiver side implementation.

phase of the AIMD algorithm described in Section 4.3. The difference is in the increase phase. With GridShield Elastic, we try to maximize energy delivered by being faster to increase allowed power in the early stages of the increase phase when the power is low, while being slower at later stages when the power is already close to the limit. This effect is achieved through a square root factor, which has these characteristics.

In GridShield Elastic, we use a utilization rate $UR(t) = \frac{P_{\text{trafo}}(t)}{P_{\text{trafo}}^{\max}}$ to track the capacity usage of the transformer. We estimate the maximum possible EV power, i.e. the maximum allowed charging power factor $\phi(t)$, based on this $UR(t)$ in (4.1).

$$\phi_{\text{est}}(t) = \frac{\phi(t-1)}{UR(t)} \tag{4.1}$$

We use this estimated maximum value $\phi_{\text{est}}(t)$ to determine how much the value of $\phi(t)$ should be increased. To do this, GridShield Elastic uses a square root factor, called the window-correlated weighting function WWF in TCP Elastic. The use of this square root factor gives GridShield Elastic its defining behavior of a fast early increase phase when the power in the grid is low, while being slow to increase when the power is already high. We deduce the value of our WWF in (4.2).

$$WWF(t) = \sqrt{\phi_{est}(t)} \tag{4.2}$$

The maximum allowed charging power factor $\phi(t)$ of GridShield Elastic is finally updated using this WWF through (4.3).

$$\phi(t) = \phi(t-1) + \frac{WWF(t)}{\phi(t-1)} \tag{4.3}$$

Similar to the AIMD implementation of GridShield, we define a scalable deadband by introducing a parameter γ, where $P_{\text{trafo}}^{\text{rest}} = \gamma P_{\text{trafo}}^{\max}$. Only when $P_{\text{trafo}}(t) < P_{\text{trafo}}^{\text{rest}}$, the additive increase phase is entered.

The performance of the Elastic GridShield algorithm can be tuned using the following parameters:

- The decrease factor β.
- The restoration limit factor γ.

4.5 PID

Proportional integral derivative (PID) controllers are an often applied solution for control engineering problems as described in Chapter 2. The implementation of a PID based controller for GridShield is described in this section. A block diagram of the algorithm is provided in Fig. 4.4. The general formula for a discrete time PID based controller is given in (4.4) [44]. A PID controller steers a signal to a given setpoint $r(t_\mathrm{k})$. For grid congestion control, the reference point is set to the maximum transformer power: $r(t_\mathrm{k}) = P_\mathrm{trafo}^\mathrm{max}$. The objective of the controller is to keep the power in the grid at the maximum power limit, i.e. it must minimize the error $e(t_\mathrm{k})$ it observes between the measured power $y(t_\mathrm{k}) = P_\mathrm{trafo}(t)$ and the reference point: $e(t_\mathrm{k}) = r(t_\mathrm{k}) - y(t_\mathrm{k})$. The controller steers the power through its control signal $u(t_\mathrm{k})$ to obtain this objective. The behavior of the controller can be tuned through the three parameters K_p, K_i and K_d. Since we use discrete time in our simulations, we account for the sample time between measurements, denoted as Δt.

$$u(t_\mathrm{k}) = K_\mathrm{p} e(t_\mathrm{k}) + K_\mathrm{i} \sum_{\mathrm{j}=1}^{\mathrm{k}} e(t_\mathrm{j}) \Delta t + K_\mathrm{d} \frac{e(t_\mathrm{k}) - e(t_{\mathrm{k}-1})}{\Delta t} \tag{4.4}$$

The parameters K_p, K_i and K_d dictate the contribution of the proportional, integral and derivative parts of the controller. The proportional part $K_\mathrm{p} e(t_\mathrm{k})$ of the controller forces a direct response to the value of $e(t_\mathrm{k})$. When violations occur, $e(t_\mathrm{k})$ becomes negative, and the proportional part also becomes negative to decrease the value of the control signal $u(t_\mathrm{k})$, which then decreases the charging power of the EVs.

The integral part $K_\mathrm{i} \sum_{\mathrm{j}=1}^{\mathrm{k}} e(t_\mathrm{j}) \Delta t$ of the controller involves a summation of the past errors. When the error is large for a prolonged period of time, e.g. we have a long period of grid limit violations, the summation term in the integral part of the controller will become very significant and thus the value of the control signal $u(t_\mathrm{k})$ will decrease, forcing the EVs to charge at a lower rate. However, EVs are not always plugged in and charging. This can cause the measured error $e(t_\mathrm{k})$ to continuously be positive due to the low charging load. This can cause an integral windup problem in the summation term in (4.4), which delays the controller's response to a negative error value [50]. Since we are mainly interested in *decreasing* the power when required, and a fast increase is only a secondary objective, we solve the integral windup problem using conditional integration, where the maximum value of the summation term in (4.4) is limited to the value of $r(t_\mathrm{k})$.

The derivative part $K_\mathrm{d}\frac{e(t_\mathrm{k})-e(t_{\mathrm{k}-1})}{\Delta t}$ of the controller counteracts sudden changes in the error, such that abrupt changes are balanced out. The more rapid the change in $e(t_\mathrm{k})$, the greater its controlling effect is. When many EVs suddenly start charging at the same time causing sudden large violations, the derivative part of the controller will become very significant and immediately decrease the charging power of the EVs by decreasing the value of the control signal $u(t_\mathrm{k})$.

Finally, the signals of the separate controller parts are summed to obtain a PID controller signal. Due to the different parts, it should respond well to various scenarios. When e.g. the derivative part is not well suited to deal with a stable but large violation, then the integral part is very well suited, whereas when there suddenly is a large error, it is the other way around. In this versatility lies the strength of a PID controller.

The measurement of the transformer power $y(t_\mathrm{k})$ is only performed at discrete time intervals, which introduces a measurement delay T_d. This delay makes the controller slow to react. To improve the speed of the controller, we take the measurement delay into account, using a linear extrapolation of the error $e(t_\mathrm{k})$ in (4.4). The extrapolation is given in (4.5), where T_d is equal to the sampling time Δt.

$$e(t_\mathrm{k}+T_\mathrm{d}) = r(t_\mathrm{k}+T_\mathrm{d}) - y(t_\mathrm{k}) + \frac{T_\mathrm{d}}{\Delta t}(y(t_\mathrm{k}) - y(t_{\mathrm{k}-1})) \tag{4.5}$$

The error is measured at the transformer, where the power is significantly higher than at a single charging station. To steer the charging power of the EVs using the error signal without overshooting due to the comparatively large value of $e(t_\mathrm{k}+T_\mathrm{d})$, the control signal $u(t_\mathrm{k})$ is normalized to the reference point $r(t_\mathrm{k})$. The resulting signal $\hat{u}(t_\mathrm{k})$ used to control the charging power of the EVs, is obtained from the value of $u(t_\mathrm{k})$ defined in (4.6), which is obtained from $u(t_\mathrm{k})$ defined in (4.7).

$$u(t_\mathrm{k}) = \begin{cases} -r(t_\mathrm{k}), & \text{if } u(t_\mathrm{k}) \leq -r(t_\mathrm{k}) \\ u(t_\mathrm{k}), & \text{if } -r(t_\mathrm{k}) < u(t_\mathrm{k}) < r(t_\mathrm{k}) \\ r(t_\mathrm{k}) & \text{if } u(t_\mathrm{k}) \geq r(t_\mathrm{k}) \end{cases} \tag{4.6}$$

$$\hat{u}(t_\mathrm{k}) = \frac{u(t_\mathrm{k})}{r(t_\mathrm{k})} \tag{4.7}$$

The normalized control signal $\hat{u}(t_k)$ takes a value between -1 and 1. Because we later multiply our message $\phi(t)$ with the control signal however, its value must be non-negative. Therefore, we define the steering signal $u^*(t_\mathrm{k}) = \hat{u}(t_\mathrm{k}) + 1$, to apply

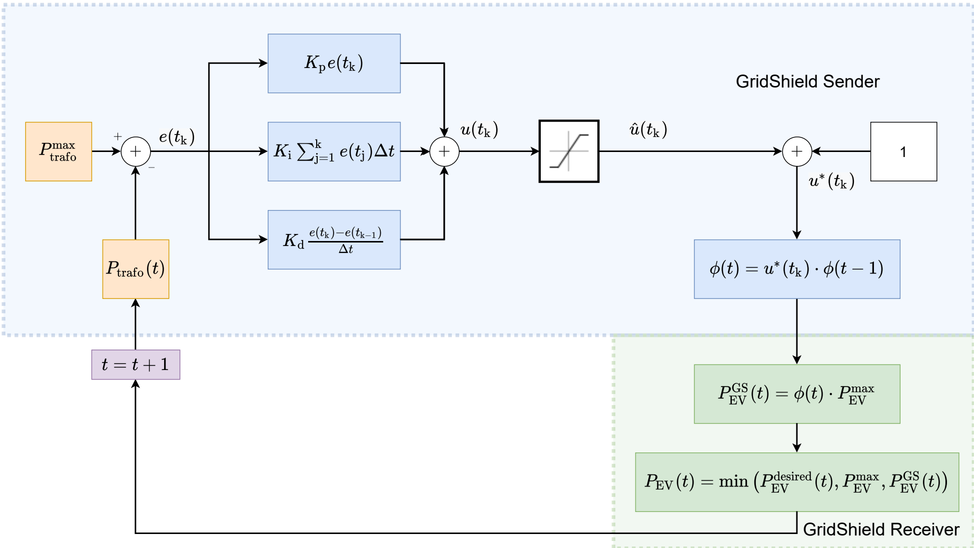

Fig. 4.4: Block diagram of PID based GridShield algorithm. Blue: sender side implementation. Green: receiver side implementation.

to our control signal. The control signal $\phi(t) = u^*(t_k)\phi(t-1)$ is sent to the EVs. The EVs adjust their power accordingly: $P_{EV}^{GS}(t) = \phi(t) \cdot P_{EV}^{max}$. As a result, when the PID based controller produces a negative value, $P_{EV}^{GS}(t)$ reduces since $u^*(t_k) < 1$ and thus the value of $\phi(t)$ reduces. When the controller produces a positive value, $P_{EV}^{GS}(t)$ is increased since $u^*(t_k) > 1$, until $P_{EV}^{GS}(t) = P_{EV}^{max}$.

The performance of the PID based GridShield algorithm can be tuned using the following parameters:

- The proportional gain K_p.
- the integral gain K_i.
- the derivative gain K_d.

4.6 GridShield Predictive

The GridShield Predictive algorithm is loosely based on the principles of droop control as described in Chapter 2. A block diagram of the algorithm is provided in Fig. 4.5. With droop control, a pre-defined curve between the measured power at the transformer and the control signal is used. When there are violations, a system controlled by a droop controller will know from this pre-defined curve what control signal is required to reduce its power consumption enough such that further grid limit violations are prevented. However, with GridShield, we cannot use a

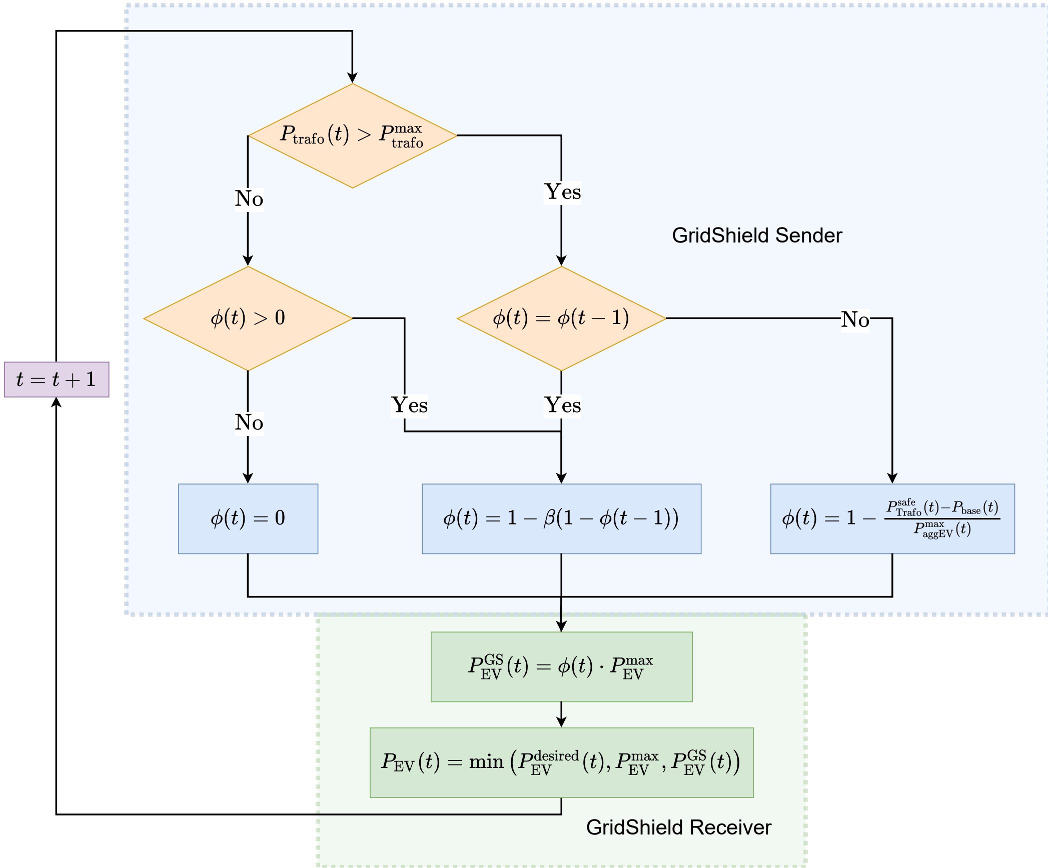

Fig. 4.5: Block diagram of Predictive GridShield algorithm. Blue: sender side implementation. Green: receiver side implementation.

pre-defined curve, since the result of transmitting a control signal will vary in time depending on e.g. the number of vehicles charging. Thus, we must make an estimation of the effect of a control signal first, before determining what our optimal value for $\phi(t)$ should be.

Because the load at the transformer is also influenced by other loads and generation in the grid, we cannot measure the aggregated charging power of the EVs directly and thus cannot immediately make an estimation of the effect of our control signal $\phi(t)$. Thus, to find what the effect of a change in $\phi(t)$ is, we must determine what the approximate aggregated charging power of the EVs $P_{\text{aggEV}}(t)$ is. We need to know this value since it is the only load in the grid that we can control with our control signal $\phi(t)$. When we know the value of $P_{\text{aggEV}}(t)$, we can use it to deduce a value $\phi^{\text{opt}}(t)$ that would result in a transformer load just below the limit of the transformer.

Since we cannot rely on direct feedback, but we do need to find how much the charging power should be reduced to get back to a non-grid violating state again, we make an approximation of the EV charging power $P_{\text{aggEV}}(t)$ currently being used by measuring the effect of a GridShield message. We cannot deduce $P_{\text{aggEV}}(t)$ directly, but we can deduce $P_{\text{aggEV}}^{\max}(t)$ by changing our control signal value $\phi(t)$. When we notice a congestion event, we immediately reduce our message $\phi(t)$ by a factor β upon measuring a congestion problem, i.e. $\phi(t) = \beta\phi(t-1)$, similar to the AIMD approach. The power reduction $\Delta P_{\text{Trafo}}(t)$ resulting from the change in our control signal $\Delta\phi(t)$ is used to derive the maximum possible charging power of the EVs $P_{\text{aggEV}}^{\max}(t)$ in (4.8).

$$P_{\text{aggEV}}^{\max}(t) = \frac{|\Delta P_{\text{Trafo}}(t)|}{\Delta\phi(t)} = \frac{|P_{\text{Trafo}}(t) - P_{\text{Trafo}}(t-1)|}{\phi(t) - \phi(t-1)} \tag{4.8}$$

Since we may already be applying a factor $\phi(t)$ to limit the EV charging power, their present aggregated charging power may have a different value than their maximum possible power. To find the share of EV charging power $P_{\text{aggEV}}(t)$ in the total power consumption, we correct for the factor $\phi(t)$ that has been applied in (4.9).

$$P_{\text{aggEV}}(t) = \phi(t) P_{\text{aggEV}}^{\max}(t) \tag{4.9}$$

From the value of $P_{\text{aggEV}}(t)$, we deduce the load on the transformer from other sources $P_{\text{base}}(t)$ in (4.10).

$$P_{\text{base}}(t) = P_{\text{Trafo}}(t) - P_{\text{aggEV}}(t) \tag{4.10}$$

Now, we derive what power the EVs can collectively use safely to charge without grid limit violations in (4.11).

$$P_{\text{aggEV}}^{\text{safe}}(t) = P_{\text{Trafo}}(t) - P_{\text{base}}(t) \tag{4.11}$$

While maintaining the power $P_{\text{aggEV}}^{\text{safe}}(t)$ could work indefinitely when the other loads in the network do not change their power in time, $P_{\text{base}}(t)$ is variable. When this causes the power to go slightly over the limit every time, that means we have to re-run our algorithm every iteration. Thus, instead of aiming to be exactly at the limit $P_{\text{Trafo}}^{\max}(t)$ which may introduce oscillations because of slight variations in $P_{\text{base}}(t)$, we introduce a deadband similar to the AIAD, AIMD and Elastic approaches. We use a factor γ that introduces a restoration limit $P_{\text{Trafo}}^{\text{rest}} = \gamma P_{\text{Trafo}}^{\max}$.

To find our optimal value $\phi^{\text{opt}}(t)$, we aim to steer the EV power such that the total power at the transformer is at a safe level $P_{\text{Trafo}}^{\text{safe}}$, exactly at the middle of the deadband, as defined in (4.12).

$$P_{\text{Trafo}}^{\text{safe}} = \frac{P_{\text{Trafo}}^{\text{rest}} + P_{\text{Trafo}}^{\text{max}}}{2} \tag{4.12}$$

We finally find our value $\phi^{\text{opt}}(t)$ through (4.13). Assuming $P_{\text{base}}(t)$ stays the same, the result will be that $P_{\text{Trafo}}(t) = P_{\text{Trafo}}^{\text{safe}}$. Over time, $P_{\text{Trafo}}(t)$ will change, but we only find a new value for $\phi^{\text{opt}}(t)$ when we leave our deadband, i.e. $P_{\text{Trafo}}^{\text{rest}}(t) > P_{\text{Trafo}}(t) > P_{\text{Trafo}}^{\text{max}}(t)$.

$$\phi^{\text{opt}}(t) = \frac{P_{\text{Trafo}}^{\text{safe}}(t) - P_{\text{base}}(t)}{P_{\text{aggEV}}^{\text{max}}(t)} \tag{4.13}$$

The performance of the Predictive GridShield algorithm can be tuned using the following parameters:

- The reduction factor β.
- the restoration limit factor γ.

4.7 Conclusion

In this chapter, we presented a list of possible algorithms that may be used to implement GridShield on the setup that was described in Chapter 3.These algorithms are based on research from various fields found in literature from Chapter 2. In Chapter 5 we present and compare performance results of the algorithms that were presented.

5 Simulations, Results and Discussion

Chapter Objective: This chapter presents and discusses the results obtained by the simulations and physical measurements that were conducted with the GridShield systems.

Chapter Contents

5.1 Introduction

In Chapter 3 we introduced the GridShield concept, and in Chapter 4 described possible algorithms that can be used to implement a GridShield system. In this chapter, we present the results obtained from simulations using various scenarios and algorithms. The goal of this chapter is to evaluate the performance of the algorithms that were presented in Chapter 4, and to present how GridShield can reduce grid limit violations in the event of EMS failures, or when there is no EMS at all.

All the simulations results described in this work are obtained using the DEMKit [51] simulator. Multiple scenarios were implemented in DEMKit to evaluate the performance of GridShield. These scenarios are of varying scale and type to test the robustness of GridShield in varying conditions. The scenarios include a model of a residential neighborhood of 80 houses in Lochem [52] presented in Section 5.2, a model of SlimPark, a small car park with 9 AC charging stations connected to a

PV installation at the University of Twente presented in Section 5.3, and a model of the ASR building in Utrecht, a large parking lot with a solar roof and 250 charging stations [53], both AC and DC, presented in Section 5.4. In all of the models, both the arrival and departure times of the EVs, the required charging energy, and base load power profiles of households have been generated when required by the Artificial Load Profile Generator (ALPG) [54]. A time base of 10 seconds was used for all simulations presented in this work. Based on the work of Martinenas et al. [25] presented in Chapter 2, who found EVs have a response time of 2 to 3 seconds, we assume that the delay from the time we send a GridShield control message to the time the result of the control message can be measured by the GridShield sender is always less than this 10 second time base. This assumption is verified in Section 5.3, where simulation results are compared to measurements obtained from the SlimPark site.

The remainder of this chapter is organized as follows: in Section 5.2 we show how the different GridShield algorithms perform in a residential neighborhood in the Dutch town of Lochem shown in Fig. 5.1, and determine which algorithm performs best in this scenario. Using the Lochem scenario, we also determine how the performance of GridShield is affected by present implementation limitations, and determine how the performance may improve in the future when these present limitations are taken away. In Section 5.3 we analyze the performance of the different algorithms again, but at a smaller scale, to find if this changes the optimal performance of GridShield. Based on the results from Section 5.2 and Section 5.3, we select the optimal parameters for a GridShield implementation and use these parameters to simulate the performance of GridShield in a multi-layer GridShield setup in Section 5.4. Finally, we summarize the results that were obtained in Section 5.5.

5.2 Residential Neighborhood Results (Lochem)

The Lochem scenario represents a validated network model of a low voltage distribution grid to which 80 single phase-connected houses are connected [52]. Every household in the scenario owns one EV that has a maximum charging power of 7.2 kW and a battery capacity of 42 kWh. The distribution grid is connected to a transformer with a maximum capacity of 40 kW per phase. In this section, we analyze the performance of the original AIAD GridShield implementation in the Lochem neighborhood, and present in what respects it can be improved. Then we show how the performance of other GridShield algorithms that were presented in

Fig. 5.1: Image of Lochem [55].

Chapter 4 compares to the original AIAD implementation. We consider the effect of the discrete charging powers described in Section 3.5.4, to explore how the performance of GridShield can be improved if we take away this technical gap and allow the EVSEs to charge at any continuous power level within their available charging power range. We also consider the difference in power behavior between power and current based charging control.

In the Lochem scenario, we consider a simulation time interval from the afternoon until midnight on a weekday. As shown in Chapter 1, people often arrive at home in the evening and hence the power profile of households shows a peak at that time, making it an interesting time period to simulate. Hence, we choose a 9 hour interval from 15:00 to 00:00. To provoke overloading of the transformer, an attack vector that represents a cyber attack is implemented. While the EVs in the scenario are normally controlled by an EMS that uses the profile steering heuristic [14] that prevents them from overloading the local grid, the attack vector overrides the EMS control signals and instead forces the EVs to alternatingly charge at very high and zero power in half hour intervals. The sudden change in charging power provoked by switching between high and zero power allows us to analyze the response time of GridShield implementations.

5.2.1 Original GridShield Implementation

The original GridShield implementation uses an AIAD algorithm. In Fig. 5.2b we see that the original GridShield implementation limits the charging power of the EVs during the attack. In Fig. 5.2a we see how the total power supplied by the grid, including the baseload, is reduced. In these figures, it takes up to 5 minutes for GridShield to start to take effect at time 20:00. This is due to the fact that GridShield changes the *maximum* charging power of the EVSEs. In the scenario, the EVs are not charging at full power and hence it takes multiple iterations before $P_{\text{EV}}^{\text{GS}}(t) < P_{\text{EV}}^{\text{Attack}}(t)$. This GridShield response delay may introduce grid damage. Hence, a GridShield control system should be fast to react to such a violation event. However, when the congestion problem is solved, the control system should also be quick to reach a safe, stable state, where the EVs charge at high power to minimize user discomfort while staying below the transformer's power limit. To address these two problems, our main objective is minimizing the Euclidean norm of the excessive power draw at the transformer, while minimizing the energy not served to customers is the secondary objective.

5.2.2 Optimization Objectives

To find which algorithm deals best with congestion problems in distribution grids, we compare the implemented algorithms based on two optimization objectives. These are the minimization of the Euclidean norm of the excessive power draw at the transformer, defined in (5.1), and the energy not served (ENS) compared to the base case defined in (5.2). In (5.2), $P_{\text{EV}}^{\text{agg}}(t)$ is the aggregated power of all EVs at time instance t during a simulation, $P_{\text{EV}}^{\text{agg,attack}}(t)$ is the aggregated power of the EVs in the attack scenario without GridShield, and $P_{\text{EV}}^{\text{agg,max}}(t)$ is the maximum power the EVs may collectively consume at time t without exceeding transformer limits, i.e. $P_{\text{EV}}^{\text{agg,max}}(t) = P_{\text{trafo}}^{\text{max}}(t) - P_{\text{base}}(t)$.

$$\|\vec{P}_{\text{viol}}\|_2 = \|\max\left(0, \vec{P}_{\text{trafo}} - P_{\text{trafo}}^{\text{max}}\right)\|_2 \tag{5.1}$$

$$\text{ENS} = \sum_{\text{t=0}}^{\text{T}} \left(P_{\text{EV}}^{\text{agg,attack}}(t)\right) \Delta t - \sum_{\text{t=0}}^{\text{T}} \min\left(P_{\text{EV}}^{\text{agg}}(t), P_{\text{EV}}^{\text{agg,max}}(t)\right) \Delta t \tag{5.2}$$

The value of $P_{\text{EV}}^{\text{agg,max}}(t)$ in (5.2) is the theoretical optimal solution, where we have no violations but are always exactly at the limit of safe energy delivery. This is

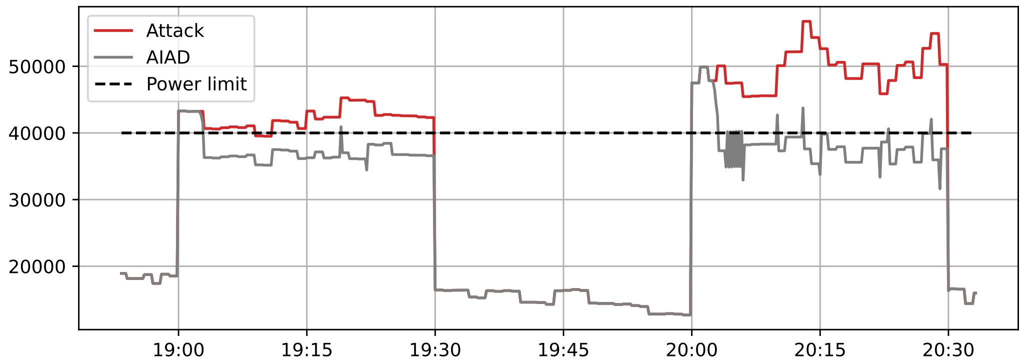

(a) Power at the highest loaded phase of the transformer. *Attack*: Attack vector with GridShield disabled; *AIAD*: original GridShield implementation.

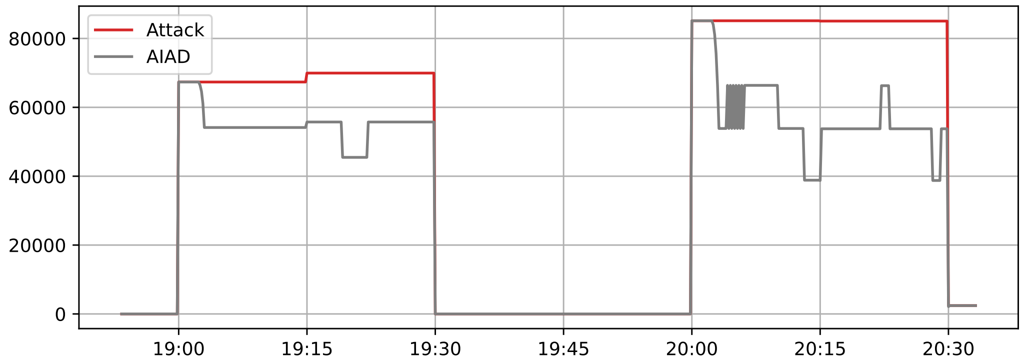

(b) Charging rates of all EVs.

Fig. 5.2: Power behavior in the Lochem grid, a comparison between having and not having GridShield.

	AIAD	AIMD			Elastic		PID			Predictive	
	α	α	β	γ	β	γ	Kp	Ki	Kd	β	γ
minimum	0.5	2	0.8	0.85	0.3	0.9	0.6	0.005	1	0.5	0.6
maximum	5	10	0.98	1	0.95	1	1.4	0.035	2	0.9	0.9
stepsize	0.5	2	0.03	0.05	0.05	0.02	0.1	0.005	1	0.05	0.05

Tab. 5.1: Parameter ranges used in the parameter sweeps of this thesis.

the energy delivery that we will compare the other algorithms to. However, when an algorithm cannot prevent some violations, more energy is served during this violation than in the optimal solution. This can result in a negative ENS. An example is the attack scenario, where $P_{\mathrm{EV}}^{\mathrm{agg,max}}(t) \leq P_{\mathrm{EV}}^{\mathrm{agg}}(t)$ resulting in a negative ENS.

Note that from a grid operation perspective, the decrease of violations is the primary objective, and the minimization of ENS is a secondary objective. We thus consider the reduction of violations the most important of our two objectives.

5.2.3 Algorithm Comparison Continuous Power Control

We first consider results where GridShield uses power based steering, and the EVs can choose from a continuous charging power range of $0\,\mathrm{kW} < P_{\mathrm{EV}}(t) < 7.2\,\mathrm{kW}$. We use the scenario of the cyber attack without an active GridShield system as our base case. The performance of the GridShield algorithms is compared to this cyber attack in Fig. 5.3. The behavior of the algorithms is characterized by the parameters introduced in Chapter 4. To find the optimal performance of the algorithms, parameter sweeps were performed and the performance with respect to our two optimization objectives. The same parameter sweeps were performed for every scenario, to maintain a fair comparison between the algorithms. The parameter sweep ranges are listed in Table 5.1. The Pareto optimal results of the parameter sweeps are presented in Fig. 5.3. The theoretical optimal solution $P_{\mathrm{EV}}^{\mathrm{agg,max}}(t)$ in (5.2) where there are no violations lies at the point $(0, 0)$ in the plot. A negative ENS can be achieved by delivering additional energy during violations, which do not occur in the theoretical optimal solution.

In Fig. 5.3, we see that all algorithms improve over the performance original AIAD implementation in terms of violation reduction, except for the PID based GridShield implementation. The GridShield Elastic algorithm obtains the lowest violations of all algorithms that were implemented in this scenario. The values of the points that provide the lowest violations are displayed in Table 5.2. In the table, we observe that GridShield Elastic decreases violations by 89.94% compared to the cyber attack, while delivering 16.48% less energy in the simulated time window than the optimal

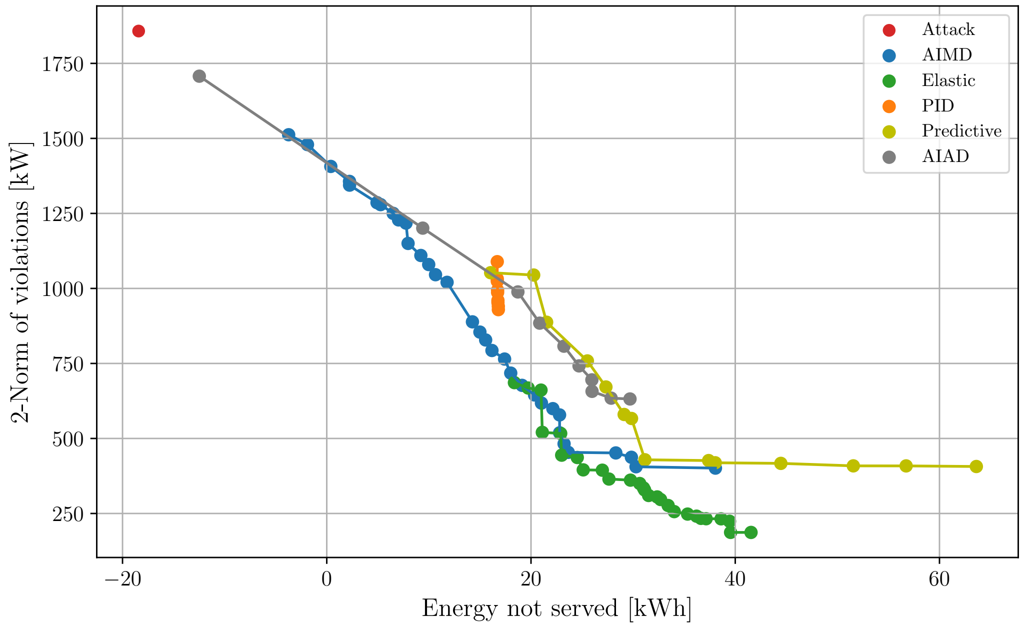

Fig. 5.3: Results of GridShield algorithm simulations in the Lochem scenario.

	2-Norm of violations [kW]	ENS [kWh]
Cyber attack	1,857.74	-18.42 (-7.31%)
AIAD	631.61 (-66.00%)	29.69 (11.78%)
AIMD	401.18 (-78.40%)	38.06 (15.09%)
PID	929.34 (-49.98%)	16.80 (6.66%)
Elastic	**186.86(-89.94%)**	**41.55 (16.48%)**
Predictive	406.58 (-78.11%)	63.61 (25.23%)

Tab. 5.2: Points with lowest violations of each algorithm in a continuous charging power control scenario.

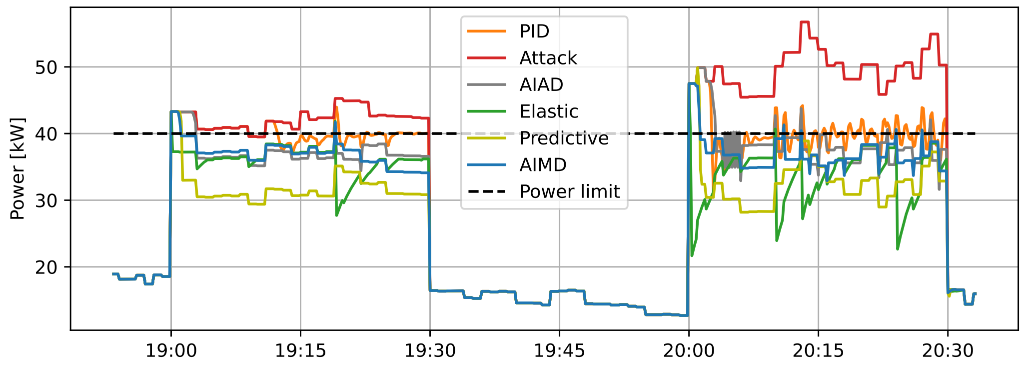

(a) Power at the highest loaded phase of the transformer.

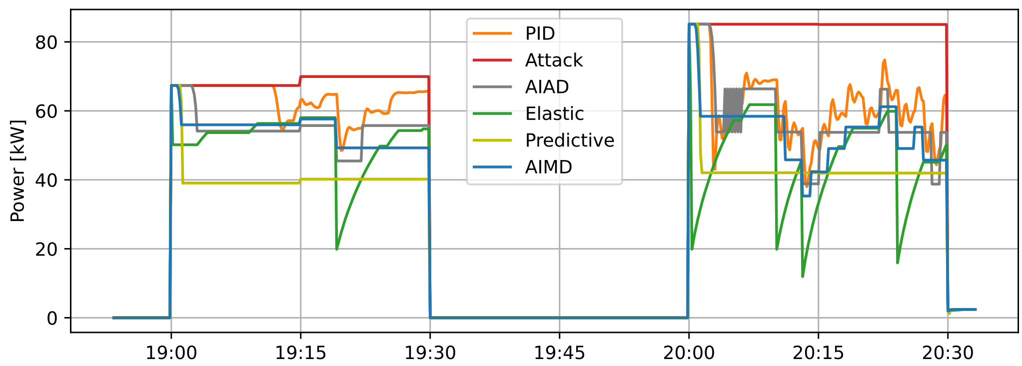

(b) Charging rates of all EVs.

Fig. 5.4: Power behavior in the Lochem grid for a continuous power control scenario.

solution. Note that this does not imply that the EVs will have a lower state of charge when they leave in the morning. The ENS values reflect the situation at 00:00, the end time of our simulation. However, as charging continues until the morning, the developed control algorithms only delay charging.

Fig. 5.4b and Fig. 5.4a show the behavior of the power in the grid when the GridShield systems are active. For every algorithm in the figure, the parameters from Table 5.1 were chosen that provided the lowest violations. For the AIAD algorithm, the restoration limit was set to a fixed value of 35 kW. The optimal parameters are presented in Table 5.3 We see that aside from the PID algorithm, every algorithm is faster to react to an initial violation caused by the cyber attack than the AIAD algorithm is. The Elastic algorithm responds the fastest of the algorithms that were tested. When comparing it to the AIMD algorithm, it uses a more aggressive β than the AIMD algorithm while maintaining a good ENS. The Predictive algorithm provides a very stable behavior, but due to the low value of γ that was chosen, it has a relatively high ENS. The PID algorithm exhibits the smoothest power curve, but it is often over the limit. The predictive algorithm requires a deadband that is

	AIAD	AIMD			Elastic		PID			Predictive	
	α	α	β	γ	β	γ	Kp	Ki	Kd	β	γ
optimal	4.5	2	0.8	0.85	0.3	0.9	1.4	0.005	2	0.65	0.5

Tab. 5.3: Optimal parameters for the algorithms in the Lochem grid for a continuous power control scenario.

too large to be competitive with the other algorithms in terms of ENS. The AIMD algorithm mainly causes more violations than the Elastic algorithm at the start of an attack iteration, where the more aggressive β of the Elastic algorithm makes it the fastest to respond.

5.2.4 Discrete Control

The results of Subsection 5.2.3 show the performance of GridShield provided that the EVSEs can choose their charging power from a continuous charging power range of $0\ \mathrm{kW} < P_{\mathrm{EV}}(t) < 7.2\ \mathrm{kW}$. However, in current EVSEs and EVs, there is often only a limited set of charging powers available which can be used to charge, as presented by Martinenas et al. [25]. With such a limitation comes a loss in control granularity, which may affect the performance of GridShield. To analyze the impact that such a limitation may have, we consider our Lochem girid again, but in this discrete control scenario the EVs only support charging rates from $1380\ \mathrm{W}$ to $7360\ \mathrm{W}$ with steps of $230\ \mathrm{W}$. We make the GridShield receivers select their charging power following the method presented in Subsection 3.5.4 to minimize the effect of the loss of control granularity.

The same parameter sweep that was performed to obtain the results presented in Subsection 5.2.3 is executed again in the discrete charging power scenario. The results of this sweep are presented in Fig. 5.5, the points with the lowest violations are presented in Table 5.4 and the corresponding parameters are presented in Table 5.5. Note that the violations and ENS of the attack also changes compared to the previous scenario: since the attack forces the EVs to charge at a high, but not at maximum power, the results of the attack also change when it cannot select the same charging power values as in the previous scenario.

When comparing Fig. 5.3 and Fig. 5.5, we see that the violations increase for all implementations when we limit the available charging powers to a discrete set. The best performing elastic algorithm more than doubles its violations from $186.86\ \mathrm{kW}$ to $458.34\ \mathrm{kW}$. Even when accounting for the increased violations with the cyber

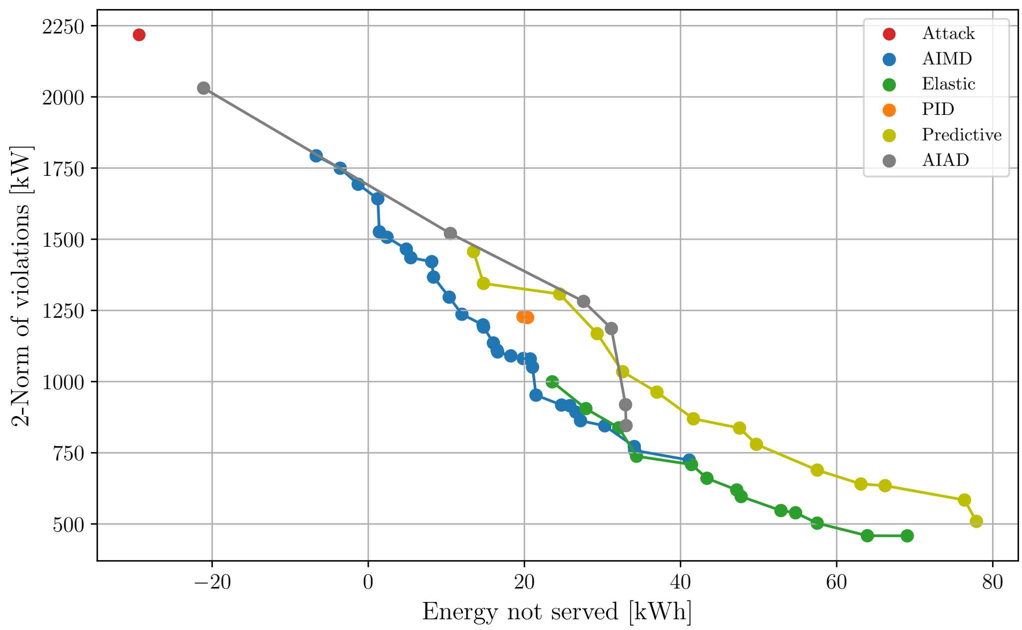

Fig. 5.5: Results of GridShield algorithm simulations in the Lochem scenario, when EVs only support a set of discrete charging powers.

discrete	**2-Norm of violations [kW]**	**ENS [kWh]**
Cyber attack	2,217.88	-29.35 (-11.32%)
AIAD	845.44 (-61.88%)	33.02 (12.73%)
AIMD	724.24 (-67.35%)	41.12 (15.85%)
PID	914.84 (-50.76%)	17.07 (6.77%)
Elastic	**458.34 (-79.33%)**	**69.04 (26.62%)**
Predictive	509.00 (-77.05%)	77.90 (30.04%)

Tab. 5.4: Points with lowest violations of each algorithm in a discrete charging power scenario.

	AIAD	AIMD			Elastic		PID			Predictive	
	α	α	β	γ	β	γ	Kp	Ki	Kd	β	γ
optimal	5	2	0.8	0.85	0.3	0.97	0.6	0.005	2	0.7	0.5

Tab. 5.5: Optimal parameters for the algorithms in the Lochem grid for a discrete charging power control scenario.

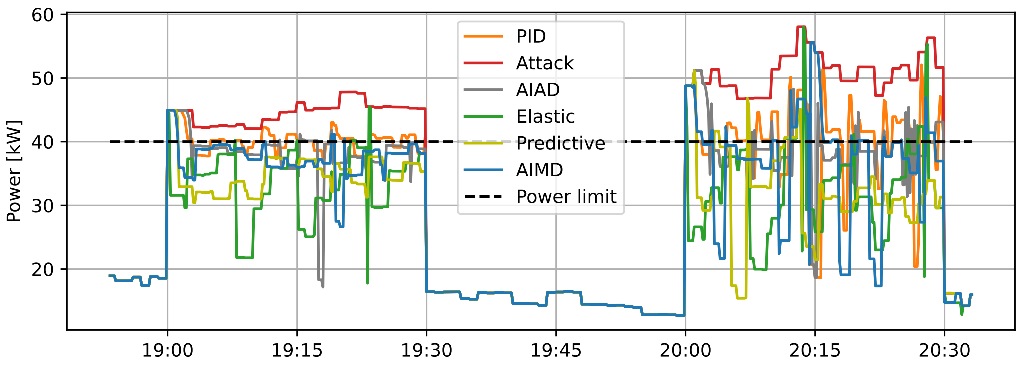

(a) Power at the highest loaded phase of the transformer.

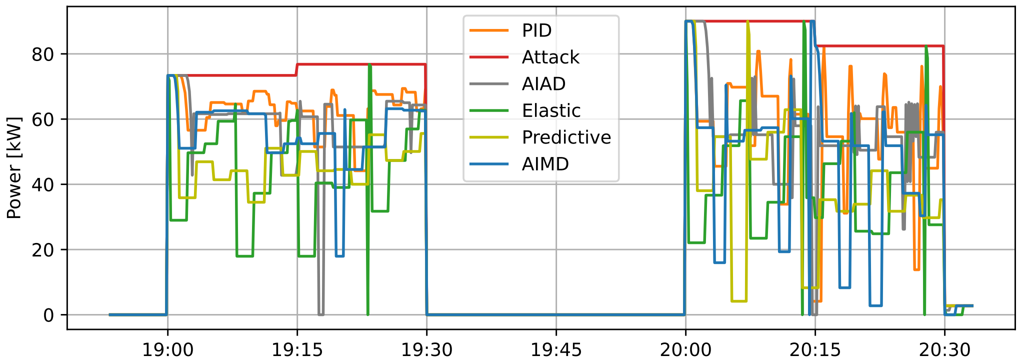

(b) Charging rates of all EVs.

Fig. 5.6: Power behavior in the Lochem grid for a discrete power control step scenario.

attack, it can prevent only half of the violations compared to continuous control, i.e. it only reduces violations by 79.33% instead of 89.94%.

Fig. 5.6a and Fig. 5.6b show why the violations become higher in the discrete charging power control scenario. All algorithms show less stable behavior; there are significant power swings with all algorithms. We see that when the message $\phi(t)$ gets to a low value, and vehicles have to decide between 0 W and 1380 W instead of choosing from a range with steps of 230 W, the swings become more pronounced due to the greater power change when an EV switches from 1380 W to 0 W or vice versa.

5.2.5 Current Based Control

In the previous sections, we considered power based control, where we measure the power at the transformer and steer the charging power of the EVs. However, transformer capacities are often rated in current, not power, and the charging rate of

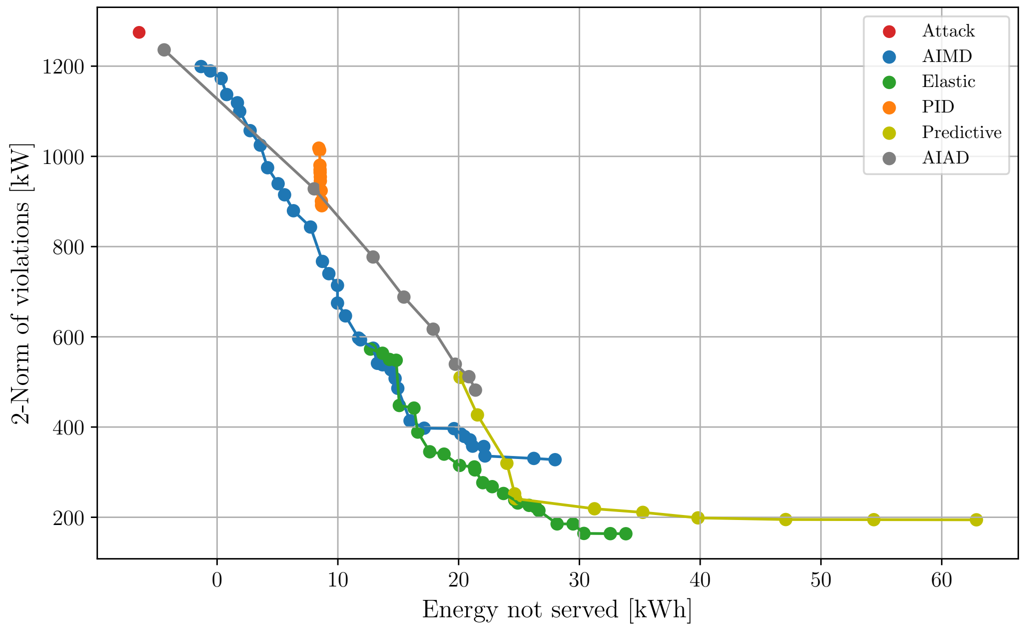

Fig. 5.7: Results of GridShield algorithm simulations in the Lochem scenario, when GridShield uses continuous current based control.

	2-Norm of violations [kW]	**ENS [kWh]**
Cyber attack	1,274.89	-6.45 (-2.73%)
AIAD	481.90 (-62.20%)	21.40 (9.04%)
AIMD	327.64 (-74.30%)	27.99 (11.83%)
PID	890.62 (-30.14%)	8.67 (3.66%)
Elastic	**163.50 (-87.18%)**	**33.85 (14.31%)**
Predictive	194.37 (-84.75%)	62.87 (26.58%)

Tab. 5.6: Points with lowest violations of each algorithm in a continuous charging current control scenario.

EVs is also often set in current instead of power. Hence, we consider what the effect of current based control is compared to power based control. While the principles of current based control are the same as power based control, results may change given that our optimization objectives are power based. The effect of current based control on our objectives hence differs from power based control because the power is the product of current and voltage, and the voltage at a node is variable.

The performance of the various algorithms in a current based control scenario are presented in Fig. 5.7. When comparing these results to Fig. 5.3, we see that the violations go down for all algorithms, and the attack as well. This is a result of the varying voltage at the nodes in the network. When comparing the different algorithms, we see that the relative performance between the algorithms is slightly

	AIAD	AIMD			Elastic		PID			Predictive	
	α	α	β	γ	β	γ	Kp	Ki	Kd	β	γ
optimal	5	2	0.8	0.85	0.3	0.91	1.2	0.005	2	0.6	0.5

Tab. 5.7: Optimal parameters for the algorithms in the Lochem grid for a continous charging current control scenario.

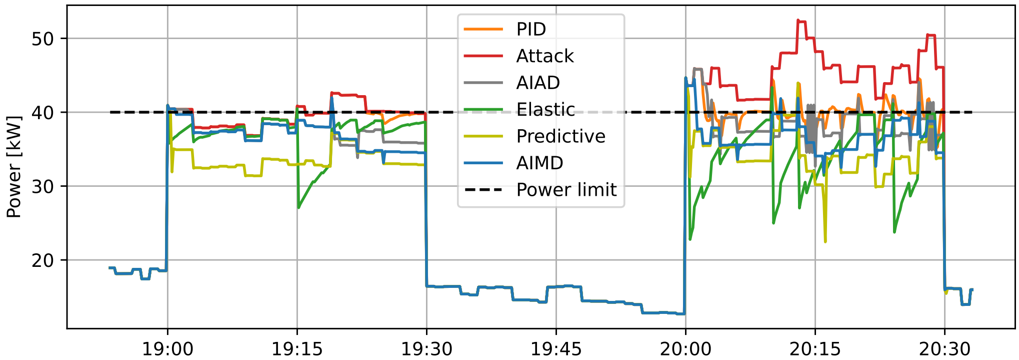

(a) Power at the highest loaded phase of the transformer.

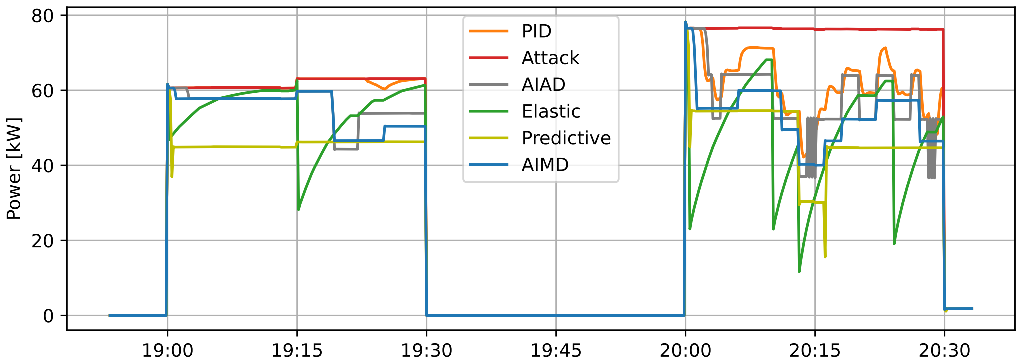

(b) Charging rates of all EVs.

Fig. 5.8: Power behavior in the Lochem grid for a continuous current control step scenario.

closer than in the power based control scenario. The optimal parameters for the current based control scenario in Table 5.7 are also different from the optimal parameters in Table 5.3. However, it is still the elastic algorithm that provides the best performance with a reduction of violations of 87.18% at a cost of 14.31% ENS.

When we consider the behavior of the power presented in Fig. 5.8a and Fig. 5.8b, we see that the behavior of the algorithms is similar to the behavior of the power based control scenario presented in Subsection 5.2.3.

5.2.6 Conclusion

In the Lochem scenario, we demonstrated that the Elastic algorithm is the best performing GridShield algorithm that was implemented given our parameter sweep, irrespective of whether we simulate with discrete or continuous charging power, and current or power based control. Since the difference in performance and behavior between current and power based control is small, we do not consider it in our other scenarios. However, the behavior of the power on the grid changes significantly when charging can only be done with discrete charging steps.

Depending on the simulation setup, the Elastic GridShield reduces violations by 79% up to 89%, at a cost of 14% to 27% ENS.

5.3 Small Car Park Results (SlimPark)

Having established results of the different GridShield algorithms in a residential neighborhood setting, we verify how GridShield performs in a smaller scale scenario in this section. To validate the simulation results that we obtain, we also show results of physical measurements of a GridShield system implemented at the SlimPark site on the university campus. In this scenario, we have no attack vector; instead, we use GridShield as a rudimentary EMS. The SlimPark site has 9 EV chargers, each charger can deliver up to $7.2\ \mathrm{kW}$ ($32\ \mathrm{A}$ per phase on three phases.) The site also has a local battery and a PV installation installed which both influence the power measured at the transformer. The location is presented in Fig. 5.9.

In this section, we first show the results of GridShield as a rudimentary EMS at the SlimPark site using continuous power control in Subsection 5.3.1, after which we compare those results to the case of discrete power control in Subsection 5.3.2. To verify the validity of the simulation results, field tests at the SlimPark site were performed, which are discussed in Subsection 5.3.3.

5.3.1 SlimPark Continuous Power Control

To compare the GridShield algorithms, we perform the same parameter sweep of Table 5.1 that was also used in the Lochem scenario to determine what parameters provide the best performance for every algorithm. For the AIAD algorithm, the restoration limit was set to a fixed value of $9.2\ \mathrm{kW}$. The results of this sweep are presented in Fig. 5.10. We see that the AIMD, Elastic and Predictive algorithm

Fig. 5.9: Image of the SlimPark location [56].

	2-Norm of violations [kW]	ENS [kWh]
Cyber attack	423.29	-5.49 (-5.30%)
AIAD	60.88 (-85.62%)	-0.28 (-0.27%)
AIMD	41.45 (-90.21%)	2.16 (2.08%)
PID	202.0 (-52.29%)	67.3 (65.0%)
Elastic	**23.37 (-94.48%)**	**10.8 (10.4%)**
Predictive	29.85 (-92.95%)	4.47 (4.32%)

Tab. 5.8: Points with lowest violations of each algorithm in a continuous charging power control scenario at SlimPark.

all perform relatively similar, and slightly better than AIAD, in this scenario where GridShield is used as a rudimentary EMS. The PID algorithm does not get such low violations as the other algorithms do. The point of the PID algorithm with the lowest violations is an outlier that has a very high compared ENS compared to the other algorithms. In Fig. 5.11a and Fig. 5.11b it becomes apparent that at these specific parameters the PID algorithm shows large oscillations, causing a large ENS value. While the other PID points in Fig. 5.10 do not show such oscillations, they also have high violations compared to the other algorithms, and we do not present them further.

Fig. 5.11a and Fig. 5.11b show that the Elastic algorithm takes up to half an hour to increase the power to the power limit again. Because in this half hour, no

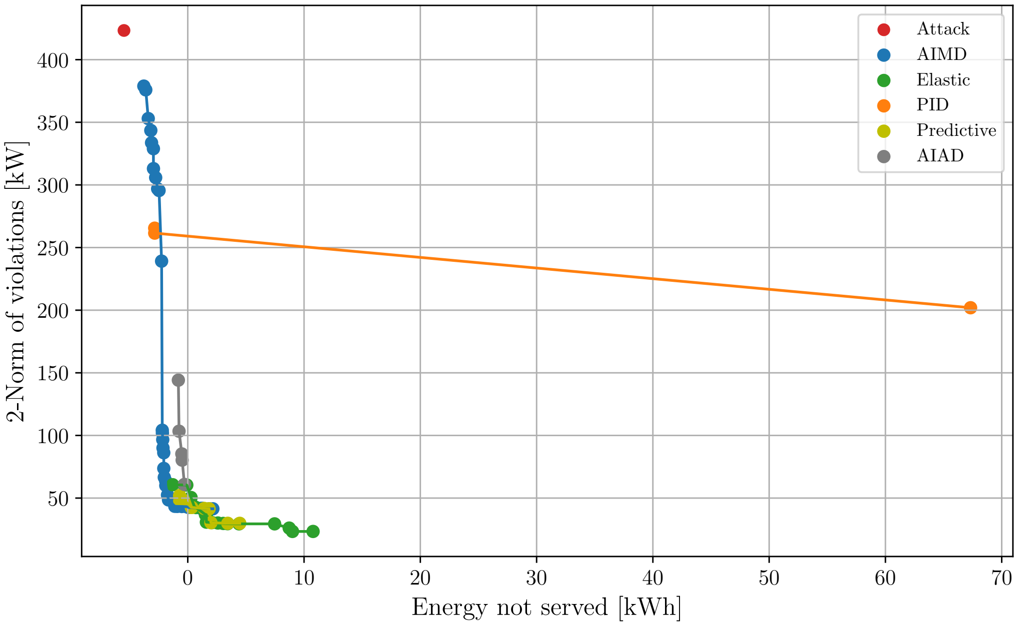

Fig. 5.10: Results of GridShield algorithm simulations in the SlimPark scenario, when GridShield uses power based continuous control.

	AIAD	AIMD			Elastic		PID			Predictive	
	α	α	β	γ	β	γ	Kp	Ki	Kd	β	γ
optimal	5	2	0.83	0.85	0.3	1	0.8	0.035	2	0.6	0.5

Tab. 5.9: Optimal parameters for the algorithms in the SlimPark scenario with a continuous charging power control scenario.

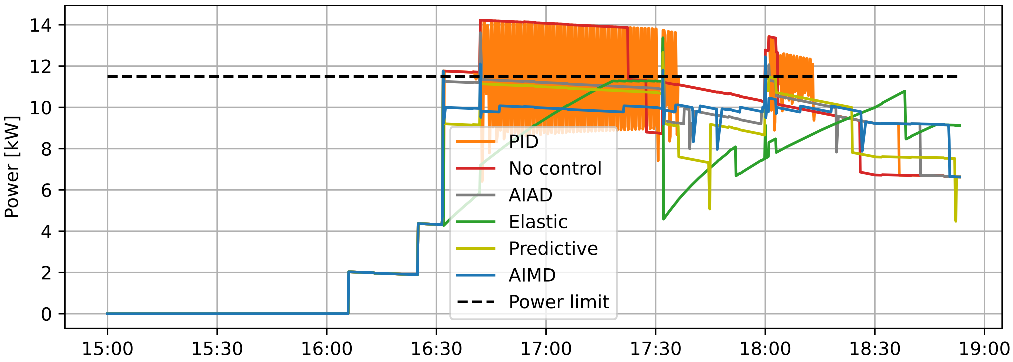

(a) Power at the highest loaded phase of the transformer.

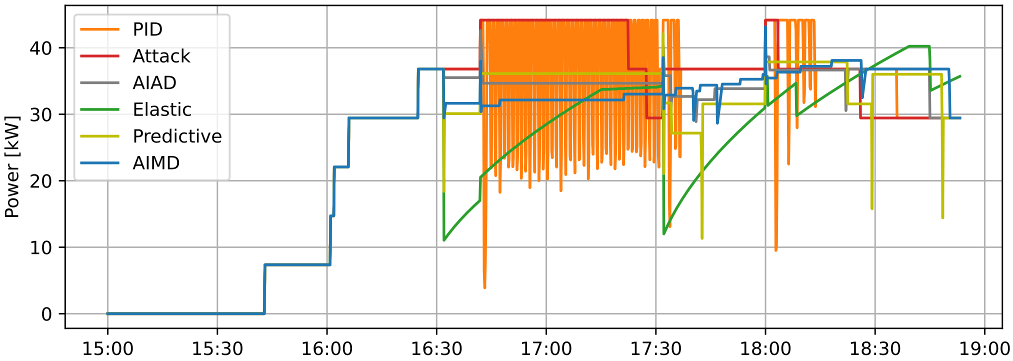

(b) Charging rates of all EVs.

Fig. 5.11: Power behavior in the SlimPark grid for a continuous power control scenario.

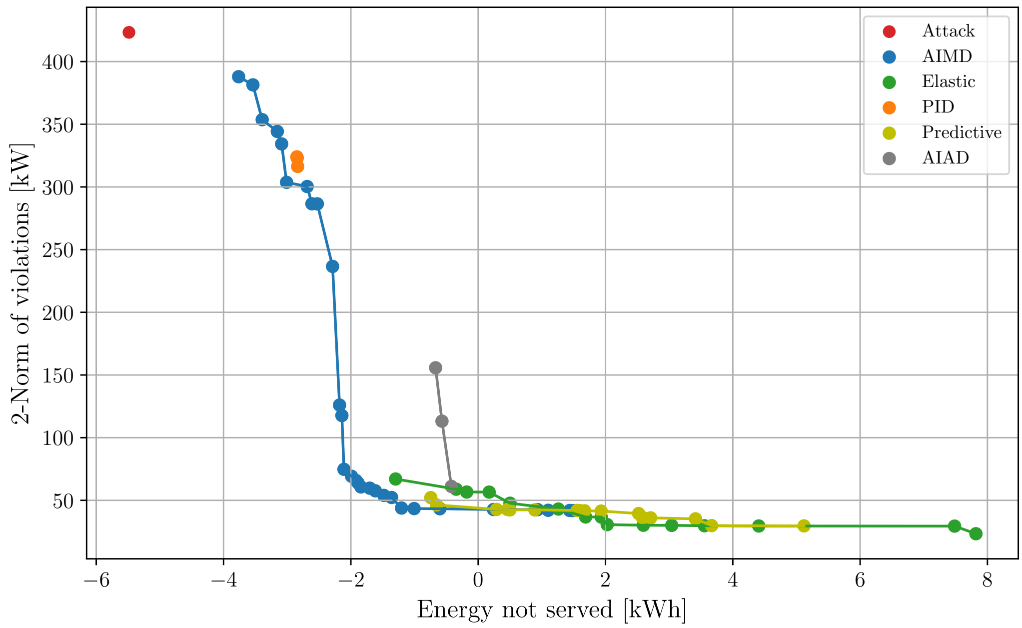

Fig. 5.12: Results of GridShield algorithm simulations in the SlimPark scenario, when GridShield uses power based discrete control.

violations occur, this implementation of Elastic with the smallest β also gets the lowest violations. The AIMD algorithm creates the least abrupt large power changes when comparing with the other algorithms, while we see the Predictive algorithm also can give large downward power changes due to its small value for β.

5.3.2 SlimPark Discrete Power Control

To analyze the impact that the discrete power control limitation may have in the SlimPark scenario, we consider our SlimPark scenario again, but in this discrete control scenario the EVs only support charging rates from 6 A to 32 A with steps of 1 A. We make the GridShield receivers select their charging power following the method presented in Subsection 3.5.4 to minimize the effect of the loss of control granularity. The results of our parameter sweep are presented in Fig. 5.10. The points with the lowest violation of each algorithm are presented in Table 5.10. We see that the Elastic algorithm is again providing the lowest violations.

The effect of the discrete charging powers is clearly visible in the increase phase of the Elastic algorithm presented in Fig. 5.13a and 5.13b. In this rudimentary EMS scenario with discrete charging powers, we see that the discrete charging powers

	2-Norm of violations [kW]	ENS [kWh]
Cyber attack	423.29	-5.49 (-5.30%)
AIAD	61.08 (-85.57%)	-0.42 (-0.41%)
AIMD	41.85 (-90.11%)	1.49 (1.44%)
PID	316.3 (-25.27%)	-2.84 (-2.74%)
Elastic	**23.37 (-94.48%)**	**7.82 (7.55%)**
Predictive	29.64 (-93.00%)	5.12 (4.95%)

Tab. 5.10: Points with lowest violations of each algorithm in a discrete charging power control scenario at SlimPark.

	AIAD	AIMD			Elastic		PID			Predictive	
	α	α	β	γ	β	γ	Kp	Ki	Kd	β	γ
optimal	5	2	0.8	0.85	0.4	0.98	0.6	0.005	2	0.9	0.6

Tab. 5.11: Optimal parameters for the algorithms in the SlimPark scenario with a discrete charging power control scenario.

(a) Power at the highest loaded phase of the transformer.

(b) Charging rates of all EVs.

Fig. 5.13: Power behavior in the SlimPark grid for a discrete power control scenario.

do not make a significant difference to the behavior or the performance of the algorithms, when comparing with the results from Subsection 5.3.1.

5.3.3 SlimPark Experimental Results

We validate the simulation results of the previous subsections through experimental data from the SlimPark location at the University of Twente campus. To validate our results, we consider a scenario where three EVs are charging at the location and their combined load is just under the limit of the transformer, which is set to 60 A in our scenario. A fourth EV also starts charging, which overloads the transformer, as presented in Fig. 5.14a. During the measurements, we used an AIMD implementation with $\alpha = 1$ A, $\beta = 0.75$ and $\gamma = 0.9$. GridShield uses a control interval of 10 seconds.

In Fig. 5.14b, we see that upon the overloading event, There is a 5 second delay before GridShield executes its next control interval. Once the next control interval occurs, GridShield decreases its allowed charging current from 32 A to 25 A (32 A $\cdot$ $\beta = 25$ A.) The power is not decreased far enough by this decrease; it takes a total of 4 GridShield control iterations before we operate within the power limit of the transformer again. Then, the additive increase phase is entered. We see that the GridShield signal goes up for two iterations, until it reaches 14 A and the transformer power is within the deadband of 54 A to 60 A, i.e. $\gamma = 0.9$. From there, the situation is stable, and we only observe some solar fluctuations on the total power for the rest of the time frame.

When we observe the EV response in Fig. 5.14c, it is interesting to note how at first, only EV3 is affected by the GridShield signal. This is due to the technical gap where EVSE units cannot directly change the current charging power, but only their maximum charging power of 32 A per phase. Since Only EV3 can charge at 32 A per phase (the other EVs charge at 3x8 A or 3x16 A) it is the only one affected by the GridShield signal. Only when the GridShield signal goes below 16 A at 14:01:40, we get a response from other EVs than EV2. This is then also visible in the transformer phase load in 5.14a, where the decrease is suddenly steeper than in the previous GridShield control iterations (now 3 EVs respond simultaneously instead of 1) and we also see that phase 2 and phase 3 are also affected by the GridShield signal for the first time.

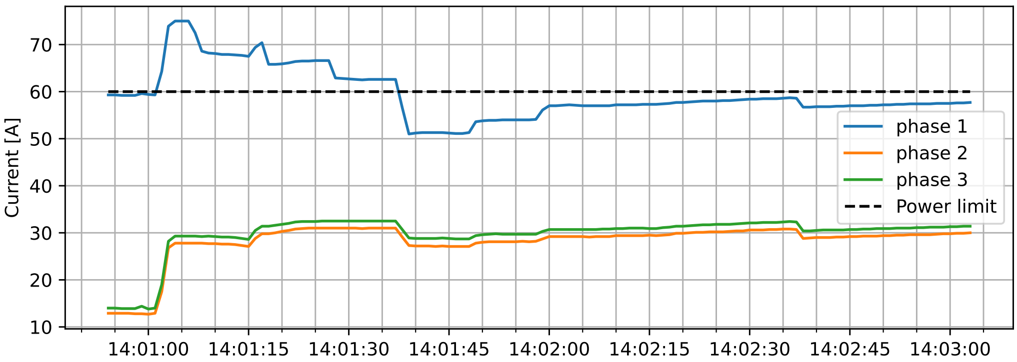

(a) Load at the three phases of the transformer. The transformer is overloaded at 14:01:03 by EV2.

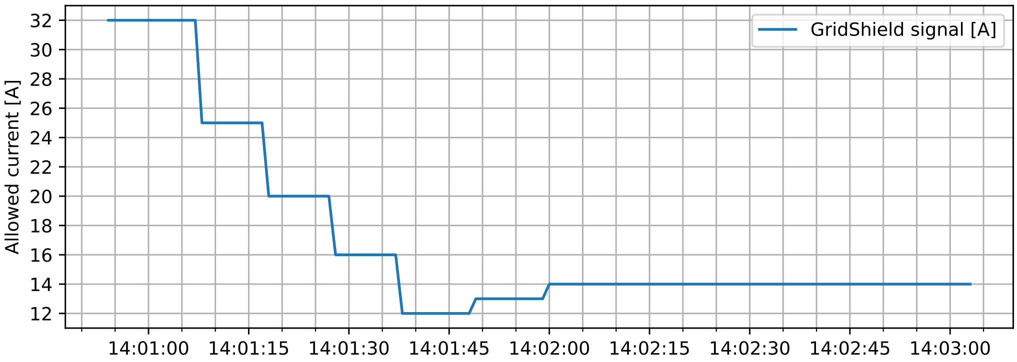

(b) GridShield response to the transformer overload. The message unit A. The limit in the message is directly applied to all phases by the GridShield receivers.

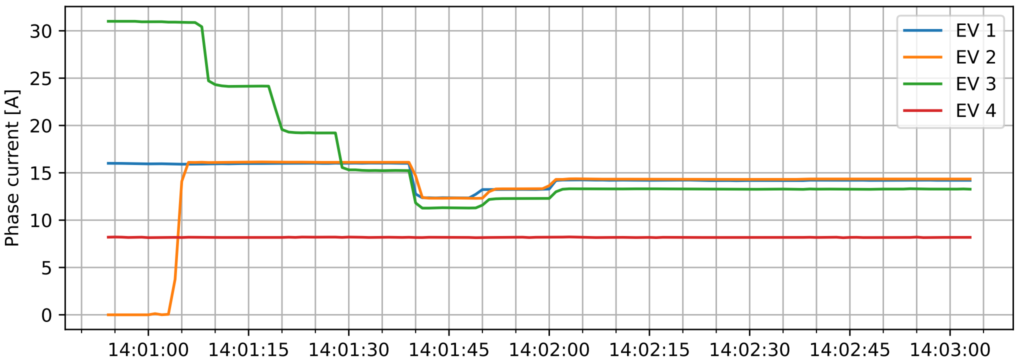

(c) Phase current of every EV. Note that EV3 only charges on one phase; the other EVs charge at three phases. EV2 overloads the transformer by starting charging at 14:01:03.

Fig. 5.14: Measurement results obtained from the SlimPark site.

5.3.4 Conclusion

In this section, we presented how GridShield can function as a rudimentary EMS in a small car park. In such a situation, GridShield can work with both continuous and discrete power control, without a significant change to performance. Finally, in Subsection 5.3.3, we verified if the GridShield system works by implementing an AIMD implementation at the SlimPark site at the campus of the University of Twente. The results show that in our scenario, GridShield can limit the charging power of EVs to stay within bounds, within a timeframe of 30 seconds after an initial violation occurs.

5.4 Large Parking Lot Results (ASR)

In the previous sections, the performance of GridShield was analyzed for a residential neighborhood and for a small car park. In this section, we evaluate the performance of GridShield at a large parking lot with a large PV array, 250 EVSE units both AC and DC, and three separate transformers supplying energy to different parts of the parking lot. The scenario is based on the ASR site that is shown in Fig. 5.15. We use the three separate transformers to present the results of a multi-layer GridShield setup, where the three separate transformers are subtransformers connected to a single main transformer as presented in Fig. 5.16. There is one high level GridShield sender module at the main transformer controlling the low level GridShield sender modules at the subtransformers. The low level GridShield sender modules send their message to the GridShield receiver modules at the EVSEs. In the scenario, the low level transformers have a maximum power of $200\ \mathrm{kW}$ per phase, and the high level transformer has a capacity of $500\ \mathrm{kW}$ per phase. We consider a continuous power control scenario.

Due to the scale and complexity of the model, simulations of the ASR scenario take significantly longer than simulations of the other two presented models, and hence no parameter sweeps are performed for the ASR scenario given time constraints. Instead, we choose the optimal parameters from the Lochem continuous power control scenario, since that scenario is most comparable in size to the ASR scenario. Measurement data from solar panels at SlimPark on a day where there were significant fluctuations in solar power is used to test the response of GridShield to such fluctuations. The measurement data is scaled up from the size of the PV array at SlimPark to the PV array at ASR. The resulting PV power in the simulated scenario is presented in Fig. 5.17. When the PV power decreases, the EVs must

Fig. 5.15: Image of the ASR location [56].

also decrease consumption rapidly to maintain within the bounds of the transformer limits. However, it is desirable that the EVs are fast to increase their power as soon as the PV power increases again.

In Subsection 5.4.1, we present the results of the simulations of the ASR scenario and consider the differences in performance between GridShield implementations for a hierarchical structure. In Subsection 5.4.2, we zoom in on the response of GridShield to the rapid fluctuations of the PV power production.

5.4.1 Hierarchical GridShield Results

A hierarchical topology of three low level GridShield sender modules is presented in the ASR scenario, with one high level GridShield sender module controlling the low level GridShield sender modules as presented in Fig. 5.16. The low level GridShield sender modules finally send their message to the GridShield receiver modules at the EVSEs. In the scenario, the low level transformers have a maximum power of 200 kW per phase, and the high level transformer has a capacity of 500 kW per phase. We consider a continuous power control scenario.

Two of the best performing algorithms in the previous scenario are presented here, to compare the differences in the approach between the algorithms. These are the

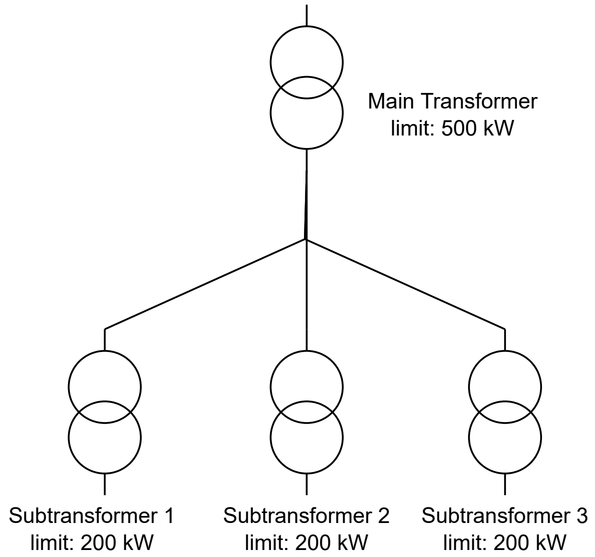

Fig. 5.16: ASR scenario transformer topology.

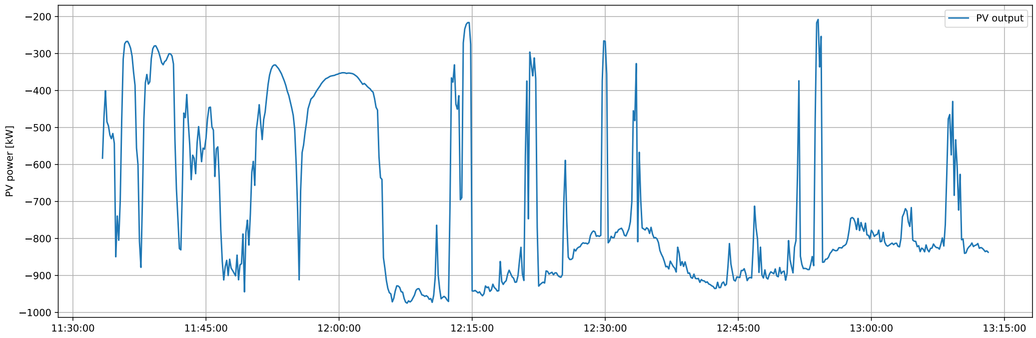

Fig. 5.17: PV total power output in the ASR scenario.

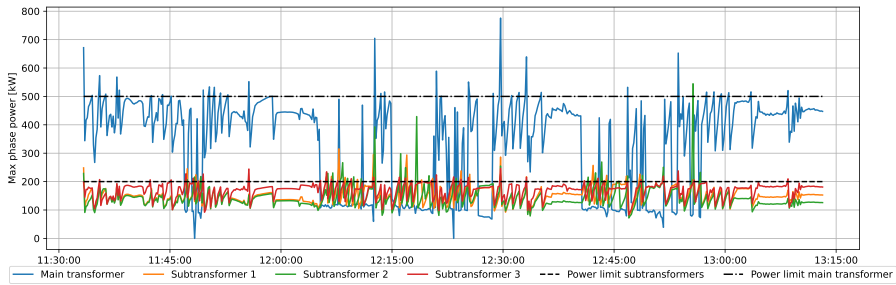

(a) Power at the highest loaded phase of the transformers.

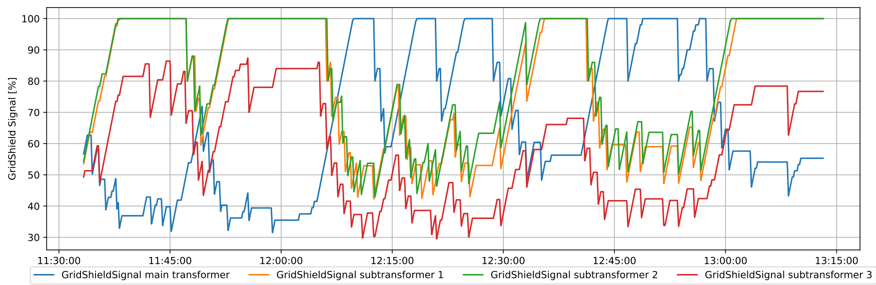

(b) GridShield signal in response to the phase load.

Fig. 5.18: Power behavior in the ASR grid when using the AIMD GridShield algorithm.

AIMD and the Elastic algorithm. While GridShield Elastic is in principle based on an AIMD algorithm, its behavior is different as is presented in Fig. 5.18a and Fig. 5.19a. The Elastic GridShield algorithm is slower to increase, which makes its behavior more stable as it has to decrease power less often. However, the AIMD algorithm is faster to increase and thus delivers more energy at a cost of more violations. When looking at the GridShield signals sent by the GridShield sender modules in Fig. 5.18b and 5.19b, it is clear that the AIMD algorithm signal fluctuates more and thus provides less stable behavior, but the total power use allowed by GridShield with the AIMD implementation is higher.

5.4.2 Response to rapid PV Fluctuations

To evaluate the performance of the AIMD and Elastic algorithms to the rapid PV power fluctuations presented in Fig. 5.17, We zoom in on the time from 12:40 to 13:13. Fig. 5.20a and Fig. 5.20b present the total EV power and the total PV power in this timeframe. We see that the AIMD algorithm is faster to increase EV power in response to an increase in PV power, compared to the Elastic algorithm. The

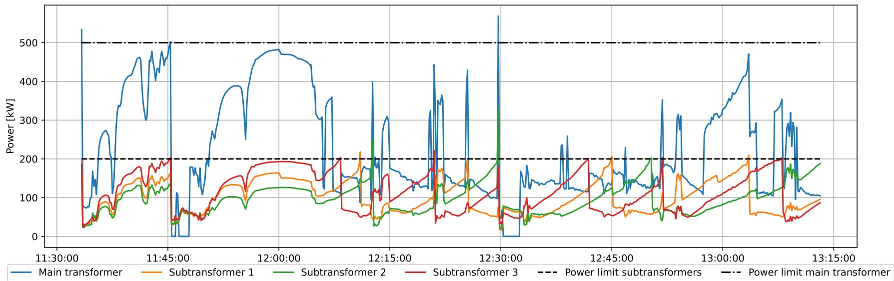

(a) Power at the highest loaded phase of the transformers.

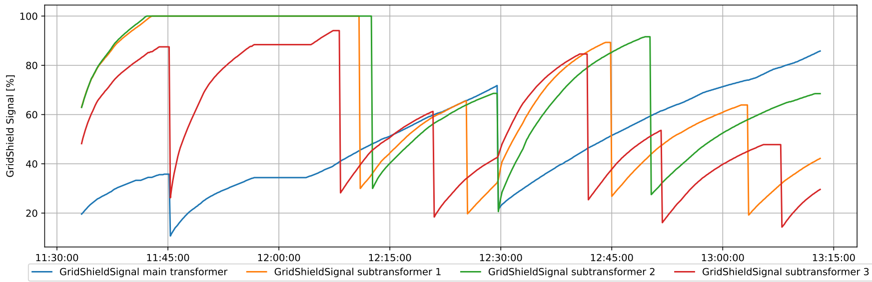

(b) GridShield signal in response to the phase load.

Fig. 5.19: Power behavior in the ASR grid when using the Elastic GridShield algorithm.

difference is especially noticeable in the time from 12:50 to 12:55, where two power drops from the PV array occur, both more than halving the energy production within 20 seconds. We see that both algorithms respond to the first production drop by reducing the charging power of the EVs. However, only the AIMD algorithm also responds to the second production drop. It was fast to increase and thus needs to decrease again at the second production drop, whereas the Elastic implementation had not recovered the charging power enough since the first production drop to have any need of responding to the second production drop.

The use of a lower β for the decrease phase in the Elastic algorithm also becomes apparent when comparing Fig. 5.20a and Fig. 5.20b. The minimum EV power of the Elastic implementation is 312 kW, whereas the minimum power of the AIMD implementation is significantly higher at 456 kW. This is mostly a result of the Elastic algorithm using a β of 0.3, whereas the AIMD algorithm uses a β of 0.8. The AIMD algorithm can thus step down the power with more granular steps.

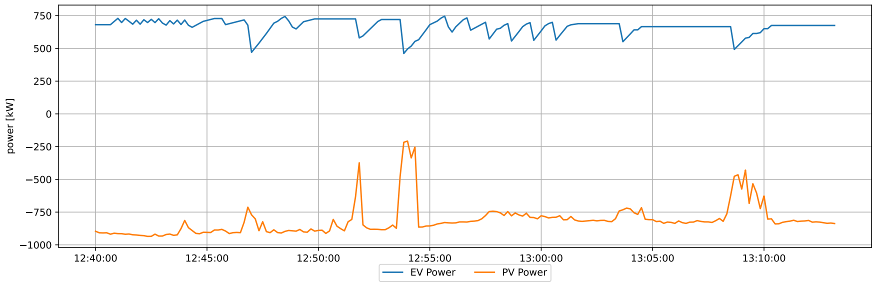

(a) GridShield response to PV fluctuations with an AIMD algorithm implementation.

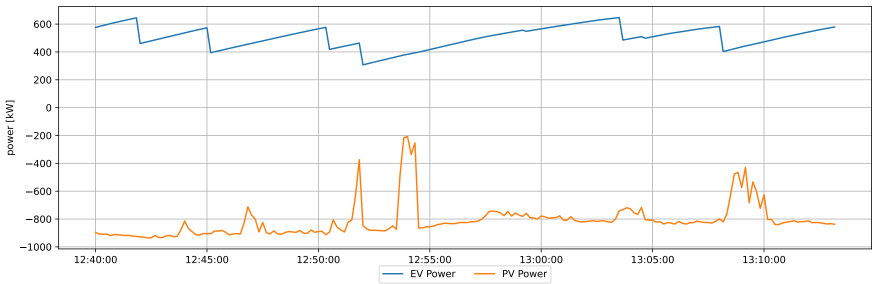

(b) GridShield response to PV fluctuations with an Elastic algorithm implementation.

Fig. 5.20: Algorithm responses to rapid PV power fluctuations.

5.5 Conclusion

In this chapter, the performance of the GridShield algorithms in different scenarios and with different control options is presented, i.e. continuous and discrete control, current and power based control. The results of the residential neighborhood of the Lochem scenario in Section 5.2 show that the presented GridShield algorithms provide a more Pareto optimal performance in terms of grid violations and ENS than the original AIAD GridShield implementation, irrespective of whether current or power based control is used, or whether a continuous or discrete set of charging powers is available.

The SlimPark scenario in Section 5.3 presents the results of using GridShield as an EMS when there is no EMS active. The results show that GridShield limits the power to reduce violations compared to the no control situation, while retaining most of the energy delivery that can be achieved while respecting grid constraints. Real-world measurements at the SlimPark site verified that GridShield can indeed limit EV power consumption when necessary.

The ASR scenario of Section 5.4 presents another public parking space, but at a significantly larger scale than the SlimPark scenario of Section 5.3. Results of two algorithms are presented, the AIMD and the Elastic GridShield algorithms. The Elastic algorithm provides a more stable behavior, but the AIMD algorithm achieves a higher energy delivery. Both algorithms show how a multi-layer GridShield setup works, where the top layer affects all lower layers when required, while if only one of the low level transformers is overloaded, only that GridShield module has to react and decrease the charging power of its EVs while the other low level transformers can stay at high power.

From the ASR scenario, it becomes apparent that while the original idea of TCP Elastic was to increase the speed of the increase phase compared to AIMD as presented in Chapter 2, in a GridShield system the Elastic algorithm is actually slower to increase than AIMD. This explains why it achieves better violations in the other scenarios, as the power in the grid with Elastic is generally lower than with an AIMD implementation. The ASR scenario also shows that the low β for the decrease phase in the Elastic algorithm is a disadvantage when GridShield is used as a rudimentary EMS, as a more granular decrease is desired in such a use case. However, the Lochem scenario shows that when GridShield is used as a defense mechanism against a cyber-attack, the rapid decrease resulting from the low value of β in the GridShield Elastic implementation can also be an advantage. The optimal GridShield implementation thus depends on what the system is used for.

6 Social Impact

Chapter Objective: This chapter discusses what the societal impact is of the installation of a GridShield system, and what can be done to optimize user behavior such that the need to activate GridShield will be kept to a minimum.

Chapter Contents

6.1 Introduction

In this chapter, we discuss the social impact of a GridShield implementation. GridShield is intended to protect a limited communal resource, i.e. the capacity of the local grid, from being overloaded. In a situation of a limited common resource, allowing everyone to take the maximum share they can acquire (which is rational from an individual point of view) leads to grid limit violations, ultimately resulting in negative consequences for all users of the resource. This effect is called the tragedy of the commons, which we explain in Section 6.2. However, Nobel prize winner Elinor Ostrom found that this apparently inevitable tragedy can be and is in fact avoided in many situations. Her work is and its implications for a local grid situation are detailed in Section 6.3. In Section 6.4, we discuss how the presence of GridShield in a community helps prevent the tragedy of the commons. Finally, we consider whether it is fair to implement GridShield in Section 6.5 after which we draw overall conclusions on the social impact of a GridShield system in Section 6.6.

6.2 The Tragedy of the Commons

The tragedy of the commons originates from an essay written in 1833 by William Forster Lloyd [57]. Lloyd described how a common resource can be over-used if it is left unregulated. In his work, he uses an example of a limited capacity pasture that is shared amongst multiple cattle herders (called a "common"), where all herders are entitled to let their cows graze on the plot of land. If all herders only put their allotted number of cattle on the common, the capacity will not be exceeded and everyone benefits. However, when one herder adds another animal to the land (thereby exceeding their allowed limit), the herder that does so benefits; he has an extra animal on the land. If there are no repercussions from the other herders, this is a rational decision. The herder violating his limit obtains the full benefits of the additional animal for himself, while the burden of the extra load on the land is shared amongst all.

When all herders do this, which is a rational decision, the common will be severely damaged and all farmers suffer the consequences. While it is rational to prevent this, it is also rational from an individual point of view to add additonal cattle. In 1968, Garrett Hardin dubbed this social dilemma "The tragedy of the commons" [58]:

> *Therein is the tragedy. Each man is locked into a system that compels him to increase his herd without limit - in a world that is limited. Ruin is the destination toward which all men rush, each pursuing his own best interest in a society that believes in the freedom of the commons.*

The dilemma of the tragedy of the commons applies to the context of GridShield by seeing the grid as the common, and the EVs as the cattle. When everyone allows their EV to charge at full power (put all their cattle in the field), the limit of the grid (the common) will be overloaded. Only when they charge at lower power (put in a few of their cows in the field at a time) the capacity of the common is respected. Thus, even if individual grid connections allow everyone to charge at full power (no one is prohibited from putting all their cows on the common at once) it is better for the community as a whole not to do so because of the limited capacity of the shared grid (or common). GridShield can prevent charging at full power when that is required, but this is undesirable: When GridShield is active, users are prevented from charging their EVs at maximum power even when they need it. On the other hand, users who do not need to charge at maximum power could charge at a lower rate, which frees up grid capacity. If they were to do so, that would mean that those in need of a charging session at high power can charge at high power without triggering GridShield.

Compelling users to prevent GridShield from activating by adapting their charging behavior, makes the charging system perform better for the community as a whole. In the remainder chapter, we discuss how this tragedy of the commons can be avoided to improve user comfort.

6.3 Solving the Tragedy

While Hardin in his article describes the tragedy of the commons as inevitable, solutions to prevent the tragedy have been proposed. Most notably, 2009 economics Nobel prize winner Elinor Ostrom theorizes that the tragedy can be avoided when the herders decide to cooperate, monitoring each others land use, and agreeing on and enforcing rules about the use of the land [60]. While this may seem a vague theory at first glance, Ostrom received the Nobel prize for the large amount of empirical evidence she gathered to prove her claim. Ostrom proposed a set of variables which contribute to the success chance of a community to self-organize and share their common-pool resources [59].

No general rules can be generated from this set of variables, but Ostrom formulated a set of design principles characterizing the rules that are applied in successful communities as given in Table 6.1. These design principles are not hard requirements, but instead conditions that help to increase the chance of success of a community sharing a common-pool resource. Ostrom found that most robust, long-term institutions for common-pool resources are characterized by most of the principles in Table 6.1. Meanwhile, fragile institutions are only characterized by a few of them. The design principles are listed here:

- Design principle 1 makes it clear for users what they can access of the common-pool, but also what the rights of others are. This allows users to take action against those that overstep their rights.
- Design principle 2 consists of two parts. The first part implies that users should perceive the rules put in place by the institution to be fair, which usually means that the assignment of benefits and costs to the users should be proportionate. The second part means that the rules must be well matched to local conditions.
- Design principle 3 requires active participation and inclusion in the making of and modification process of the agreed rules. By keeping participants included, the chance that they continue to perceive the rules as fair increases and design principle 2 remains effective over time.

- Design principle 4 demands that it is monitored whether the rules are abided by by individual users, such that sanctions can be put in place when the rules are not complied with.
- Design principle 5 requires that sanctions get progressively harder when a user repeatedly breaks rules. This makes repeated breaking of the rules unattractive, but also means that small disagreements about interpretation of the rules for a first time does not directly result in a harsh punishment.
- Design principle 6 entails that when a disagreement about the rules occurs between two users, there should be a method to quickly resolve the issue through a third party.
- Design principle 7 and 8 relate to autonomy. When the rights of an institution to mediate are recognized by national, regional and local governments, the legitimacy of the rules devised by the users will be challenged less in courts and other external settings. Design principle 8 requires that day-to-day problems can be solved in smaller subgroups, even when such a group is part of a larger institution.

6.4 GridShield Communities

A GridShield community, e.g. a group of households connected to the same transformer, always has a shared common-pool resource: the capacity of the grid. Whether in a public parking lot or in a neighborhood, the grid capacity is always the common-pool resource that a GridShield community shares. In this section, we evaluate how Ostroms design principles apply to EV charging.

- The limits of the grid are well-defined as the limit of the local transformer. However, this limit is not known to most users. Additionally, Dutch law mandates that users can withdraw power up to the power limit that they pay for at all times. Yet, when everyone uses the full capacity they pay for, the grid will not cope and all users will be left without electricity. To adhere to design principle 1, this additional shared limit must become apparent to the users. Thus, insight in the present capacity available on the grid must be provided to them. This could be in the form of an app, or an indicator device such as a screen in the EV charging station.

- When a user wishes to use a high charging power at a given moment, they should somehow incur costs that are proportional to benefits others receive when they choose to use a lower power. A market system should be in place to allow for this and provide a fair system to users in accordance with design principle 2.
- For design principle 3, it is important that users can communicate about the rules that they want to have in their system. In a local neighborhood, this requires active participation from users. In a public parking lot, this is nigh impossible since different users come and go.
- Monitoring the condition of the transformer only requires measuring the load, for which devices are already in place. More important for design principle 4 is to know what users are causing the largest violations. A problem here is that often an EV charging station is unaware of its current load, meaning that significant changes are required to measure violations at a user level.
- For design principle 5, users must be gradually sanctioned harsher depending on the extent of their violation and the context. For this design principle, GridShield becomes of significance. Users charging at a high power when transformer conditions do not allow for it, will be punished first when GridShield activates. Others who charge at a lower power will only be affected by GridShield later.
- To resolve conflicts about fairness as in design principle 6, a local arena should be put in place. To resolve problems quickly, it is desirable to have a log of who was affected by GridShield and how much. A legal framework is required to be able to collect this data whithout violating privacy regulations. This information is important to make a fair judgement to users that often contribute a large share to grid limit violations and thus GridShield activations.
- For communities to be able to organise themselves, they must be recognized by external government authorities (design principle 7) and if necessary, need to be able to form in multiple layers of nested enterprises. Rules regarding charging power at given times must be decided upon by the local community, e.g. by their representatives in a municipality, and recognized by external authorities. GridShield can be a standardized system that many communities use, which can then be recognized by higher level government authorities.
- Local LV grids are always part of a larger MV grid, which is part of the national grid. These higher level grids are also limited to a certain capacity. For design principle 8, it is important that het local LV grids can adapt to requirements

from a larger grid it is connected to. A GridShield system working on multiple levels can be put into place, which can help in applying design principle 8.

In summary, GridShield can directly contribute to design principle 5, 6, 7 and 8 for communities sharing a local grid to charge their EVs. Since a GridShield event affects all users of the grid, a local community can monitor when it is triggered, and investigate later who was responsible for triggering GridShield. This means that GridShield also makes the implementation of design principle 4 easier.

6.5 Fairness

A recurring theme in Ostroms design principles is the fairness of design principle 2. Many other design principles are in place to accommodate a greater sense of fairness. Thus, we look at the fairness aspects of a GridShield implementation in more detail.

The AIMD algorithm, coming from the Internet TCP, was developed with fairness in mind as presented in Section 2.3.2. The algorithm converges to a fair and even distribution of the available bandwidth or grid capacity by design, without need for direct communication between users. However, when individual users have different maxima to their own grid capacity, or to the maximum charging power of their EVs, differences in the capacity assigned to users by a GridShield implementation with AIMD-based algorithms may still occur.

This is a result of how in any GS implementation, some vehicles will be affected differently than others. By design, GridShield works via the polluter-pays principle (PPP) [61], a widely used principle where the person responsible for damage or costs to a system is also the one incurring the costs for restoration. Since GridShield imposes limits on the *maximum* charging power of an EVSE, but not on the *actual* charging power, those who own an EV that charges at a higher power are affected sooner than those charging at lower powers.

Since some vehicles charge on one phase only at a high current, while others charge on multiple phases, an EV charging on one phase may have an impact on that phase that is very large, despite the vehicle charging at a lower overall rate than another EV charging on multiple phases. This brings up a fairness discussion. Should the EV charging on one phase be the only EV affected by GridShield, since the phase it is charging at is also the phase that is being overloaded? This might be in accordance with PPP, but the EV charging on multiple phases is also consuming power on the overloaded phase. But then should everyone have an equal reduction in charging power, even when the EV charging on multiple phases is not the main polluter?

To answer these questions, GridShield could be designed such that it has two modes; one where it only limits EVs charging at the overloaded phase, and one where it can always limit power on all phases. Communities should decide upon what is a good implementation/rule for them, such that a sense of fairness is obtained and design principle 2 is adhered to in the best way.

6.6 Conclusion

Local communities can use GridShield to contribute to design principle 5, 6, 7 and 8 directly. According to Ostroms principles, this means that using GridShield in a local grid can increase the chances of preventing the tragedy of the commons from coming to be. Therefore, we conclude that GridShield can provide a contribution to communities that want to use their local grid in the fairest and most optimal way.

Tab. 6.1: Design principles illustrated by long-enduring common-pool resource institutions, adapted from [59]

Principle	Explanation
1. Clearly defined boundaries	Individuals or households with rights to withdraw resource units from the common-pool resource and the boundaries of the common-pool resource itself are clearly defined.
2. Congruence	a. The distribution of benefits from appropriation rules is roughly proportionate to the costs imposed by provision rules. b. Appropriation rules restricting time, place, technology and/or quantity of resource units are related to local conditions.
3. Collective-choice arrangements	Most individuals affected by operational rules can participate in modifying operational rules.
4. Monitoring	Monitors, who actively audit common-pool resource conditions and user behaviour, are accountable to the users and/or are the users themselves.
5. Graduated sanctions	Users who violate operational rules are likely to receive graduated sanctions (depending on the seriousness and context of the offence) from other users, from officials accountable to these users, or from both.
6. Conflict-resolution mechanisms	Users and their officials have rapid access to low-cost, local arenas to resolve conflict among users or between users and officials.
7. Minimal recognition of rights to organise	The rights of users to devise their own institutions are not challenged by external governmental authorities.
For common-pool resources that are part of larger systems:	
8. Nested enterprises	Appropriation, provision, monitoring, enforcement, conflict resolution and governance activities are organised in multiple layers of nested enterprises

7 Conclusions and Future Work

Chapter Objective: In this chapter, conclusions are drawn from the presented results, to answer the research questions of Chapter 1, after which suggestions for future work are presented.

Chapter Contents

The energy transition creates a transition to high power electrical appliances, which need high power electrical energy. The current electrical grid is not designed to work with such devices, and reinforcing it takes a long time. To continue the transition, energy management systems are introduced to more optimally use the existing grid infrastructure. In this work, we presented GridShield, a system that can function as a backup for a failing EMS, but can also act as a rudimentary EMS in a location where no EMS has been installed.

In Chapter 3 the model and components of the GridShield system are presented. The GridShield system operates using the algorithms that are presented in Chapter 4. The functioning and performance of GridShield is analyzed in Chapter 5, where both simulation results and a real-world test of GridShield are presented. Chapter 6 deals with the social impact of the implementation of a GridShield system, and provides suggestions to increase the chance that it will be accepted by communities.

The remainder of this chapter presents answers to the research questions of Chapter 1 in Section 7.1. Finally, suggestions for directions for future work are presented in Section 7.2.

7.1 Conclusions

From the results presented in this work, the main research question presented in Chapter 1 can be answered. To answer this question, we first answer the sub-questions that were formulated to deal with this main question:

> *What are the main objectives of such an EV charging control emergency fallback system and how can its performance be measured?*

The main objective of an EV charging control emergency fallback system is to minimize the violations of the maximum grid capacity, i.e. the capacity of a central connection point such as a transformer, in the event that the combined load of EVs that are charging starts to exceed grid limits. However, a secondary objective is to also minimize the energy not served to the EVs, since limiting the charging power of the EVs more than necessary results in a decrease of user comfort. A good EV charging control emergency fallback system makes a good trade-off between these two objectives.

To measure the grid capacity violations, great violations should be assigned a proportionally larger weight than small violations. Hence, the 2-norm of the violations occurring should be taken to quantify the violations. The energy not served can be quantified by integrating the energy that is served to EVs in a scenario, and comparing that energy to the energy served in a reference situation where a theoretical optimal solution without violations is applied.

> *How can general control concepts aid in avoiding grid congestion?*

While the electricity grid is physically different from a chemical plant, or from the Internet, similarities between grid congestion and e.g. process stability or congestion problems on the Internet have been observed. In all these cases, a system must be maintained to operate within its boundaries. While control concepts from those research fields do not directly deal with the electricity grid, these concepts thus may still be applied to an EV charging control emergency fallback system. The PID based GridShield algorithm presented in this work is based on the PID controller concept from the control engineering field, while the AIMD and Elastic algorithms are based on concepts from TCP used in the Internet. The results in this thesis show that the problem of grid congestion is similar to the problem of network congestion in the Internet, since the AIMD and Elastic algorithms are generally the best performing algorithms that were tested when considering the performance metrics of the previous research question.

How could an EV charging emergency fallback system be practically implemented?

Since an EV charging control emergency fallback system must prevent overloading of a central connection point such as a transformer, it must have a module at this central point that measures the load on the grid. When it measures an overload, it should decrease the charging power of all EVSEs connected to the central connection point. To implement this, a module must also be connected to every EVSE that can limit the power of the EVSE when the central module measures an overload.

The communication between the central module and the modules at the EVSEs should be implemented on a standalone network, completely decoupled from the Internet. This makes it more robust against cyber attacks and local Internet outages. Thus, a LoRa communication network between the central sender module and the modules at the EVSEs was implemented to obtain measurement results at the SlimPark site of the University of Twente, which are presented in Chapter 5.

How will EV charging emergency fallback systems impact user comfort and social behavior?

A local electricity grid is a system used by a community that must share the available capacity. While in the past, the simultaneity between users and their energy consumption were so low that the grid capacity never had to be considered by a user, the energy transition and the accompanying increase of high power electrical devices such as EVs change that paradigm. Where users by law are allowed to use the full capacity of their household connection continuously, the implication of all community members is that the grid will overload and that grid assets will be damaged. To avoid this tragedy of the commons from coming to be on the grid, an additional set of rules must be created that dictates how much grid capacity can be used by individual users depending on the current state of the grid. These rules could include incentives to use less grid capacity when the grid load is high, or punishment when using too much capacity, or both.

An EV charging emergency fallback system can contribute to making such a set of rules. It ensures that a community as a whole cannot damage their local grid by greedily charging their EVs. If all users agree that it is fair that the EV charging emergency fallback system is installed to prevent grid damage, this is a first step to making a system where a limited capacity grid can be shared amongst a community without ending up in the tragedy of the commons. While GridShield in the worst case lets users charge at a lower power than desired, thus impacting user comfort, it contributes to a social system that fairly distributes the grid resources amongst the community. By making users aware of this, it can have a positive impact on social behavior amongst users.

Having answered the sub-questions, we can now answer the main research question:

> ***How to robustly and adequately implement emergency fallback control of EV charging to avoid grid congestion?***

In this work, we present GridShield, an emergency fallback mechanism that controls EV charging to avoid grid congestion through a standalone separate uni-directional communication network for robustness and reliability. This setup shields the system from vulnerabilities of other common (shared) communication channels, such as external events or cyber-attacks. GridShield uses a transmitter at a central connection point that can communicate to receivers at EVSE units that they should limit their charging power by a certain amount. By basing the control algorithm of GridShield on the TCP Elastic concept, which was originally introduced for Internet applications, GridShield reduces grid limit violations by 85% up to 94% in the presented scenarios compared to when no control is applied. GridShield thus significantly reduces the grid limit violations caused by EV charging, while doing so at a cost of 7.5% to 26.6% energy not served compared to a theoretical optimal solution. We therefore conclude that the GridShield system adds robust and adequate emergency fallback control to avoid grid limit violations.

7.2 Future Work

The results presented in this thesis show that the presented approaches for GridShield provide good results in terms of our objectives, compared to having no active GridShield system. However, there are multiple research directions and future work recommendations which can improve upon the presented work, both to improve its performance and to broaden its applicability. This section provides a few ideas for these directions and recommendations.

7.2.1 Topology

In this work, we discussed a centralized and a decentralized variant of GS. In the centralized variant, we send a more elaborate message to the receivers that dictates what they must do. In the decentralized variant, we send a very simple message and the receivers base their actions on that. For future work, it is interesting to combine these approaches: sending a more elaborate message about the grid state, which the receivers can then use to run a local algorithm. Through such an approach, the receivers do not only have to base their actions on the state of the GridShield sender module, but can also take local information such as the local voltage into account. The use of such information could improve the performance of the GridShield system.

7.2.2 Algorithm Optimization

To find the optimal implementation of the presented algorithms, parameter sweeps were used. This raises the question of how the algorithms would have performed when other parameter ranges were chosen, as choosing a different parameter range may provide different outcomes. When comparing the AIMD and Elastic parameter sweeps presented in this work, it must be noted that the value of β goes significantly lower in the sweeps for the Elastic than for the AIMD implementation. A more elaborate sweep for the AIMD algorithm should be done to make a fairer comparison. Adding a sensitivity analysis to the parameter sweeps may help in determining what the optimal parameters of a given implementation may be.

Another interesting topic is the performance of different algorithms/parameters in different scenarios. In this work, we see that the optimal parameters for the implementations are similar between the Lochem and SlimPark scenarios, but they are not exactly equal. The comparison between the ASR and the Lochem scenario shows that the same parameters do not always perform best in all scenarios. In the cyber-attack of the Lochem scenario, it becomes apparent that the low β value of the Elastic algorithm is advantageous for a rapid response, but in the ASR scenario where GridShield is a rudimentary EMS, a slower but more granular decrease phase is desirable. Research into what parameters average the best results over a wide range of scenarios would be an interesting addition to this work, and could aid in developing a GridShield system that is generally applicable in a wide range of use cases.

the Elastic implementation is too slow as is apparent from the ASR scenario in Chapter 5. To compensate for the slow increase because of the long control signal intervals, we can compensate by rewriting equation (4.3) into equation (7.1). By dividing the denominator term $\phi(t-1)$ by Δt, we account for the long time delay and can possibly get a faster increase phase from GridShield Elastic. More research into the increase phase of GridShield Elastic may make it live up to its promise of a better increase phase implementation compared to AIMD.

$$\phi(t) = \phi(t-1) + \frac{WWF(t)}{\phi(t-1)/\Delta t} \tag{7.1}$$

7.2.3 V2G

As detailed in Chapter 3, the standard behavior of GridShield is to limit the charging power of EV chargers. To broaden the applicability of GridShield, V2G functionality could be taken into account for when future EVs and EVSEs support V2G energy delivery. To do so, the GridShield message $\phi(t)$ should be modified. Where in the GridShield implementation presented in this thesis, we always have a message $0 \leq \phi(t) \leq 1$, where $\phi(t) = 0$ means the EVs stop charging and $\phi(t) = 1$ means the EVs may charge at maximum power. To support V2G, we can extend our possible message range with additional values $1 \leq \phi(t) \leq 2$. When $\phi(t) = 1$, no V2G energy is supplied, while $\phi(t) = 2$ means maximum V2G energy should be provided.

Having V2G functionality presents another problem: Too much power can be injected into the grid. In such a situation, GridShield could also be adapted to limit the power delivery by the EVs. When too much power is being injected into the grid instead of consumed, the value of $\phi(t)$ can be made negative. The factor $-1 \geq \phi(t) \geq 0$ then becomes the amount by which V2G power injection from the EVs must be decreased:

$$P_{GS}^{EV,V2G}(t) = \hat{P}_{max}^{EV,V2G} \cdot (1 + \phi(t)) \tag{7.2}$$

When reducing the V2G power injection to 0 is not enough, ϕ can be reduced further: a factor $-2 \geq \phi(t) \geq -1$ then forces the EV to consume energy from the grid when possible. When $\phi(t) = -1$, no energy is charged by the EV, while $\phi(t) = -2$ means the EV must charge at full power. The resulting GridShield system would be more complex, but also more flexible and broadly applicable, making it an interesting research direction.

7.2.4 Other Device Types

While the focus in this work has been on EV power control, the concept of GridShield can also be extended to other device types. Examples of other device types that

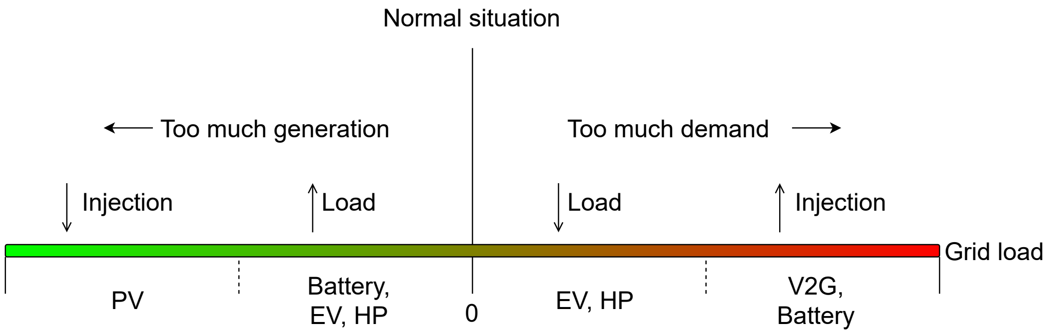

Fig. 7.1: GridShield application areas. On the green (left) side of the line there is too much generation, on the red (right) side of the line there is too much production.

can be controlled by GridShield are presented in Fig. 7.1. A proposal for device priorities is also included in this figure. When there is too much demand, first the load of EVs and HPs controlled by GS should be brought down. Only when that is not enough, active injection by batteries and V2G enabled EVs should be forced by GridShield as a means to balance supply and demand locally. The other way around, it is desirable to first actively increase load by forcing batteries, EVs and HPs to consume more energy, to maximize the usage of available green energy, before resorting to curtailment of PV production.

To control other device types, the message $\phi(t)$ should be extended to also include a byte signalling what device type the GridShield message is for. After this authentication byte, the message $\phi(t)$ as described in this work can be transmitted. When a device can both consume and supply power, such as a V2G enabled EV, the extension of $\phi(t)$ for bi-directional devices proposed in Section 7.2.3 can also be applied to that device. It is recommended to implement this identification byte such that it has a range of possible additional values left, so that it becomes easier to incorporate additional device types besides EVs, HPs, PV and home batteries in the future.

7.2.5 Standardization

By making GridShield compatible with a range of device types, it can become a standard for grid capacity protection in any location. However, social systems and regulations must be made for every device type, which is an entire different field of study by itself and requires a lot of attention. To go through the energy transition, we must make optimal use of the available grid infrastructure that was once built by a different, less energy dependent society. GridShield could be a step in the right direction.

Bibliography

[1]“Cop26 the glasgow climate pact.” (), [Online]. Available: %5Curl%7Bhttps://ukcop26.org/wp-content/uploads/2021/11/COP26-Presidency-Outcomes-The-Climate-Pact.pdf%7D,%20journal=%7BUN%20Climate%20Change%20Conference%20UK%202021%7D,%20publisher=%7BUN%7D,%20year=2021 (cit. on p. 2).

[2]I. v. Halm. “How can the eu end its dependence on russian gas?” (May 2022), [Online]. Available: https://www.energymonitor.ai/policy/how-can-the-eu-end-its-dependence-on-russian-gas (cit. on p. 2).

[3]Z. Wanat and A. Hernandez. “Brussels spells out plan to end dependence on russian energy.” (May 2022), [Online]. Available: https://www.politico.eu/article/eu-plan-end-dependence-russia-energy/ (cit. on p. 2).

[4]M. Niewold. “Te weinig capaciteit op stroomnet om nieuwe bedrijven aan te sluiten.” (Jun. 2021), [Online]. Available: https://www.rtlnieuws.nl/economie/artikel/5238110/netbeheerder-liander-kan-niet-bolwerken-bedrijven-wachtlijst (cit. on p. 3).

[5]RVO. “Subsidieregeling Elektrische Personenauto’s Particulieren (SEPP).” (Apr. 2022), [Online]. Available: https://www.rvo.nl/subsidies-financiering/sepp (cit. on p. 3).

[6]ANWB. “Alle fiscale voordelen voor elektrische auto’s op een rij.” (Dec. 2020), [Online]. Available: https://www.anwb.nl/auto/elektrisch-rijden/alle-fiscale-voordelen-voor-elektrische-autos-op-een-rij (cit. on p. 3).

[7]Centraal Bureau voor de Statistiek (CBS). “Hoeveel rijden personenauto’s?” (Nov. 2021), [Online]. Available: https://www.cbs.nl/nl-nl/visualisaties/verkeer-en-vervoer/verkeer/verkeersprestaties-personenautos (visited on Mar. 7, 2022) (cit. on p. 4).

[8]International Energy Agency (IEA), “Technology roadmap - smart grids,” 2011 (cit. on p. 4).

[9]Commission for Energy Regulation (CER), “Cer smart metering project - electricity customer behaviour trial” (cit. on p. 5).

[10]“Energy management system application program interface (EMS-API),” International Electrotechnical Commission (IEC), Standard, 2005 (cit. on p. 8).

[11]M. F. Zia, E. Elbouchikhi, and M. Benbouzid, “Microgrids energy management systems: A critical review on methods, solutions, and prospects,” *Applied Energy*, vol. 222, pp. 1033–1055, 2018. DOI: https://doi.org/10.1016/j.apenergy.2018.04.103 (cit. on p. 9).

[12]P. Siano, “Demand response and smart grids—a survey,” *Renewable and Sustainable Energy Reviews*, vol. 30, pp. 461–478, 2014. DOI: https://doi.org/10.1016/j.rser.2013.10.022 (cit. on p. 9).

[13]K. McKenna and A. Keane, “Residential load modeling of price-based demand response for network impact studies,” *IEEE Transactions on Smart Grid*, vol. 7, no. 5, pp. 2285–2294, 2016. DOI: 10.1109/TSG.2015.2437451 (cit. on pp. 9, 10).

[14]M. Gerards, H. Toersche, G. Hoogsteen, *et al.*, “Demand side management using profile steering,” in *PowerTech, 2015 IEEE Eindhoven*, IEEE Power & Energy Society, Jun. 2015. DOI: 10.1109/PTC.2015.7232328 (cit. on pp. 9, 47).

[15]BDEW, German Association of Energy and Water Industries, “Discussion paper - smart grid traffic light concept,” 2015 (cit. on pp. 11, 12).

[16]L. Degroote, B. Renders, B. Meersman, and L. Vandevelde, “Neutral-point shifting and voltage unbalance due to single-phase dg units in low voltage distribution networks,” *2009 IEEE Bucharest PowerTech*, pp. 1–8, 2009 (cit. on p. 13).

[17]S. Weckx, C. Gonzalez, and J. Driesen, “Combined central and local active and reactive power control of pv inverters,” *IEEE Transactions on Sustainable Energy*, vol. 5, no. 3, pp. 776–784, 2014. DOI: 10.1109/TSTE.2014.2300934 (cit. on pp. 13, 14).

[18]C. Gonzalez, J. Geuns, S. Weckx, *et al.*, “Lv distribution network feeders in belgium and power quality issues due to increasing pv penetration levels,” in *2012 3rd IEEE PES Innovative Smart Grid Technologies Europe (ISGT Europe)*, 2012, pp. 1–8. DOI: 10.1109/ISGTEurope.2012.6465624 (cit. on p. 13).

[19]S. Paudyal, O. Ceylan, B. P. Bhattarai, and K. S. Myers, “Optimal coordinated ev charging with reactive power support in constrained distribution grids,” in *2017 IEEE Power Energy Society General Meeting*, 2017, pp. 1–5. DOI: 10.1109/PESGM.2017.8274266 (cit. on p. 14).

[20]U. B. Tayab, M. A. B. Roslan, L. J. Hwai, and M. Kashif, “A review of droop control techniques for microgrid,” *Renewable and Sustainable Energy Reviews*, vol. 76, pp. 717–727, 2017. DOI: https://doi.org/10.1016/j.rser.2017.03.028 (cit. on p. 15).

[21]M. Reza, D. Sudarmadi, F. Viawan, W. Kling, and L. Van Der Sluis, “Dynamic stability of power systems with power electronic interfaced dg,” in *2006 IEEE PES Power Systems Conference and Exposition*, IEEE, 2006, pp. 1423–1428 (cit. on p. 15).

[22]J. Slootweg and W. Kling, “Impacts of distributed generation on power system transient stability,” in *IEEE Power Engineering Society Summer Meeting,*, IEEE, vol. 2, 2002, pp. 862–867 (cit. on p. 15).

[23]M. Marinelli, S. Martinenas, K. Knezović, and P. B. Andersen, “Validating a centralized approach to primary frequency control with series-produced electric vehicles,” *Journal of Energy Storage*, vol. 7, pp. 63–73, 2016. DOI: https://doi.org/10.1016/j.est.2016.05.008 (cit. on pp. 15, 16).

[24] K. Knezović, S. Martinenas, P. B. Andersen, A. Zecchino, and M. Marinelli, “Enhancing the role of electric vehicles in the power grid: Field validation of multiple ancillary services,” *IEEE Transactions on Transportation Electrification*, vol. 3, no. 1, pp. 201–209, 2017. DOI: 10.1109/TTE.2016.2616864 (cit. on pp. 15, 16).

[25] S. Martinenas, K. Knezović, and M. Marinelli, “Management of power quality issues in low voltage networks using electric vehicles: Experimental validation,” *IEEE Transactions on Power Delivery*, vol. 32, no. 2, pp. 971–979, 2017. DOI: 10.1109/TPWRD.2016.2614582 (cit. on pp. 15, 16, 31, 46, 53).

[26] Y. Yang and S. Lam, “General aimd congestion control,” in *Proceedings 2000 International Conference on Network Protocols*, 2000, pp. 187–198. DOI: 10.1109/ICNP.2000.896303 (cit. on pp. 17, 36).

[27] A. Hartmanns, H. Hermanns, and P. Berrang, “A comparative analysis of decentralized power grid stabilization strategies,” in *Proceedings of the 2012 Winter Simulation Conference (WSC)*, 2012, pp. 1–13. DOI: 10.1109/WSC.2012.6465083 (cit. on p. 17).

[28] A. Hartmanns and H. Hermanns, “Modelling and decentralised runtime control of self-stabilising power micro grids,” in *Leveraging Applications of Formal Methods, Verification and Validation. Technologies for Mastering Change*, T. Margaria and B. Steffen, Eds., Berlin, Heidelberg: Springer Berlin Heidelberg, 2012, pp. 420–439 (cit. on p. 17).

[29] S. Stüdli, E. Crisostomi, R. Middleton, and R. Shorten, “A flexible distributed framework for realising electric and plug-in hybrid vehicle charging policies,” *International Journal of Control*, vol. 85, no. 8, pp. 1130–1145, 2012. DOI: 10.1080/00207179.2012.679970. eprint: https://doi.org/10.1080/00207179.2012.679970 (cit. on p. 17).

[30] D.-M. Chiu and R. Jain, “Analysis of the increase and decrease algorithms for congestion avoidance in computer networks,” *Computer Networks and ISDN Systems*, vol. 17, no. 1, pp. 1–14, 1989. DOI: https://doi.org/10.1016/0169-7552(89)90019-6 (cit. on pp. 17, 18).

[31] W. R. Stevens, *TCP Slow Start, Congestion Avoidance, Fast Retransmit, and Fast Recovery Algorithms*, RFC 2001, Jan. 1997. DOI: 10.17487/RFC2001 (cit. on p. 18).

[32] S. Stüdli, M. Corless, R. H. Middleton, and R. Shorten, “On the modified aimd algorithm for distributed resource management with saturation of each user’s share,” in *2015 54th IEEE Conference on Decision and Control (CDC)*, 2015, pp. 1631–1636. DOI: 10.1109/CDC.2015.7402444 (cit. on p. 18).

[33] M. A. Alrshah, M. A. Al-Maqri, and M. Othman, “Elastic-tcp: Flexible congestion control algorithm to adapt for high-bdp networks,” *IEEE Systems Journal*, vol. 13, no. 2, pp. 1336–1346, 2019. DOI: 10.1109/JSYST.2019.2896195 (cit. on pp. 18, 20, 36).

[34] U. Hengartner, J. Bolliger, and T. Gross, “Tcp vegas revisited,” in *Proceedings IEEE INFOCOM 2000. Conference on Computer Communications. Nineteenth Annual Joint Conference of the IEEE Computer and Communications Societies (Cat. No.00CH37064)*, vol. 3, 2000, 1546–1555 vol.3. DOI: 10.1109/INFCOM.2000.832553 (cit. on p. 19).

[35] H. Jamal and K. Sultan, “Performance analysis of tcp congestion control algorithms,” *International journal of computers and communications*, vol. 2, no. 1, pp. 18–24, 2008 (cit. on p. 19).

[36]E. Weigle and W.-c. Feng, “A case for tcp vegas in high-performance computational grids,” in *Proceedings 10th IEEE International Symposium on High Performance Distributed Computing*, 2001, pp. 158–167. DOI: 10.1109/HPDC.2001.945186 (cit. on pp. 19, 20).

[37]A. A. Ghassan, I. Mahamod, and J. Kasmiran, “Characterization and observation of (transmission control protocol) tcp-vegas performance with different parameters over (long term evolution) lte networks,” *Scientific Research and Essays*, vol. 6, no. 9, pp. 2003–2010, 2011. DOI: 10.5897/sre11.252 (cit. on p. 19).

[38]A. Esterhuizen and K. Aes, “Tcp congestion control comparison,” in *Southern African Telecommunication Networks and Applications Conference (SATNAC)*, 2012 (cit. on p. 20).

[39]N. Cardwell, Y. Cheng, C. S. Gunn, S. H. Yeganeh, and V. Jacobson, “Bbr: Congestion-based congestion control,” *ACM Queue*, vol. 14, September-October, pp. 20–53, 2016 (cit. on p. 20).

[40]K. "Ang, G. Chong, and Y. Li, “Pid control system analysis, design, and technology,” IEEE, Jul. 2005 (cit. on p. 21).

[41]J. Zhang and L. Guo, “Theory and design of pid controller for nonlinear uncertain systems,” *IEEE Control Systems Letters*, vol. 3, no. 3, pp. 643–648, 2019. DOI: 10.1109/LCSYS.2019.2915306 (cit. on p. 21).

[42]B. Yang, T. Yu, H. Shu, *et al.*, “Energy reshaping based passive fractional-order pid control design and implementation of a grid-connected pv inverter for mppt using grouped grey wolf optimizer,” *Solar Energy*, vol. 170, pp. 31–46, 2018. DOI: https://doi.org/10.1016/j.solener.2018.05.034 (cit. on p. 21).

[43]K. M. Tan, V. K. Ramachandaramurthy, J. Y. Yong, and M. Tariq, “Experimental verification of a flexible vehicle-to-grid charger for power grid load variance reduction,” *Energy*, vol. 228, p. 120 560, 2021. DOI: https://doi.org/10.1016/j.energy.2021.120560 (cit. on p. 21).

[44]G. Hoogsteen, “A cyber-physical systems perspective on decentralized energy management,” English, Ph.D. dissertation, University of Twente, Netherlands, Dec. 2017. DOI: 10.3990/1.9789036544320 (cit. on pp. 21, 39).

[45]A. O’Dwyer, “Pi and pid controller tuning rules: An overview and personal perspective,” in *2006 IET Irish Signals and Systems Conference*, 2006, pp. 161–166 (cit. on p. 21).

[46]T. Samad, “A survey on industry impact and challenges thereof [technical activities],” *IEEE Control Systems Magazine*, vol. 37, no. 1, pp. 17–18, 2017. DOI: 10.1109/MCS.2016.2621438 (cit. on p. 22).

[47]P. to Phase, *Netten voor distributie van elektriciteit*. Phase to Phase, 2009 (cit. on p. 23).

[48]ElaadNL. “Thuisladen, nationale agenda laadinfrastructuur - elaad nl.” (2021), [Online]. Available: https://www.elaad.nl/nationale-agenda-laadinfrastructuur/thuisladen/ (cit. on p. 26).

[49]J. Kerkhoven, *Proof of concept sociale module voor laadpalen, decentrale variant: Lokaal congestiemanagement door middel van smart charging met behulp van loray*, Feb. 2020 (cit. on p. 34).

[50]Y. Peng, D. Vrancic, and R. Hanus, “Anti-windup, bumpless, and conditioned transfer techniques for PID controllers,” *IEEE Control Systems Magazine*, vol. 16, no. 4, pp. 48–57, 1996. DOI: 10.1109/37.526915 (cit. on p. 39).

[51]G. Hoogsteen, J. L. Hurink, and G. J. M. Smit, “Demkit: A decentralized energy management simulation and demonstration toolkit,” in *2019 IEEE PES Innovative Smart Grid Technologies Europe (ISGT-Europe)*, 2019, pp. 1–5. DOI: 10.1109/ISGTEurope.2019.8905439 (cit. on p. 45).

[52]G. Hoogsteen, A. Molderink, G. Smit, *et al.*, “Charging electric vehicles, baking pizzas, and melting a fuse in lochem,” English, *CIRED: Open Access Proceedings Journal*, vol. 2017, no. 1, pp. 1629–1633, Oct. 2017. DOI: 10.1049/oap-cired.2017.0340 (cit. on pp. 45, 46).

[53]“Utrechtse burgemeester opent grootste laadparkeergarage ter wereld bij asr.” (Sep. 2021), [Online]. Available: https://www.asrnederland.nl/nieuws-en-pers/pers/utrechtse-burgemeester-opent-grootste-laadparkeergarage-ter-wereld-bij-asr (cit. on p. 46).

[54]G. Hoogsteen, A. Molderink, J. Hurink, and G. Smit, “Generation of flexible domestic load profiles to evaluate demand side management approaches,” Undefined, in *2016 IEEE International Energy Conference (ENERGYCON)*, eemcs-eprint-27137 ; Conference date: 04-04-2016 Through 08-04-2016, IEEE Power & Energy Society, Apr. 2016, p. 1279. DOI: 10.1109/ENERGYCON.2016.7513873 (cit. on p. 46).

[55]GroenLinks. “Lochem is schitterend, ook vanuit de lucht.” (Sep. 2016), [Online]. Available: https://lochem.groenlinks.nl/nieuws/lochem-schitterend-ook-vanuit-de-lucht (cit. on p. 47).

[56]“Energy in twente.” (2021), [Online]. Available: https://twente.energy/ (cit. on pp. 59, 67).

[57]W. F. Lloyd, *Two lectures on the checks to population*, English. Oxford University, 1833, p. 75 (cit. on p. 74).

[58]G. Hardin, “The tragedy of the commons,” *Science*, vol. 162, no. 3859, pp. 1243–1248, 1968. DOI: 10.1126/science.162.3859.1243. eprint: https://www.science.org/doi/pdf/10.1126/science.162.3859.1243 (cit. on p. 74).

[59]E. Ostrom, *Governing the Commons: The Evolution of Institutions for Collective Action*, ser. Political Economy of Institutions and Decisions. Cambridge University Press, 1990. DOI: 10.1017/CBO9780511807763 (cit. on pp. 75, 80).

[60]M. Burke, “People in economics: The master artisan,” *Finance & Development*, vol. 48, no. 3, 2011. DOI: 10.5089/9781451953633.022.A002 (cit. on p. 75).

[61]M. R. Khan, “Polluter-pays-principle: The cardinal instrument for addressing climate change,” *Laws*, vol. 4, no. 3, pp. 638–653, 2015. DOI: 10.3390/laws4030638 (cit. on p. 78).

Colophon

This thesis was typeset with $\LaTeX\,2_\varepsilon$. It uses the *Clean Thesis* style developed by Ricardo Langner. The design of the *Clean Thesis* style is inspired by user guide documents from Apple Inc.

Download the *Clean Thesis* style at http://cleanthesis.der-ric.de/.